A Study of the Thermal Interactions of Sustainable Asphalt Concrete Pavements

by

Miguel Angel Díaz Sánchez

A thesis submitted to the Graduate Faculty of
Auburn University
in partial fulfillment of the
requirements for the Degree of
Master of Science

Auburn, Alabama
December 14, 2013

Keywords: asphalt concrete, thermal properties,
sustainable pavements

Approved by

David Timm, Chair, Brasfield & Gorrie Professor, Civil Engineering
Rod E. Turochy, Associate Professor, Civil Engineering
Randy West, Director, National Center for Asphalt Technology

Abstract

A study of the thermal interactions of select sustainable technologies, such as reclaimed asphalt pavements (RAP), recycled asphalt shingles (RAS), ground tire rubber (GTR), and foamed asphalt in cold recycled materials was performed using the structural sections built as part of the fifth research cycle at the National Center for Asphalt Technology (NCAT) Test Track. The study focused on two stages in the life of asphalt concrete (AC) pavements, initial construction and in-service life. Results revealed that even if theoretical models for predicting the initial cooling of AC were satisfactory, the use of RAS, GTR-modified binders, and foamed cold mix bases had a direct effect on the temperature predictions, warranting further investigation. A subsequent analysis of the built pavements established that the use of these sustainable technologies affected the thermal properties of asphalt concrete pavements, which could impact the structural and functional performance of the pavement.

Acknowledgments

The author would like to thank his family and his girlfriend for their unconditional support and motivation. The author would also like to thank Dr. David Timm and the advisory committee for their guidance throughout the development of this thesis. Gratitude is also expressed to the staff at the National Center for Asphalt Technology. Finally, the author would like to acknowledge the Alabama Department of Transportation, the Alabama Department of Environmental Management, The North Carolina Department of Transportation, The South Carolina Department of Transportation and the Virginia Department of Transportation for their support of this research.

Table of Contents

List of Tables

List of Figures

CHAPTER ONE

INTRODUCTION

1.1 BACKGROUND

With the ever-increasing global demand for construction and rehabilitation of transportation infrastructure, a collective necessity for pavement structures capable of meeting the needs of present road users without compromising future generations, becomes evident. The pavement engineering community is challenged with the development of innovative technologies and construction methods that take into account environmental, economic and social indicators, targeting sustainable development. The concept of sustainable pavements is used to define pavement structures and materials that systematically minimize the consumption of non-renewable resources, while maximizing the reuse of existing materials and generating a minimum of pollutants in a cost-effective manner, which directly benefits society.

Under this notion of sustainability, the asphalt industry has deployed multiple initiatives in response to a variety of government regulations, economic factors and changes in public attitudes (Prowell et al., 2011). As a result, a number of innovative technologies and techniques have been developed and are gaining popularity amongst agencies, contractors and users. Materials such as reclaimed asphalt pavements (RAP), recycled asphalt shingles (RAS) and ground tire rubber (GTR) which would otherwise be disposed of in landfills, have been incorporated. Pioneering construction processes have

been developed to reuse the existing pavement materials as an enhanced foundation for new pavement structures. Methods for enhancing recycled materials, such as asphalt foaming, have been improved by equipment manufacturers. All these efforts have contributed to the accelerated advancement towards more sustainable roads and pavements, observed in recent years.

With this enhanced development of innovative sustainable technologies and methods for asphalt pavements arises an essential need for continued assessment of the constructability and performance of such advances. The properties and characteristics of the new materials must be continuously assessed and studied to ensure their effectiveness and practicality. Although the adequate structural and functional capacity of these materials has been validated on multiple occasions, there is an essential need to study their interactions with the environment from a constructability and performance perspectives.

The ultimate behavior of a well-designed asphalt mixture during construction and throughout the service life of the pavement is closely related to its behavior under varying environmental conditions, especially temperature. Asphalt concrete properties are greatly affected by temperature variations and is constantly interacting with the surrounding environment by absorbing and emitting heat. These thermal interactions between asphalt concrete pavements and the surrounding environment are vital during paving operations as they control the time available to compact and achieve proper density in the asphalt layer. Similarly, during the service life of the pavement, these thermal interactions define the functional and structural performance of the asphalt layers, as well as the impact of the pavement on the ambient air temperatures, especially in large cities, known as the

Urban Heat Island (UHI) Effect. In that way, a detailed study of the thermal interactions of sustainable asphalt concrete materials would allow for a better understanding of the performance during the construction and service life of sustainable pavements.

1.2 OBJECTIVES

The objective of this study was to evaluate the effect of innovative sustainable technologies on the thermal interactions of asphalt pavements and the environment. For this, two different stages during the life of a pavement were considered, construction and early service life of the pavement. For each case, individual objectives were established:

1. Construction:
    - 1.1 Evaluate the effect of sustainable technologies on the construction cooling rate of asphalt concrete layers
    - 1.2 Evaluate the accuracy of current cooling prediction software (i.e., MultiCool) with the inclusion of RAS, high RAP contents, and GTR-modified asphalt binders.
    - 1.3 Evaluate the effect of foamed cold mix as underlying base layer on the construction cooling rate of conventional asphalt concrete layers placed above the foamed cold mix.
2. Early service life:
    - 2.1 Evaluate the thermal interactions of sustainable technologies during the early service life of asphalt pavements.
    - 2.2 Evaluate the effect of RAS, high RAP contents, and GTR-modified asphalt binders on the temperature fluctuations of asphalt pavements.

2.3 Evaluate the effect of RAS, high RAP contents, and GTR-modified asphalt binders on the thermal energy stored by asphalt pavements.

2.4 Evaluate the effect of RAS, high RAP contents, and GTR-modified asphalt binders on the thermal properties of asphalt pavements.

1.3 SCOPE

To meet the objectives, an investigation was performed using the structural test sections from the 2012 structural study at the National Center for Asphalt Technology (NCAT) Test Track. To evaluate the effect of innovative sustainable technologies on the cooling rate of asphalt pavement layers, a critical assessment of the accuracy of a commonly used computer program, MultiCool, in predicting the cooling rate of the mixtures used in the structural experiment was performed. Specific weather information, mixture characteristics and as-built properties were used as inputs to generate simulated cooling curves in MultiCool. A statistical analysis of the results was conducted to compare the simulated cooling curves to field measurements under controlled conditions. An evaluation of the effect of RAS, high RAP contents, and GTR-modified binders on the construction cooling of asphalt concrete was performed.

To determine the contribution of sustainable technologies on the thermal response of asphalt pavements, a study was conducted to analyze energy storing and thermal conduction capacities of the pavement sections included in the structural experiment. The study was based on average hourly pavement temperature measurements taken between January 1st and June 19th, 2013. Hourly measurements of the ambient air temperature, wind velocity and solar radiation, made by an on-site weather station, were also used to estimate the energy stored by the pavement and the heat conducted through the asphalt

layer. A statistical analysis of the results allowed comparing the sections included in the experiment to analyze the possible effect of high RAP contents, RAS, and GTR-modified binders on the thermal properties of asphalt concrete pavements.

1.4 ORGANIZATION OF THESIS

The results of the study were divided into six chapters. A literature review, included in Chapter Two, was conducted in an attempt to describe the concepts behind heat transfer mechanisms between the asphalt concrete and the surrounding environment. Chapter Three includes a detailed description of the test sections included in the 2012 NCAT Test Track structural study, the construction process, and the experimental plan followed for the study. Chapter Four evaluates the effect of sustainable technologies on the cooling rate of asphalt pavements. The results of a statistical comparison between field temperature measurements and simulated cooling curves obtained with the MultiCool program are presented. Additionally, the results of an assessment of the accuracy of the MultiCool model in predicting the cooling rate of the sustainable mixtures used for the study are explained. Chapter Five analyzes the thermal response and heat energy storage of the sections included in the study during the early service life of the pavement. Also included in this chapter is a statistical comparison of the thermal properties measured from field measurements. Chapter Six concludes the aspects of this investigation and provides recommendations based on the findings of this study.

CHAPTER TWO

LITERATURE REVIEW

2.1 INTRODUCTION

Asphalt concrete is a thermorheologically dependent material with a complex viscoelastic deformation behavior, affected by various factors, such as time (i.e. rate of loading, loading time, rest period), temperature, stress state, mode of loading, aging, and moisture. All of these elements play an important part in the success of an asphalt concrete pavement. However, the ultimate behavior of a well-designed asphalt mixture during construction and throughout the service life of the pavement is closely related to its performance under varying environmental conditions, especially temperature. In fact, asphalt concrete is sensitive to temperature variations and is constantly interacting with the surrounding environment by absorbing and emitting heat. As mentioned before, these thermal interactions between asphalt concrete pavements and the surrounding environment define the constructability and long-term performance of the asphalt layers. Therefore, a correct understanding of the heat transfer mechanisms between the asphalt concrete and the surrounding environment would assist paving crews during construction and potentially improve pavement performance predictions. For this, a literature review was conducted in an effort to describe and characterize the heat transfer mechanisms in asphalt concrete.

2.2 HEAT TRANSFER MECHANISMS IN ASPHALT CONCRETE

In civil engineering, heat is defined as a form of energy that can be transferred from one system to another as a result of a temperature difference between the two systems (Cengel, 2010). In all cases, this transfer occurs from the system with the higher temperature towards the system with the lowest temperature, until the two systems reach the same temperature and thermal equilibrium occurs. In practice, heat transfer may be classified as being steady (also called steady-state) or transient (also called unsteady) (Cengel, 2010). Steady heat transfer considers that the temperature in the system remains constant with time and location, while transient heat transfer integrates all possible thermal variations with time and position within the system. Although most heat transfer problems encountered in practice are transient in nature, an abridged steady-state analysis is usually used to simplify the complex calculations needed to model transient heat transfer (Cengel, 2010). This simplification is based on the assumption that materials are isotropic and have the exact same properties in all directions, and even if composite materials (i.e. asphalt concrete) are anisotropic in nature, this assumption may be deemed reasonable.

A pavement structure can be modeled as a large planar wall, where three individual systems interact: the base, the asphalt concrete, and the surrounding air. Differences in temperature amongst these three systems allow for heat to be transferred from the high-temperature medium towards the low-temperature medium. Assuming all three mediums are isotropic, the heat transfer is expected to be transient, occurring in the direction perpendicular to the surface of the pavement. In that case, the variations of temperature in all other directions may be ignored and the heat transfer mechanisms may

be considered “one-dimensional”. In such conditions, three primary mechanisms of heat transfer can be identified: conduction occurring from the asphalt layer to the base, convection occurring from the asphalt layer to the surrounding air, and solar radiation directly applied at the surface of the asphalt layer. The general concept of one-dimensional heat transfer between the asphalt layer (gray), the base (textured) and the surrounding environment is presented in Figure 2.1, where the direction of heat transfer is represented by arrows. Each heat transfer mechanism is described in more detail in the following sections.

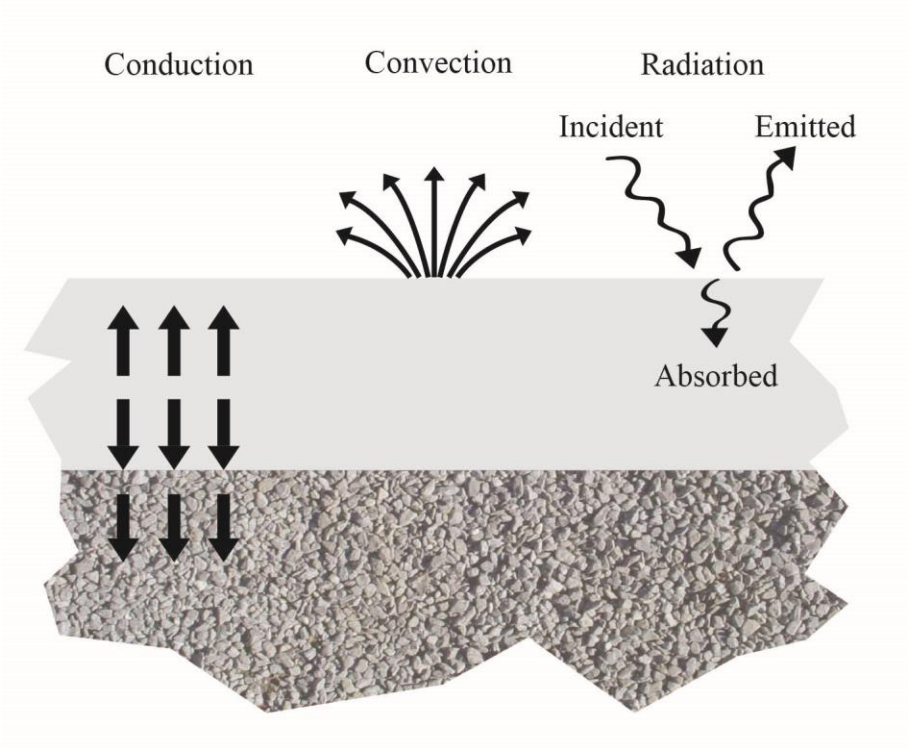

FIGURE 2.1 One-Dimensional Heat Transfer in a Pavement Structure

.

2.2.1 Heat Conduction

The transfer of energy from the more energetic particles in a medium to the adjacent less energetic particles in the same or in a neighboring medium is called conduction (Cengel, 2010; Vargas-Nordcbeck and Timm, 2011a). According to Cengel (2010), experiments have shown that the rate of heat transfer (Q) through a planar layer (i.e. asphalt and base layers) is proportional to the temperature difference across the layer and the heat transfer area, but is inversely proportional to the thickness of the layer. Therefore, heat conduction in an asphalt pavement can be described by Fourier's law of heat conduction, which states that the heat flux or rate of heat transfer, in a given direction is directly proportional to the temperature gradient (change in temperature/change in depth) in the same direction (Chadbourn, 1998; Vargas-Nordcbeck and Timm, 2011a; Corlew 1968). This proportionality is determined by the thermal conductivity of the material, which represents a measure of the ability of the material to conduct heat (Cengel, 2010).

Although the thermal conductivity of a material generally varies with temperature, most practical applications allow assuming an average value to simplify the analysis (Cengel, 2010). In that way, assuming a constant thermal conductivity throughout the asphalt layer; one-dimensional heat conduction is defined in Equation 1. In this specific case, the heat transfer area is constant and the heat flux (rate of heat transfer per unit area normal to the direction of heat transfer) is a better approach to illustrate the heat transfer mechanism. Moreover, the negative sign on the right side of the equation denotes the direction of heat transfer, from higher temperatures to lower temperatures.

$$q_{cond} = -k_{ac} \cdot \frac{dT}{dz} \quad (1)$$

Where: q_{cond} = Conduction heat flux in the vertical direction (W/m^2)

k_{ac} = Thermal conductivity of asphalt concrete (W/m·K)

$\frac{dT}{dz}$ = Temperature gradient (change in temperature/change in depth)

The energy required to raise the temperature of a unit mass of asphalt concrete by one degree as the pressure is held constant is called the specific heat at constant pressure (c_p). Furthermore, the combined effect of the density (ρ) and the specific heat (c_p), also known as the heat capacity, represents the ability of a material to store thermal energy. The rate of heat propagation through the asphalt layer, or thermal diffusivity, can then be viewed as the ratio of the heat conducted to the heat stored in asphalt concrete, as shown in Equation 2. A small value of thermal diffusivity means that heat is mostly absorbed by the material and only a small amount of heat is conducted further. Inversely, larger thermal diffusivity values indicate that less heat is being stored by the material, thus heat is propagating faster in the medium.

$$\alpha = \frac{k_{ac}}{\rho \cdot c_p} \quad (2)$$

Where: α = Thermal diffusivity (m^2/s)

k_{ac} = Thermal conductivity of asphalt concrete (W/m·K)

ρ = Density (kg/m^3)

c_p = Specific heat at constant pressure (J/kg·K)

In general, heat transfer within an asphalt layer is transient in nature. Thus temperature can be considered to vary with time and position in the direction perpendicular to the surface. The conservation of energy principle (adopted as the first law of thermodynamics) states that the net change in the total energy of a system during a process is equal to the difference between the total energy entering and the total energy leaving the system (Cengel, 2010). Consequently, the rate of energy transfer in an element of thickness Δz in an asphalt layer is described by the difference between the rates of heat conduction at a depth z and a depth $z + \Delta z$. This change in energy is mainly controlled by the thermal diffusivity of asphalt concrete as an indication of the ability of the material to propagate thermal energy. The one-dimensional heat conduction equation in an asphalt layer for the case of constant conductivity under transient heat conduction with no heat generation reduces to Equations 3 and 4 (Chadbourn, 1998, Vargas-Nordcbeck and Timm, 2011a; Corlew 1968, Cengel, 2010).

$$k_{ac} \cdot \frac{d^2T}{dz^2} = \rho \cdot c_p \cdot \frac{dT}{dt} \tag{3}$$

$$\frac{d^2T}{dz^2} = \frac{1}{\alpha} \cdot \frac{dT}{dt} \tag{4}$$

Where: k_{ac} = Thermal conductivity of asphalt concrete (W/m·K)

T = Temperature (K)

z = Depth (m)

ρ = Density (kg/ m^3)

c_p = Specific heat at constant pressure (J/kg·K)

t = Time (s)

α = Thermal diffusivity (m^2/s)

Thermal conductivity, thermal diffusivity and heat capacity are three main thermal properties required to define transient heat conduction in an asphalt layer. Although, the complexity and variety of paving materials makes it difficult to determine precise thermal properties for asphalt concrete (Carlson et al., 2010), most references recommend precise values for specific heat, heat capacity, thermal conductivity, and thermal diffusivity for asphalt materials. Similarly, numerous testing procedures have been developed to determine these properties in the laboratory. The following sections address each of these thermal properties individually, while briefly summarizing some of the typical values reported in the literature and certain testing procedures used to determine them.

Thermal Conductivity of Asphalt Concrete

The thermal conductivity of asphalt concrete can be defined as the rate of heat transfer through a unit thickness of the material per unit area per unit temperature difference (Cengel, 2010). As mentioned before, it is a measure of the ability of asphalt materials to conduct heat. Higher values of thermal conductivity indicate that the material is a good heat conductor, while an extremely low value would be characteristic of an insulator.

Thermal conductivity has been confirmed to slightly decrease with increasing temperature and to increase with increasing density (Chadbourn et al., 1996), causing considerable complexity in the conduction analysis of asphalt concrete. For this reason,

common practice suggests to determine the thermal conductivity at an average temperature and density, and treat it as a constant in the calculations, resulting in Equations 1 and 3. Although these temperature and density susceptibilities may cause some uncertainty in the analysis, sufficiently accurate results can be obtained by assuming that the thermal conductivity remains constant at some average value (Cengel, 2010).

Asphalt concrete, consisting of a mineral matrix and small amounts of asphalt binder and air (NCAT, 2009; Mamlouk and Zaniewski, 2009), may be considered an inhomogeneous material susceptible to vary within the same mix design (Carlson et al., 2010). Therefore, accurately establishing a common thermal conductivity value for asphalt concrete is complicated as it would depend on the specific composition of each particular asphalt mixture. In effect, the lack of mixture-specific thermal conductivity data has been partly attributed to the complexity and variety of paving materials (Cengel, 2010). The mineral matrix consists of a distribution of aggregate particle sizes which may be mineralogically diverse within a given mixture, and are certainly diverse from one geographic region to another. The asphalt binder is a temperature susceptible viscous hydrocarbon material generally selected depending on the temperature conditions and the traffic loads. Finally, air voids are strictly related to the density of the mixture resulting from roller compaction in the field. Although the mineral aggregates and the asphalt binder are different in nature, they may be considered as one single solid phase for thermal conductivity analysis purposes (Côté, 2013). Therefore, the definition of asphalt concrete can be narrowed down for the analysis of thermal conductivity, as proposed by Côté et al. (2013), identifying it as a two-phase porous material with a solid phase

composed by the aggregates and the asphalt binder and a gas phase between 3% and 10% by volume after compaction.

In general, the thermal conductivity of asphalt concrete can be determined in the laboratory by placing a compacted specimen (either a flat slab or a cylinder) between a heat source and a heat sink with either constant temperature or constant heat flow. While the specimen is allowed to reach thermal equilibrium, thermal conductivity can be calculated from the variation in temperatures taken at several depths in the specimen (Chadbourn et al., 1998).

Highter and Wall (1984) established that the thermal conductivity of asphalt concrete is directly related to the temperature of the mixture. Subsequent research revealed that, in general, thermal conductivity of asphalt concrete decreases with increasing temperature (Chadbourn et al., 1996; Mrawira and Luca, 2002; Côté et al., 2013). However, other properties, such as density and aggregate type, have a more significant effect on the thermal conductivity of asphalt concrete (Tageler and Dempsey, 1973). In fact, thermal conductivity increases with increasing density of the asphalt mixture (Highter and Wall, 1984; Chadbourn, 1996; Côté et al., 2004; Mrawira and Luca, 2002; Luca and Mrawira, 2005; Mrawira and Luca, 2006). In other words, a higher amount air voids affects the mechanism of heat conduction in the asphalt mixture. In the solid phase (i.e. aggregates and asphalt binder) heat conduction is due to the combined effects of two components: the lattice vibrational waves induced by the periodic motion of molecules at relatively fixed positions (also called lattice) and the energy transported via the free flow of electrons between adjacent particles in the medium. However, in the gas phase (i.e. air voids) heat conduction is attributed to the random collisions of

molecules with varying kinetic energies, from the more energetic molecules to the less energetic ones (Cengel, 2010). In that way, the thermal conductivity in the gas phase of an asphalt mixture is lower than that of the solid phase. Therefore, the presence of additional air voids in the layer (i.e. lower density), would reduce the overall thermal conductivity of the asphalt mixture, explaining the results reported in the literature (Highter and Wall, 1984; Chadbourn, 1996; Côté et al., 2004; Luca and Mrawira, 2005; Mrawira and Luca, 2006). Furthermore, a recent study published by Côté et al. (2013), introduces the concept of a variable thermal conductivity as a function of the density of the asphalt concrete, and proposes an equation to predict the thermal conductivity for a known density, with an expected error of no more than 25%.

Specific Heat and Heat Capacity of Asphalt Concrete

The internal energy of asphalt concrete may be viewed as the sum of the kinetic and potential energies of its individual molecules. Due to the particular conditions of asphalt pavements, the potential energy of the inner molecules in the asphalt mixture may be considered to remain constant. The kinetic energy, on the other hand, is known to increase with increasing temperature, resulting in the energy transfer between molecules that leads to the heat conduction phenomenon. For this reason, the portion of internal energy associated with the kinetic energy of the molecules is commonly called sensible heat, as it determines the heat conduction in asphalt materials (Cengel, 2010).

Sensible heat of asphalt concrete fluctuates with the temperature changes in the system. The specific heat is the thermal property that allows defining the susceptibility of a material to potential variations in the surrounding temperature. As mentioned before,

the specific heat of asphalt concrete may be defined as the energy necessary to raise the temperature of a unit mass of a substance by one degree. In that way, specific heat is a direct measure of the ability of asphalt concrete to store thermal energy (Cengel, 2010).

Kersten (1949) determined that the specific heat of dry aggregates increases with temperature. Similarly, as mentioned by Chadbourn et al. (1998), Saal found that the specific heat of asphalt binders also increases with increasing temperatures. In that way, the specific heat of the solid phase in asphalt concrete, described before as the combination of the mineral aggregates and the asphalt binder, may be considered to increase with increasing temperature.

For any material, the product of its density (ρ) and its specific heat (c_p) is called the heat capacity. Both the specific heat and the heat capacity represent the heat storage capability of the material. However, the specific heat expresses it per unit mass, whereas the heat capacity expresses it per unit volume (Cengel, 2010). The heat capacity is the denominator in Equation 2, and may be directly determined if the other two thermal properties (i.e. thermal conductivity and thermal diffusivity) are known.

Specific heat of asphalt concrete may be determined by submerging a specimen at a known, constant temperature in a lower temperature fluid, contained in an insulated vessel. The rise in temperature of the fluid allows calculating the specific heat of the submerged solid (Chadbourn et al., 1998).

Thermal Diffusivity of Asphalt Concrete

Thermal diffusivity, defined as the ratio of the thermal conductivity and the heat capacity, represents the rate of heat diffusion through asphalt concrete. While the thermal conductivity represents how well the material conducts heat, the heat capacity determines how much energy is stored by the material. Therefore, as mentioned before, thermal diffusivity can be viewed as the ratio of heat conducted through the material to the heat stored per unit volume (Cengel, 2010). In general terms, the thermal diffusivity represents the speed at which heat is released by the material to the surrounding mediums. In other words, thermal diffusivity is a measure of the heat propagation speed (Chadbourn et al., 1996).

In most cases, thermal diffusivity may be determined by measuring the temperature at different points in a specimen under constant heat flow, as a function of time. However, most methods for determining the thermal diffusivity require very sophisticated and accurate heating and temperature measurement equipment (Chadbourn et al., 1998).

Determination of Asphalt Concrete Thermal Properties

Literature on the thermal properties of pavement materials is relatively abundant. Although certain computer simulations for one-dimensional heat transfer may be used to backcalculate the most probable thermal conductivity and diffusivity of asphalt concrete (Corlew and Dickson, 1968; Jordan and Thomas, 1976), direct measurements under fully controlled conditions were found to be necessary to obtain reliable experimental values (Côté et al., 2013). Several testing procedures have been used in the past to

experimentally determine typical values of thermal conductivity, thermal diffusivity and heat capacity for asphalt concrete, while studying the effect of the varying characteristics of asphalt mixtures.

As stated by Chadbourn et al. (1998), most testing procedures attempt to approximate one-dimensional constant conductive heat flux in laboratory compacted specimens. In a slab specimen, this is achieved by insulating its sides or by using a sufficiently small thickness-to-length ratio. Similarly, in the case of a cylindrical specimen this can be achieved by using a line heat source located along the central axis of a specimen with a small diameter-to-length ratio. In general, laboratory testing methods may be categorized in two main groups, those based on steady heat transfer, and those that consider transient heat conduction in the analysis. Although, the majority of commonly used test methods would be included in the first group, the procedures tend to be time consuming, which has led to the development of faster tests under transient heat conditions.

Methods Based on Steady-State Heat Conduction. The American Society for Testing and Materials (ASTM) standard C177 – *Standard Test Method for Steady-State Heat Flux Measurements and Thermal Transmission Properties by Means of the Guarded Hot Plate Apparatus* – establishes the criteria for the laboratory measurement of the steady-state heat flux through a flat specimen using a thermal conductivity instrument. This test allows determining the thermal conductivity by applying a known temperature through an asphalt concrete slab of known dimensions. Once steady state heat transfer is reached, the temperatures of the sample faces are measured, which allows determining the thermal

conductivity as the ratio of the generated heat flux (Q) over the variations in temperature (ΔT) multiplied by the variations in thickness (ΔX) (Wolfe, 1983). However, as mentioned by Carlson et al. (2010), this test is not recommended for highly inhomogeneous materials, such as asphalt concrete.

ASTM standard C518 – *Standard Test Method for Steady-State Thermal Transmission Properties by Means of the Heat Flow Meter Apparatus* – provides a rapid means of determining the steady-state thermal transmission properties of thermal insulations and other materials. In this test, a slab specimen is subjected to a constant heat flux by maintaining the two opposite surfaces at constant temperature differences. The thermal conductivity is then determined by directly measuring the thermal gradient between the two surfaces of the specimen. However, this method requires inconveniently long testing times to reach thermal equilibrium (Tan et al., 1997). Furthermore, the heat flow meter apparatus requires frequent calibration using ASTM C177, affecting testing variability.

ASTM standard C1114 – *Standard Test Method for Steady-State Transmission Properties by Means of the Thin Heater Apparatus* – can be used to determine the steady-state thermal transmission properties of flat-slab specimens of thermal insulation materials with uniform density having low lateral heat flow. According to the standard, the use of a thin heater apparatus can reduce lateral heat flow and avoid the need for active-edge guarding. However, the test method doesn't describe a particular apparatus, but a procedure for qualifying one that meets the concept of a thin heater. Furthermore, although Mrawira and Luca (2002) mentioned this standard as a possible procedure for

estimating the thermal properties of asphalt pavement materials, no indication of its use was found in the literature.

ASTM Specification C 1045 – Standard Practice for Calculating Thermal Transmission Properties under Steady State Conditions – provides a uniform procedure to calculate the apparent thermal conductivity as a function of the temperature relationship. Thermal transmission properties are calculated from the temperature difference generated under the steady-state, one-dimensional tests previously mentioned.

Côté and Konrad (2005) proposed a thermal conductivity testing method based on steady state heat flow, in which a cylindrical specimen of 100mm in diameter and 75 mm in height is placed between two heat exchangers connected to an independent, insulated temperature controlled bath. A heat transfer cell, insulated with 100 mm thick insulating shields, in used and heat fluxes are measured at both ends of the specimen using thermoelectric heat flux meters that also include 5 independent thermocouples for simultaneous temperature measurements at different locations on both flat ends of the specimen.

Methods Based on Transient Heat Conduction. ASTM standard D5334 – *Standard Test Method for Determination of Thermal Conductivity of Soil and Soft Rock by Thermal Needle Probe Procedure* – allows measuring the thermal conductivity of a cylindrical specimen under transient heat transfer. A heating probe and a thermocouple are inserted into a laboratory compacted cylindrical specimen. While a constant current is applied to the heating probe, the temperature change over time is measured, which allows determining the thermal conductivity of the asphalt mixture. Although this test procedure

is specified for soils and soft rocks, it has been successfully used to measure the thermal conductivity of asphalt concrete (Chadbourn, 1998).

Kavianipour and Beck (1977) developed a method to measure the thermal properties of semi-infinite, homogeneous bodies subject to in-situ, transient heating conditions. This method, based on Laplace transform, allows determining the thermal diffusivity when only temperatures are measured. Furthermore, the thermal conductivity and the specific heat may be determined if the surface heat flux is known.

Fwa et al. (1995) proposed an effective method to estimate the thermal conductivity and thermal diffusivity of asphalt concrete slab specimens under transient heat conduction. Although two test setups and two analysis schemes were investigated, the recommended procedure is based on a horizontal slab specimen with the top surface cooled by air flowing at a constant velocity. The thermal properties are determined by analyzing the temperature change at the center of a slab specimen. In this way, a constant convection coefficient may be used to calculate the thermal conductivity and thermal diffusivity of the slab.

In developing a pavement cooling prediction model, Chadbourn et al. (1998) designed a test to determine the thermal diffusivity of asphalt concrete slab specimens and modified the thermal probe method presented in ASTM D5334 to measure the thermal conductivity of laboratory compacted cylindrical specimens. The “slab cooling method for thermal diffusivity of asphalt concrete” proposed by the authors, uses thermocouples embedded in an asphalt concrete slab in a specific configuration, with the top face exposed to ambient temperatures and all other surfaces insulated. Temperature readings taken at different depths in the slab, for regular time steps in small time

intervals, allow directly determining the thermal diffusivity from a first-order time-temperature relationship and a second-order space-temperature relationship. The "thermal probe method for thermal conductivity of asphalt concrete", on the other hand, suggests the use of high-conductivity cement, workable enough to draw a stainless steel tube (with a diameter of 1.6 mm and a length of 50 mm) containing the thermal probe. The procedures instructed by the ASTM standard are maintained in order to calculate the thermal conductivity of the specimen.

Tan et al. (1997) proposed a laboratory procedure to determine the thermal conductivity and thermal diffusivity of asphalt concrete based on transient heat conduction on a flat slab specimen. The suggested method, which is similar to the method proposed by Fwa et al. (1995), uses a high-precision temperature chamber to control stability and uniformity on the top surface of the specimen while all other faces are insulated using polystyrene. A horizontal airflow, parallel to the surface of the specimen, is applied while the temperature is increased from 25°C to 60°C in approximately 30 seconds. Using the plane wall theory, the authors propose a data reduction method to calculate thermal conductivity and the thermal diffusivity of asphalt concrete.

Mrawira and Luca (2002) developed a relatively simple device that employs a flat plate with heaters as a heat emitter and two other identical plates as heat receivers to measure the thermal diffusivity of asphalt concrete. The proposed testing apparatus is used with two slab specimens placed between the heat emitter and the receivers, insulating all the free edges of the slabs. Four pairs of thermocouples allow measuring and monitoring temperature variations through the specimen. The one-dimensional heat

flow in the proposed setup was validated by performing a two-dimensional finite element (FE) analysis and its applicability was verified by conducting tests in the laboratory.

Typical Values Found in the Literature

Since the late 1940's a vast number of attempts to measure the thermal diffusivity and thermal conductivity of asphalt concrete have been performed. Kersten (1949) conducted a study to investigate the thermal properties of a variety of soils, and an asphalt-gravel paving mixture with cutback asphalt molded at one single density and tested in dry conditions. The results showed a slight increase of the thermal conductivity with increasing temperature, ranging from 1.48 W/m·K at -19.6°F to 1.50 W/m·K at 40.1°F. However, no statistical difference between these values was found and a mean value of 1.49 W/m·K was reported.

In developing a numerical solution for calculating the time-and-space dependent temperature distribution in hot-mix asphalt concrete during compaction, Corlew and Dickson (1968) suggested using a thermal conductivity of 1.21 W/m·K. Jordan and Thomas (1976) developed a similar model and suggested using thermal conductivity values ranging between 0.80 W/m·K and 1.06 W/m·K for the analysis. This model was validated by comparing the cooling curves predicted by the computer software with field measurements of experimental test sections, finding a good agreement between the two.

Kavianipour and Beck (1977) measured the thermal properties of two full depth asphalt pavements in Michigan. It was found that the thermal conductivity and the thermal diffusivity decreased with increasing pavement temperature, with results ranging from 2.88 W/m·K at 0°F to 2.28 W/m·K at 100°F for the thermal conductivity and

between 1.44×10^{-6} m^2/s at 0°F and 1.15×10^{-6} m^2/s at 100°F. Similarly, the heat capacity was found to decrease with increasing temperature, ranging from 2.00×10^{6} $J/m^3\cdot K$ at 0°F to 1.97×10^{6} $J/m^3\cdot K$ at 100°F. Additionally, Kavianipour and Beck (1977) conducted a thorough literature review revealing a relatively good agreement of the results obtained in the literature for heat capacity. Nonetheless, considerable variation was found in the results reported for thermal conductivity and thermal diffusivity.

A book published by Turner and Malloy (1981), addressing the design of insulation systems to correctly provide for expansion and contraction of piping and equipment, suggested an asphalt concrete thermal conductivity of 0.76 W/m·K to calculate the heat transfer in underground applications.

Fwa et al. (1995) determined the thermal properties of two dense graded mixtures with similar volumetric composition but different gradations. The reported thermal conductivities ranged between 1.41 W/m·K, for the finer mixture and 1.80 W/m·K for the coarser mixture. A similar trend was observed for the thermal diffusivity, ranging between 5.83×10^{-7} m^2/s and 6.96×10^{-7} m^2/s for the fine and coarse graded mixtures, respectively.

Chadbourn et al. (1996) determined thermal conductivity values from direct thermal diffusivity measurements for two asphalt mixtures with different gradations (dense graded asphalt and SMA) and a 120/150 penetration asphalt, compacted at different densities. The obtained results showed that the thermal diffusivity decreased as temperature increased for both mixtures, with values ranging from 1.1×10^{-6} m^2/s to 1.3×10^{-6} m^2/s at 70° to 0.5×10^{-6} m^2/s to 0.7×10^{-6} m^2/s at 140°C. Thermal conductivity values for the SMA mixture ranged from 0.6 W/m·K to 1.5 W/m·K, while the dense-

graded mixture had values ranging between 2.0 W/m·K and 2.5 W/m·K. Although the thermal conductivity of the SMA mixture was found to be statistically lower than that of the dense graded mixture, in both cases the thermal conductivity was found to increase with increasing density. However, the SMA mixture presented a much steeper slope.

Tan et al. (1997) determined the thermal properties of two typical asphalt mixtures, one containing coarse aggregates and the other one containing finer aggregates. The reported thermal conductivities ranged from 1.32 W/m·K to 1.37 W/m·K for the fine mixture, while the coarse mixture had values raging between 1.33 W/m·K and 1.49 W/m·K. Nonetheless, the coarse mixture had a slightly higher density than the fine mixture, suggesting that the variations in thermal conductivity may be due to either the gradation or the density of the mixtures. Furthermore, the thermal diffusivity values reported ranged from 5.22×10^{-7} m^2/s to 5.50×10^{-7} m^2/s for the fine mixture, and between 5.47×10^{-7} m^2/s and 6.09×10^{-7} m^2/s for the coarser mixture. The heat capacity values were calculated using Equation 2.

Mrawira and Luca (2002) measured the thermal properties of two asphalt mixtures with different densities and measured air voids of 2.5% and 8%, under different moisture conditions. The obtained thermal conductivity ranged from 1.71 W/m·K to 2.2 W/m·K in saturated conditions and between 1.72 W/m·K and 1.81 W/m·K in dry conditions, revealing that higher air voids and increased moisture contents affect the thermal conductivity of asphalt concrete. Thermal diffusivity values, on the other hand, ranged from 5.2×10^{-7} m^2/s to 7.2×10^{-7} m^2/s for specimens with 2.5% air voids and from 4×10^{-7} m^2/s to 12×10^{-7} m^2/s for specimens with 8% air voids.

Luca and Mrawira (2005) measured the thermal properties of a dense-graded, 12.5-mm nominal maximum aggregate size (NMAS) asphalt mixture, with 6% PG58-34 asphalt binder, compacted to 67, 99, 133, and 212 gyrations using the superpave gyratory compactor. The obtained results didn't show a specific trend between the thermal properties and the density of the specimens. Nonetheless, thermal conductivity values, ranging from 1.45 W/m·K to 1.81 W/m·K, were found to be more consistent than previous studies, with a coefficient of variation of 6.6%. The obtained thermal diffusivity values ranged from 4.42×10^{-7} m^2/s to 6.39×10^{-7} m^2/s, with a higher coefficient of variation of 11.0%.

More recent studies focused on investigating the effects of mix design factors on the thermal properties of asphalt concrete. Mrawira and Luca (2006) used two different aggregates, three gradations and four compaction levels to examine the effect of these properties on the thermal behavior of asphalt concrete. Contrary to most previous findings, the authors established that the amount of air voids (i.e. density) does not have consistent effects on the thermal properties of dense-graded asphalt mixtures. Although the thermal conductivity decreased with increasing air voids for crushed-gravel aggregates (from 1.70 W/m·K to 2.11 W/m·K), this was not the case for what they called hornfels aggregates, for which thermal conductivity ranged between 1.56 W/m·K and 1.94 W/m·K without a specific trend. Similarly, the thermal diffusivity values reported didn't show a specific trend for any of the mixtures tested, ranging from 3.9×10^{-7} m^2/s to 6.1×10^{-7} m^2/s for the crushed gravel and between 3.8×10^{-7} m^2/s and 6.0×10^{-7} m^2/s for hornfels aggregates.

Côté et al. (2013) conducted a study to measure the thermal conductivity of two different asphalt mixtures with two different aggregates, crushed basalt and crushed chlorite schist, and a PG58-34 asphalt binder. The authors found that thermal conductivity decreased with increasing air voids, from 1.49 W/m·K to 1.19 W/m·K. However, the mixtures containing chlorite schist presented a thermal conductivity 15% higher than the mixtures containing crushed basalt aggregates, leading to the conclusion that the aggregate type influences the thermal conductivity as a function of its own thermal conductivity.

A review of available literature revealed a wide range of thermal conductivity values for asphalt concrete, varying from 0.6 W/m·K (Chadbourn et al., 1996) to 2.88 W/m·K (Kavianipour, 1977). Similarly, thermal diffusivity values ranged between 3.50×10^{-7} m^2/s (Highter and Wall, 1984) and 14.40×10^{-7} m^2/s (Kavianipour and Beck, 1977). Table 2.1 summarizes the thermal properties found in the literature.

TABLE 2.1 Typical Values Found in the Literature for Asphalt Concrete

Source	Thermal Conductivity k_{ac} (W/m·K)	Heat Capacity $\rho c_p \times 10^6$ (J/m^3·K)	Thermal Diffusivity $\alpha \times 10^{-7}$ (m^2/s)
Kersten (1949)	1.49	Not Investigated	Not Investigated
Aldrich [a]	1.5	Not Investigated	Not Investigated
Saul [a]	2.23	Not Investigated	Not Investigated
O'Blenis [a,b]	0.85 – 2.32	Not Investigated	4.61 – 11.98
Barber [b]	1.22	2.08	5.86
Corlew and Dickson (1968)	1.21	2.05	5.86
Jordan and Thomas (1976)	0.80 – 1.06	2.00 – 2.16	3.70 – 5.30
Kavianipour and Beck (1977)	2.28 – 2.88	2.00 – 1.97	11.50 – 14.40
Wolfe et al. [d]	1.00 – 1.75	1.98 – 2.35	5.16 – 8.26
Kirk [c]	0.9 – 1.9	Not Investigated	Not Investigated
Turner and Malloy (1981)	0.76	Not Investigated	Not Investigated
Phukan [d]	1.05 – 1.520	Not Investigated	Not Investigated
Highter and Wall (1984)	0.80 – 1.60	Not Investigated	3.50 – 7.50
Himeno [d]	Not Investigated	Not Investigated	6.00 – 11.00
Solaimanian and Kennedy [b]	1.46	Not Investigated	Not Investigated
Solaimanian and Bolzan [d]	0.74 – 2.88	Not Investigated	Not Investigated
Fwa et al. (1995)	1.41 – 1.80	2.42 – 2.59	5.83 – 6.96
Chadbourn et al. (1996)	0.6 – 2.5	1.20 – 1.90	5.00 – 13.00
Tan et al. (1997)	1.32 – 1.49	Not Investigated	5.22 – 6.09
Mrawira and Luca (2002)	1.71 – 2.20	1.42 – 1.83	4.00 – 12.00
Côté et al. (2004)	0.6 – 1.2	Not Investigated	Not Investigated
Luca and Mrawira (2005)	1.45 – 1.81	2.69 – 3.29	4.42 – 6.39
Mrawira and Luca (2006)	1.38 – 2.11	2.31 – 4.80	3.80 – 6.10
Mieczkowski (2007)	0.698	2.366	2.950
Côté et al. (2013)	1.19 – 1.49	Not Investigated	Not Investigated

[a] Reported by Kavianipour (1967)
[b] Reported by Fwa et al. (1995)
[c] Reported by Côté et al. (2013)
[d] Reported by Luca and Mrawira (2005)

2.2.2 Convection Heat Transfer

Convection is the mode of heat transfer between a solid surface and an adjacent fluid (liquid or gas), which is in motion relative to the solid (Chadbourn et al., 1998; Cengel, 2010). In other words, convection heat transfer involves the combined effect of the bulk fluid motion, known as advection, and the conduction due to random motion of the molecules in the fluid (Bergman et al., 2011). Faster fluid motion causes greater convection heat transfer, but in the absence of any bulk fluid motion, heat transfer between the solid surface and the fluid occurs by pure conduction between the two mediums (Cengel, 2010).

As mentioned before, in the case of asphalt concrete, convective heat transfer occurs between the asphalt concrete surface and the surrounding air. Heat is first transferred by conduction from the more energetic particles in the pavement to the air molecules adjacent to the surface of the pavement. The random motion of the air molecules and the bulk motion of the air remove the heated air near the surface, replacing it with cooler air. If wind is present, the heated air adjacent to the pavement surface is forced away from the surface of the pavement and is replaced by cooler air, giving way to a phenomenon called forced convection. In contrast, in the absence of wind, variations in the density of the air molecules adjacent to the surface, caused by temperature differences, induce buoyancy forces that transport the heated air away from pavement and replace it with cooler air. This phenomenon is called natural or free convection.

Convection heat transfer is very difficult to model due the complex fluid motion of air. However, the rate of convection heat transfer is proportional to the temperature differential between the ambient air and the surface of the asphalt layer (Chadbourn et al.,

1998), which is conveniently expressed by Newton's law of cooling presented in Equation 5. The proportionality constant is called the convection heat transfer coefficient (h), an experimentally determined parameter whose values depend on all the variables influencing convection such as the surface geometry, the nature of fluid motion, the properties of the fluid, and the bulk velocity of the fluid.

$$q_{conv} = h \times (T_a - T_s) \quad (5)$$

Where: q_{conv} = Convection heat flux in the vertical direction (W/m^2)

h = Convection heat transfer coefficient ($W/m^2 \cdot K$)

T_a = Meant air temperature (K)

T_s = Temperature of the pavement surface (K)

As stated by Cengel and Ghajar (2010), experience shows that the fluid properties affecting convection heat transfer include its dynamic viscosity, thermal conductivity, density, and specific heat. Furthermore, experimental observations indicate that air in motion comes to a complete stop at the pavement surface interface, causing the velocity at that point to be insignificant. This phenomenon, known as the no-slip condition (Bergman et al., 2011), is responsible for the development of a specific velocity profile in which the air velocity is zero at the surface of the pavement and increases exponentially with increasing distance. The existence of this no-slip condition at the boundary between the pavement and the air implies that that heat transfer from the solid surface to the adjacent fluid layer occurs by pure conduction and may be expressed by Fourier's law, as described in Equation 6.

$$q_{conv} = q_{cond} = -k_{air} \cdot \frac{dT}{dz} \quad (6)$$

Where: q_{conv} = Convection heat flux in the vertical direction (W/m^2)

q_{cond} = Conduction heat flux in the vertical direction (W/m^2)

k_{air} = Thermal conductivity of air (W/m·K)

$\frac{dT}{dz}$ = Temperature gradient (change in temperature/change in height)

Equations 5 and 6 can be equated as they both define the heat transfer at the boundary between the asphalt pavement and the surrounding air. The convection heat transfer coefficient can then be found as shown in Equation 7.

$$h = \frac{-k_{air} \cdot (dT/dz)}{T_a - T_s} \quad (7)$$

Where: h = Convection heat transfer coefficient ($W/m^2 \cdot K$)

k_{air} = Thermal conductivity of air (W/m·K)

T_a = Mean air temperature (K)

T_s = Temperature of the pavement surface (K)

dT/dz = Temperature gradient (change in temperature/change in height)

Determination of the Convection Heat Transfer Coefficient

Numerous procedures involving theoretical and/or empirical relationships for determining the convection heat transfer coefficient may be found in the literature. In general these procedures are based on obtaining the convective heat transfer coefficient from the Nusselt number, which in turn is based on two other properties, known as the Reynolds number and the Prandtl number (Corlew and Dickson, 1968).

Since heat transfer through any fluid layer (i.e. surrounding air) occurs by the combined effect of conduction and convection, it is common practice to use the Nusselt number, as defined in Equation 8, to describe heat transfer in the fluid layer. The Nusselt number represents the enhancement of heat transfer through a fluid layer as a result of convection relative to conduction across the same fluid layer (Cengel, 2010).

$$Nu = \frac{q_{conv}}{q_{cond}} = \frac{h \times (\Delta T)}{k_{air} \cdot (\Delta T/L)} = \frac{h \cdot L}{k_{air}} \quad (8)$$

Where: Nu = Nusselt number (dimensionless)

q_{conv} = Convection heat flux in the vertical direction (W/m^2)

q_{cond} = Conduction heat flux in the vertical direction (W/m^2)

h = Convection heat transfer coefficient ($W/m^2 \cdot K$)

ΔT = Change in temperature (K)

L = Length of the fluid (m)

k_{air} = Thermal conductivity of air ($W/m \cdot K$)

The Nusselt number can be expressed as a function of Reynolds and Prandtl numbers alone (Cengel, 2010). The Reynolds number results from the dynamic analysis of air flow. As the flow of any fluid, air can flow under two different regimes, known as laminar and turbulent flow. Laminar flow, characterized by smooth streamlines and highly-ordered, constant motion, is mainly controlled by viscous forces. Turbulent flow, on the other hand, is dominated by inertial forces, producing vortices and highly-disordered motion under velocity fluctuations. Generally, air flow over a pavement surface initiates as laminar and gradually becomes turbulent as it remains in constant contact with the surface. In fact, the transition from laminar to turbulent flow depends highly on the geometry and roughness of the pavement surface (Cengel, 2010).

The Prandtl number is a dimensionless parameter that describes the relative thickness of the flow region over the surface of the pavement in which the temperature variation in the direction normal to the surface is significant, known as the thermal boundary layer. Defined as the ratio of momentum diffusivity, or kinematic viscosity, to thermal diffusivity, the Prandtl number specifies the correlation between the viscous diffusion rate and the thermal diffusion rate, depending only on the type and state of the fluid. In that way, Prandtl numbers higher than one indicate that thermal diffusivity dominates the convection heat transfer, while Prandtl numbers lower than one indicate that momentum diffusivity is dominant.

Corlew and Dickson (1968) used a set of charts, developed by Irving and Hartnett, to obtain the Nusselt number as a function of the Reynolds number. The convection heat transfer coefficient was directly obtained from the Nusselt number. According to the authors, the use of these charts accounted for the transition from laminar

to turbulent flows at a lower Reynolds number in presence of increased free-stream turbulence expected for the rough surface of asphalt concrete.

An alternative method allows determining the convection coefficient as a function of the wind velocity. Originally proposed for black body surfaces by Alford et al., the model was found to provide sufficiently accurate results for asphalt pavements by Chadbourn et al. (1998). This simple equation was used in developing a pavement cooling model presented later in this document and is presented as Equation 9.

$$h = r_{BB} + (h_0 - r_{BB}) \times \left(\frac{v}{v_0}\right)^{0.75} \quad (9)$$

Where: h = Convection heat transfer coefficient for wind velocity, v ($W/m^2 \cdot K$)

r_{BB} = Black body radiation coefficient (7.4 $W/m \cdot K$)

h_0 = Convection coefficient for v_0 (34 $W/m^2 \cdot K$)

v = Wind velocity (m/s)

v_0 = Reference wind velocity (6.7 m/s)

Hermansson (2001) proposed an empirical model, shown in Equation 10, to calculate the heat convection coefficient that considers the combined effect of the wind velocity, the pavement surface temperature and the ambient temperature. The model was later validated by Mrawira and Luca (2002), who proposed to use it in combination with an equation developed under the Strategic Highway Research Program (SHRP) that allows estimating the pavement surface temperature.

$$h = 698.24 \times \left[0.00144 \times \left(\frac{T_s + T_a}{2}\right)^{0.3} \times v^{0.7} + 0.00097 \times (T_s - T_a)^{0.3}\right] \quad (10)$$

Where: h = Convection heat transfer coefficient for wind velocity, v ($W/m^2 \cdot K$)

T_s = Temperature of the pavement surface (K)

T_a = Meant air temperature (K)

v = Wind velocity (m/s)

2.2.3 Radiation Heat Transfer

Radiation is the energy emitted by matter in the form of electromagnetic waves or photons as a result of the changes in the electronic configurations of the atoms or molecules (Cengel, 2010). In that way, radiation heat transfer does not require the presence of an intervening medium, occurs at the speed of light, and suffers no attenuation in a vacuum. These conditions allow a fraction of the thermal energy generated by the sun to be transferred to the pavement surface.

In the same way as the convection phenomenon, the radiation process is very complex as it involves heat originating from the sun and the surrounding environment and penetrating into a certain depth below the surface of the pavement (Chadbourn et al., 1998). In fact, radiation is a volumetric phenomenon by which all solids and fluids emit, absorb, or transmit radiation to varying degrees. However, in the case of an asphalt pavement exposed to thermal radiation, the exchange of energy may be assumed to only occur at the surface of the pavement. In effect, the radiation emitted by the interior regions of the pavement can never reach the surface, while the radiation incident on the pavement is absorbed within a few microns from the surface (Cengel, 2010).

The maximum rate of radiation heat absorbed or emitted by a specific body (i.e. asphalt pavement, surrounding environment) is given by the Stefan-Boltzmann law, which states that the transferred energy is directly proportional to the fourth power of the absolute temperature of the body. The proportionality constant is known as the Stefan-Boltzmann constant in honor to Jozef Stefan and Ludwig Boltzmann who derived it in 1879, specifically to describe blackbody radiation. A blackbody is an idealized surface which absorbs or emits the maximum possible amount of radiation at a specified temperature without reflecting or transmitting any energy. In reality, no surface is capable of absorbing or emitting radiation perfectly, so certain factors are needed to account for the energy absorbed and redirected by the surface. The fraction of the radiation energy absorbed by the pavement is known as absorptivity or absorptance. Similarly, the fraction of the energy redirected is called emissivity or emittance. These two factors have values ranging between 0 and 1, where a value of one would represent a blackbody, considered a perfect absorber and emitter.

Multiple theories have been proposed to describe the interactions of the radiation at the pavement's surface (Hermansson, 2001). The majority of these models have been developed in an effort to describe the temperature cycling of the pavement as a function of daily temperature. However, two methods stand out for their simplicity and applicability, and they are described in the following sections.

Effect of from the Surrounding Environment and Solar Radiation

This method, originally suggested by Chadbourn et al. (1998), considers the combined effect of radiation heat transfer from the surrounding environment and the solar radiation on the surface of the pavement.

Surrounding Environment. The pavement surface is surrounded by air, which may be considered as a much larger surface. Therefore, radiation heat transfer between these two surfaces is proportional to the difference between the fourth power of the pavement temperature and the fourth power of the surrounding air temperature. The proportionality in this case is defined by the Stefan-Boltzmann constant and the emissivity of the pavement surface, whereas the emissivity and the surface area of the surrounding surface do not have any effect on the net radiation heat transfer (Cengel, 2010). The heat flux due to radiation heat transfer attribute to the surrounding environment is expressed as Equation 11.

$$q_{rad1} = \varepsilon \times \sigma \times (T_s^4 - T_a^4) \quad (11)$$

Where: q_{rad1} = Radiation heat flux from surrounding environment (W/m^2)

ε = Pavement emissivity or emittance (dimensionless)

σ = Stefan-Boltzmann constant (5.669×10^{-8} $W/m^2 \cdot K^4$)

T_s = Temperature of the pavement surface (K)

T_a = Meant air temperature (K)

Solar Radiation. As mentioned before, a fraction of the thermal energy emitted by the sun is transmitted to the pavement by radiation. Chadbourn et al. (1998) proposed a method to calculate the hourly net solar heat flux on a pavement surface as a function of its geographic location (i.e. latitude), the time (i.e. day, hour) and the estimated cloud coverage. The energy absorbed by the pavement may then be calculated as a function of its absorptivity according to Equation 12.

$$q_{rad2} = \alpha \times H_s \quad (12)$$

Where: q_{rad2} = Solar heat flux (W/m^2)

α = Pavement absorptivity or absorptance (dimensionless)

H_s = Net solar flux calculated after Chadbourn et al. (1998)

Radiation Balance

This method, originally proposed by Solaimanian and Kennedy (1998), was used as part of the Superpave methodology to determine the surface temperature of the pavement. Hermansson (2001) questioned the validity of this model, stating that the original model tended to overestimate the maximum temperature, and suggested a new method based on the same radiation balance concept. The procedure considers the combined effect of short-wave and long-wave radiation on the pavement surface.

Outgoing Long-Wave Radiation. The earth's surface is assumed to behave as a black body and emit long-wave radiation following the Stefan-Boltzmann law, as shown in equation 13.

$$q_{olw} = \varepsilon \times \sigma \times T_s^4 \quad (13)$$

Where: q_{olw} = Radiation heat flux due to outgoing long-wave radiation (W/m^2)

ε = Pavement emissivity or emittance (dimensionless)

σ = Stefan-Boltzmann constant (5.669×10^{-8} $W/m^2 \cdot K^4$)

T_s = Temperature of the pavement surface (K)

Long-Wave Counter-Radiation. The radiation absorbed by the pavement and emitted back to the surrounding environment is known as counter-radiation (Hermansson, 2001). The effect of this counter-radiation is described as a function of the pavement absorptivity according to Equation 14.

$$q_{acr} = \alpha \times \sigma \times T_a^4 \quad (14)$$

Where: q_{acr} = Absorbed counter-radiation heat flux (W/m^2)

α = Pavement absorptivity or absorptance (dimensionless)

σ = Stefan-Boltzmann constant (5.669×10^{-8} $W/m^2 \cdot K^4$)

T_a = Meant air temperature (K)

Short-Wave Radiation. The surface of the sun has a very high temperature, approximately 6000°K, and it therefore emits high-frequency, short-wave radiation (Hermansson, 2001). A fraction of this radiation is scattered in the atmosphere, and the fraction of this diffused radiation that reaches the pavement is called diffuse incident radiation. On the other hand, the solar radiation that reaches the surface of the pavement

directly, without being scattered through the atmosphere is called direct short-wave radiation. The total radiation to which the pavement is exposed varies with the weather, location and time. Furthermore, Hermansson (2000), proposed a simplified way of calculating the incident shortwave radiation absorbed by the pavement surface as function of the measured albedo, defined as the ratio of reflected radiation from the surface to incident radiation upon it.

Determination of Pavement Emissivity and Absorptivity

The two methods described previously require the use of two pavement properties, emissivity and absorptivity. Numerous sources in the literature provide relatively consistent values for these properties. Cengel (2010) specified that, in general, the emissivity of an asphalt pavement ranges between 0.85 and 0.93. Similarly, Corlew and Dickson (1968) used a value of 0.95 for the thermal emissivity, which was later validated by Chadbourn et al. (1998). Hermansson (2001) used a curve-fitting method to estimate pavement surface emissivity from different test sections included in the Long Term Pavement Performance Program (LTPP). The proposed emissivity values ranged between 0.75 and 0.85, depending on the location of the pavement.

Corlew and Dickson (1968) reported an absorptivity of 0.85 for asphalt concrete. Solaimanian and Kennedy (1993) established a value of 0.7 for pavement absorptivity, based on field measurements. Similarly, Hermansson (2000) defined absorptivity as one minus the pavement albedo, reporting values between 0.75 and 0.90.

2.3 PAVEMENT COOLING DURING CONSTRUCTION

High quality, smooth asphalt pavement surfaces are the result of many key factors, including proper materials selection, mixture design, production, placement and compaction. Ultimately, the prolonged existence and performance of the pavement relies on well managed construction processes that adapt to ever-changing field conditions. However, once paving operations have begun, adequate control of the mixture temperature during compaction is the most important factor in achieving proper densification of asphalt concrete (Chadbourn et al., 1998; Timm et al., 2001; Vargas-Nordcbeck and Timm, 2011a). Furthermore, deficient monitoring of rolling operations may result in densities below the specified thresholds, which detrimentally affects the long-term performance of the pavement. Significant decreases in the fatigue life and strength, and increased moisture-related damage and permanent deformation may result from deficient densification of the AC layer (Chang et al., 2009).

During construction, as the compaction process is underway, asphalt concrete loses temperature by the heat transfer mechanisms described in the previous section. The cooling rate is then determined by the specific thermal properties of asphalt concrete, such as thermal conductivity, thermal diffusivity and heat capacity, and by certain external factors such as the underlying material, the ambient temperature, the velocity of the wind, and the solar radiation. All these factors combined determine the time available for compaction, which in turn controls all construction activities in a paving project. Furthermore, multiple efforts have been made over the years to accurately determine the time available for compaction for a specific asphalt mixture in the field and substantial research has been developed to assist contractors during this delicate stage.

In order to understand how the heat transfer mechanisms apply to the pavement cooling during construction, it is necessary to address the theory behind the compaction process. The following sections address the mechanics of asphalt concrete compaction and summarize multiple methods and models used in the literature to estimate its cooling rate as function of the conditions in the field.

2.3.1 Compaction of Asphalt Concrete Pavements

Asphalt concrete compaction may be defined as the process of compressing a given volume of asphalt concrete into a smaller volume (Asphalt Institute, 2007). In this process, the aggregate particles a rearrange and air is expelled from the mixture (Huerne, 2004). In that way, the mix under compaction changes from a loose, plastic, non-cohesive state into a coherent mass possessing a high degree of tensile strength (Kari, 1967). The principal goal of asphalt concrete pavement compaction is to achieve an optimum air void content, which provides a smooth riding surface and increases the bearing capacity of the material (Bijleveld, 2012). In fact, asphalt paving technologists around the world agree that the density of a well-designed asphalt mixture is the most prominent measurement for road quality (Varsenev, 2012).

The construction of an asphalt concrete pavement starts at the asphalt plant, where heated aggregates are combined with a liquid asphalt binder and possible additives and/or fibers, at temperatures in the range of 120°C and 150°C (Chadbourn et al., 1998). The mixture may be stored in a silo or surge bin until it is transported by trucks to the construction site. In the field, asphalt concrete may be deposited directly into the paver or a material transfer vehicle (MTV) or placed in a windrow to be picked up and moved

through a paver. Subsequently, the paver spreads the mixture in a specified thickness, while providing a modest amount of initial compaction. Definitive compaction is applied by a series of steel-wheel and pneumatic rollers until proper density is achieved before the material cools down, impeding the plastic flow of pavement layer. While the mixture design and control is properly specified and abundantly addressed in the literature, the paving process depends heavily on the experience of the paving crew (Bijleveld et al., 2012). Asphalt compaction usually begins as soon as the mix can support the roller weight and the roller operator is responsible for empirically determining the best time to start compacting based on experience ad trial an error for the specific site conditions and mixture characteristics.

Four basic types of self-propelled compactors are typically used to achieve satisfactory density of asphalt mixtures; static steel wheel rollers, pneumatic tire rollers, vibratory rollers, and combination rollers (NAPA, 2002). The National Asphalt Pavement Association (NAPA) provides a comprehensive guide on the selection and all possible applications of each one of these rollers. Common practice separates the rolling operations in three different phases. The first stage, known as breakdown compaction, should produce the majority of the target density in the asphalt layer, beginning at the highest possible mixture temperature without distorting the mat. Intermediate compaction, which occurs immediately after the breakdown phase, is the final step in reaching target density and the initial step in smoothing the surface. The last rolling stage, known as finish rolling, is intended to improve the surface smoothness by removing the drum marks or tire marks from pneumatic-tire rollers while the mat is still warm.

When laid asphalt concrete is loaded with a heavy roller, the material is pushed away from the drum or the pneumatic tires causing minor deformations, mostly prevented by counter pressure and internal cohesion of the mixture (Bijleveld et al., 2012). Compaction of an asphalt mixture may then be considered to behave somewhere between a cohesive and non-cohesive soil (Chadbourn et al., 1998). Initially, compaction is achieved through distortion and reorientation of the aggregate particles as the asphalt binder keeps them together, much like a cohesive soil. During this stage the binder viscosity needs to be great enough to resist the compactive effort of the rollers, but sufficiently low so that when the loads are applied air can be expelled from the mixture. After a certain point, as the binder viscosity increases, reorientation of the aggregate particles is resisted by friction forces at the contact points between the aggregate faces, behaving like a non-cohesive soil. At this stage, the air present in the mixture is trapped within the asphalt layer and the gain in density and stiffness are negligible with further compaction. If compaction is still needed to reach the proper density, very high forces may be necessary to continue compressing the aggregate skeleton; however, the smoothness of the pavement may be compromised (Bijleveld et al., 2012).

As stated by Chadbourn et al. (1998), for practical purposes, the workability of a mixture is defined by two main components, spreadability and compactibility. The spreadability describes the ability of a loose mixture to be spread evenly over the road surface by the paver, while the compactibility refers to the mixture's ability to be compressed into a compact mass. In that way, the term workability defines the capacity of an asphalt mixture to be produced, handled, placed and compacted with minimum application of energy. The shape, size, texture, porosity and gradation of the aggregates,

as well as the binder viscosity and the volumetric properties of the mixture have been found to have a direct effect on the compactability of the asphalt layers (Chadbourn et al., 1998; Cabrera, 1991). In an effort to define the compactability of a mixture, multiple empirical formulations that associate the density of the material at different compaction stages with the accumulative compaction energies have been proposed (Wang, 2011).

Due to the many influencing factors, it is difficult to develop simple mathematic compaction models to describe the compaction process and relate it with the end product properties such as density, modulus and performance (Wang, 2011). Huerne (2004) investigated the compaction process with a non-standard finite element methods (FEM) approach called the arbitrary Lagrangian Eulerian method. The behavior of a mixture during compaction was simulated considering the asphalt concrete behaves somewhere between a solid and a liquid. It was established that the asphalt concretes behaves differently during the different stages in the compaction process. After the pre-compaction of the paver, before the aggregate particles are reoriented, the layer behaves in the elastic range. During compaction, as the aggregate particles are moving, the behavior is visco-plastic. However, as the material gets more compacted and the final density starts to be achieved, the layer becomes visco-elastic. According to Bijleveld et al. (2012), a similar behavior had been reported by Frigge in 1987. Similarly, based on a detailed discussion of the theories and backgrounds of compaction from a micromechanics approach, Wang (2011) proposed the use of a visco-plasticity, parallel layer model to account for the large non-linear, irrecoverable deformations involved in the compaction process.

2.3.2 Asphalt Concrete Temperature during Compaction

The temperature of the mixture has the greatest influence on the compaction and densification of an asphalt concrete pavement (NAPA, 2002). If the temperature is excessively high, the mixture is overstressed, according to Kari's (1967) definition. In such a state, the low stability of the mixture may be easily overcome by the weight of the roller, resulting in lateral movements underneath the drum or the rubber tires. As the mat cools down, the viscosity of the asphalt binder increases, reducing its ability to be compressed into a more dense state. However, once a mixture reaches a certain temperature, commonly referred to as a cessation temperature, further rolling cannot overcome the stiffness of the mixture, and further rolling may lead to cracking without additional improvements in the density. This underscores the importance of determining and maintaining an optimal temperature, between the unstable and cessation temperature, at which maximum densification can be achieved. Although this optimal temperature range varies with the properties of the mixture, once paving operations have begun, adequate density can only be ensured by determining an optimal compaction temperature in the field (Chadbourn et al., 1998).

A significant amount of literature addresses the optimal compaction temperature and multiple approaches have been proposed over the years for its determination. Some researchers have proposed specifying a minimum compaction temperature of 80°C, below which further compaction is impractical (Corlew and Dickson, 1968; Tageler and Dempsey, 1973). Other studies have focused on using the rheological properties of the asphalt binder to determine appropriate compaction temperatures. However, more

comprehensive approaches suggest using the heat transfer mechanisms previously described, to model the heat loss of the mixture accounting for the conditions in the field.

Compaction Temperature based on Binder Rheology

In 1962, the Asphalt Institute published specific guidelines for determining mixing and compaction temperatures of conventional asphalt mixtures, based on the viscosity of the asphalt binder. The optimal compaction temperature was defined as the temperature corresponding to a binder viscosity of 280±30 cP, as determined from the temperature-viscosity plot (Asphalt Institute, 1962). Furthermore, ASTM Specification D2493 – Standard Viscosity-Temperature Chart for Asphalts – provides detailed guidelines for plotting the measured viscosity at specific temperatures in a way that allows estimating the mixing and compaction temperatures in the laboratory. Although this approach has been reported to work well in the laboratory for neat binders, it may result in excessive temperatures for more viscous binders such as polymer-modified or rubber-modified binders (Decker, 2006). To solve this problem, the Asphalt Institute and the National Asphalt Pavement Association (NAPA) recommended reducing the compaction temperatures between 14°C and 25°C to avoid overheating the binder (Bahia et al., 2006). This method is still being used today for mixture design in the laboratory, where the rotational viscometer is employed to establish the relationship between temperature and viscosity. The temperature-viscosity plot approach is simple and provides reasonable compaction temperatures when the asphalt binder behaves as a Newtonian fluid at high temperatures (Tang and Haddock, 2006). However, modified binders show significant non-Newtonian behavior at common compaction temperatures (Bahia et al., 2001). In

fact, modified asphalt mixtures are more difficult to compact in the field due to their relatively high viscosity at these temperatures (Bahia et al., 2006).

According to Bahia et al. (2006), an attempt to introduce a revised procedure for establishing mixing and compaction temperatures in the laboratory was made as part of NCHRP Project 9-10: Applicability of Superpave Protocols to Mixtures Produced with Modified Asphalts. As a result, a procedure to determine the low shear viscosity (LSV) of the binder using the rotational viscometer was introduced, and target limits were defined based on the assumption that compaction of the compaction is dominated by the high viscosity at low shear rates. However, the proposed procedure required following a time-consuming and complicated curve fitting method, which generated mixed results in multiple validation studies, and therefore was never implemented.

Following the work introduced by NCHRP Project 9-10, multiple studies were conducted to determine more accurate compaction temperatures for modified asphalt binders. Yildrim et al. (2000) postulated that due to the thin films of asphalt, shearing during compaction is dominated by very high shear rates, and thus recommended the use of high-shear viscosity (HSV) measurements to determine mixing and compaction temperatures. As a result, individual consideration of the high-shear rate was found insufficient to solve the problem, and considering higher limits for the viscosity of the binder resulted in more reasonable compaction temperatures that were verified for a variety of modified asphalts used in Texas (Bahia et al., 2006). Salomon and Zhai (2002) introduced the activation energy, correlated to asphalt viscosity through Arrhenius equation, as the binder physical property best related to effective mixing and compaction.

It was found that higher compactive efforts to achieve the same density in gyratory compaction were necessary for higher activation energy values.

The National Center for Asphalt Technology (NCAT) introduced an instrumented mixer to measure the resistance of loose mixtures to mixing. The workability of the mixtures was defined as the inverse of the torque required to rotate the paddle within the sample. A preliminary attempt was made to utilize workability data to determine realistic compaction temperatures, but the results were inconclusive (Gudimettla, 2003). Bahia et al. (1998) and Guler et al. (2000) developed a device to measure the shear resistance of the mixture and determine its resistance to densification using the Superpave gyratory compactor (SGC). This special device called pressure distribution analyzer (PDA), allowed for the determination of what was called the compaction energy index (CEI), defined as the area under the densification curve between a relative density corresponding to the 8^{th} gyration and the density at 92% G_{mm}, and the compaction force index (CFI), defined as the area under the curve showing the variation of the shear resistance and the number of gyrations to 92% G_{mm}.

DeSombre et al. (1998) conducted a study to define which parameters affect compaction for modified binders under the hypothesis that optimum compaction occurs at the temperature where the shear stress is the lowest. Results, for a limited number of binders, indicated that shear stress generally increases as the temperature decreases, but the power required to achieve a specific density depends largely on aggregate type and gradation, while the temperature and the asphalt grade were found to have minimal effects on compaction resistance. Khatri et al. (2001) developed a procedure to determine the compaction temperatures by calculating the zero-shear viscosity (ZSV) temperatures

based on traditional compaction temperatures determined at a viscosity of 6.0 Pa-s. For Newtonian asphalt binders the viscosity is independent of the shear rate, while relative variations may be observed for non-Newtonian binders. Therefore, the ZSV method allows determining more accurate compaction temperatures for unmodified and modified asphalt binders. A validation study, carried by Tang and Haddock (2006) for asphalt mixtures in Indiana, revealed that using the ZSV method maintained the optimum binder content and allowed to achieve adequate densities in the field, making it a viable solution for the determination of the compaction temperature.

Bahia et al. (2006) proposed a solution for determining the mixing and compaction temperatures of modified asphalt binders by measuring the viscosity at various shear rates. Based on the concept that modified binders are shear thinning, a procedure for measuring the low-shear viscosity (LSV) was detailed and it was recommended to use levels of 3000 cP to estimate reasonable compaction temperatures for mixtures with modified binders.

Leiva-Villacorta and West (2008) used the accumulated compaction pressure (ACP) concept to quantify the compactive effort applied to an asphalt mixture in the laboratory. Different factors such as gradation type, aggregate size, lift thickness, mixture temperature and asphalt grade were analyzed and correlated to the compactive effect in the field. As a result, a simple method was proposed to measure the field compactability of asphalt concrete as a function of the mixture characteristics. An additional field validation of this concept was performed by Leiva-Villacorta (2007) using field density measurements from different test sections at the NCAT Test Track during the 2000 and 2003 research cycles. A model correlating the field and laboratory compactability of

asphalt mixtures, as a function of common quality control operations, was proposed. The model was subsequently validated using sixteen surface mixtures from NCHRP Project 9-27.

More recent research conducted under NCHRP Project 09-39 attempted to determine a simple, reliable, and accurate procedure for determining the mixing and compaction temperatures for virgin and modified binders. Three candidate methods, referred to as the High Shear Rate Viscosity, the Steady Shear Flow test and the Phase angle method, were compared in the laboratory. The results published in NCHRP Report 648 (2010), revealed that both the Steady Shear Flow and the Phase Angle methods provided reasonable mixing and compaction temperatures for commonly used binders across the United States, and their use was recommended, specifically for modified binders (West et al., 2010).

In general, all these studies consider developing extensive laboratory testing to determine the compaction temperatures in the field and, for the most part, the results are largely based on the rheological properties of the binder. However, the mixture temperature at the time of compaction is affected by conditions at the asphalt plant, paving operations, thermal properties of the materials, thickness and gradual densification of the pavement layer, and environmental conditions, such as air temperature, wind velocity and solar radiation (Chadbourn et al., 1998). Even if minimum laydown and compaction temperatures have been proposed (Corlew and Dickson, 1968; NAPA, 2002), varying field conditions may cause the optimum compaction time frame to expand or compress, depending on the rate of cooling.

Cooling Models Based Heat Transfer Mechanisms

Multiple one-dimensional solutions to the pavement cooling phenomenon have been developed in an attempt to model the rates of cooling. Corlew and Dickson (1968) used a numerical or finite difference solution based on transient-heat transfer, to develop a computer program that allowed calculating the cooling rates of asphalt concrete over an asphalt base. Factors such as wind velocity, solar altitude, and various environmental conditions were combined with default values for thermal conductivity, specific heat, density, and absorptance and emittance, to determine the time available for compaction. Convective heat transfer was determined by using charts that allowed obtaining a Nusselt number as a function of the Reynolds number determined by the wind velocity. Solar radiation was graphically determined as a function of the altitude of the sun, and corrected for the specific altitude of the pavement. To define heat conduction, constant physical properties were assumed, although the authors recognized that possible variations were expected with temperature and degree of compaction. These same properties were used in the program to model the heat transfer through the asphalt base, although possible modifications were permitted by the code in case a different base was expected.

In an attempt to simplify the procedure for determining the compaction time, Tageler and Dempsey (1973) used a similar heat transfer model to develop a series of theoretical nomographs and charts that allowed determining the optimal compaction time for asphalt concrete. Climatic inputs, which influence radiation and convection heat transfer, were used in an initial chart to determine a heat loss factor. Subsequent charts developed for specific mat thicknesses, pavement structures, and mixture temperatures,

allowed determining the compaction time in minutes as a function of the surface temperature. An example of these charts is presented in Figure 2.2. For practical purposes, the authors defined the available compaction time as the time needed for the HMA to reach an average temperature of 175°F. Although the charts were established for a specific geographical latitude of 40 degrees north and a maximum elevation of 4000 feet, a relatively simple procedure was suggested to account for different latitudes and elevations. The charts considered the wind velocity, the base temperature, the initial temperature of the mixture, and the layer thickness as the most influencing factors on the compaction of asphalt concrete. Based on this, final recommendations on minimum lift thicknesses and temperatures were provided for cold weather paving operations.

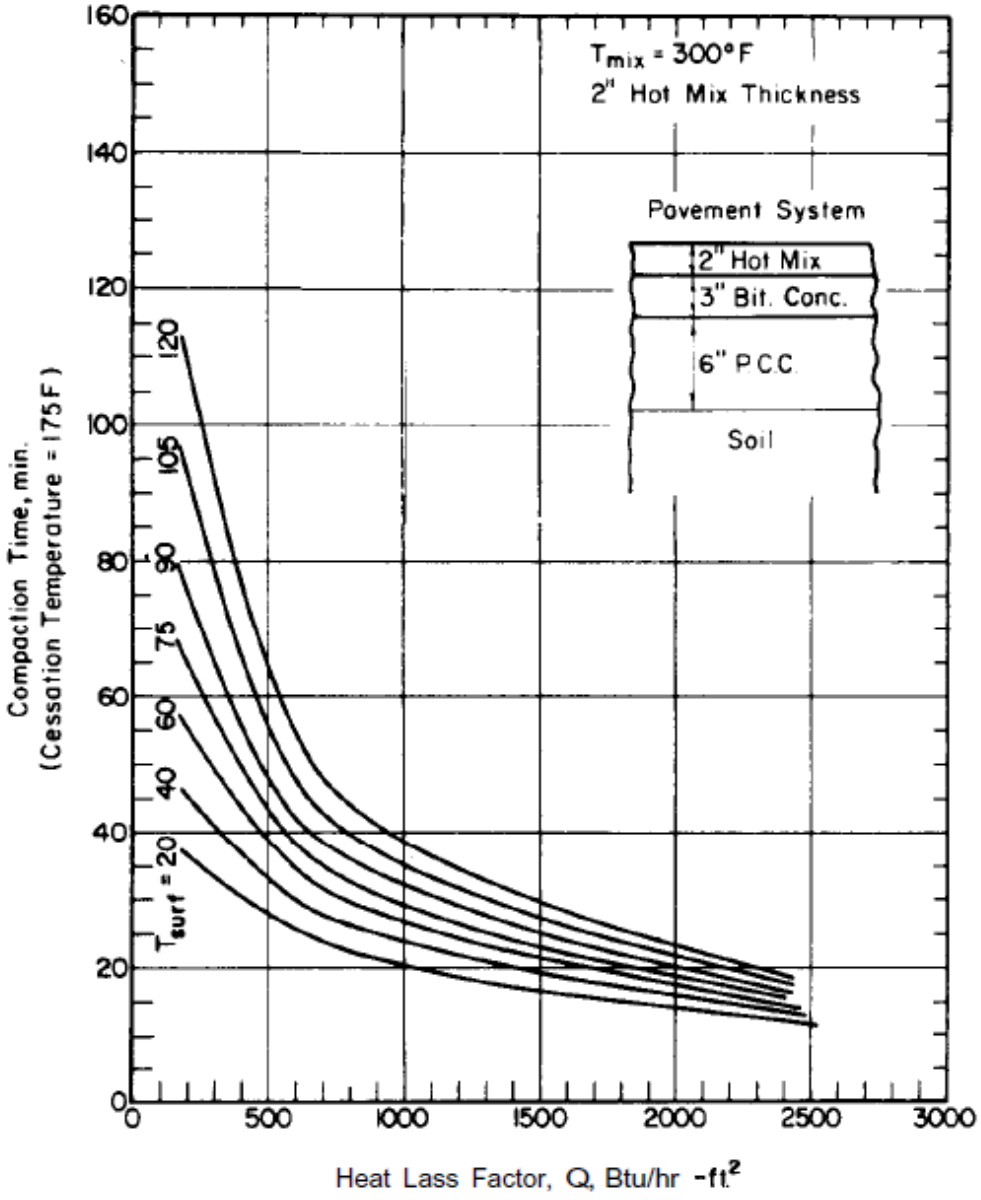

FIGURE 2.2 Compaction time curves proposed by Tageler and Dempsey (1973)

A similar approach was taken by Jordan and Thomas (1976), at the United Kingdom's Transport and Road Research Laboratory (TRRL). A computer model was developed to simulate the cooling behavior of hot paving materials, based on transient heat transfer theory. The accuracy of the model was validated by comparing the cooling curves obtained in five experimental sections with the outputs from the software, showing a good agreement between measured and predicted compaction times. Additionally, a sensitivity analysis using the computer program revealed that initially, the larger rate of heat loss occurred at the interface between the asphalt concrete and the bottom layer, but after a certain time, the surface rate of heat loss became dominant. Furthermore, the results showed that even if increasing the lift thickness for compaction operations had little effect on the overall rate of heat loss, thicker lifts tended to lose a smaller portion of their initial heat content, maintaining a higher temperature for longer periods of time. Based on this model, Daines (1985) presented a set of tables that allowed predicting the compaction time in the field, as a function of the layer thickness and the environmental conditions. Simultaneously, a similar method was proposed by Hunter and McGuire (1986).

Wolfe et al. (1983) used heat transfer theory to develop a simple pavement cooling predictive model capable of being used with a hand-held Hewlett-Packard 97 programmable calculator. The versatility of the model allowed determining the compaction time at the job site with ease, making it a useful solution for contractors and paving crews. Furthermore, validation studies performed with measured temperatures under laboratory and field condition proved that the computer simulation was satisfactory for predicting cooling times up to 20 minutes, as shown in Figure 2.3.

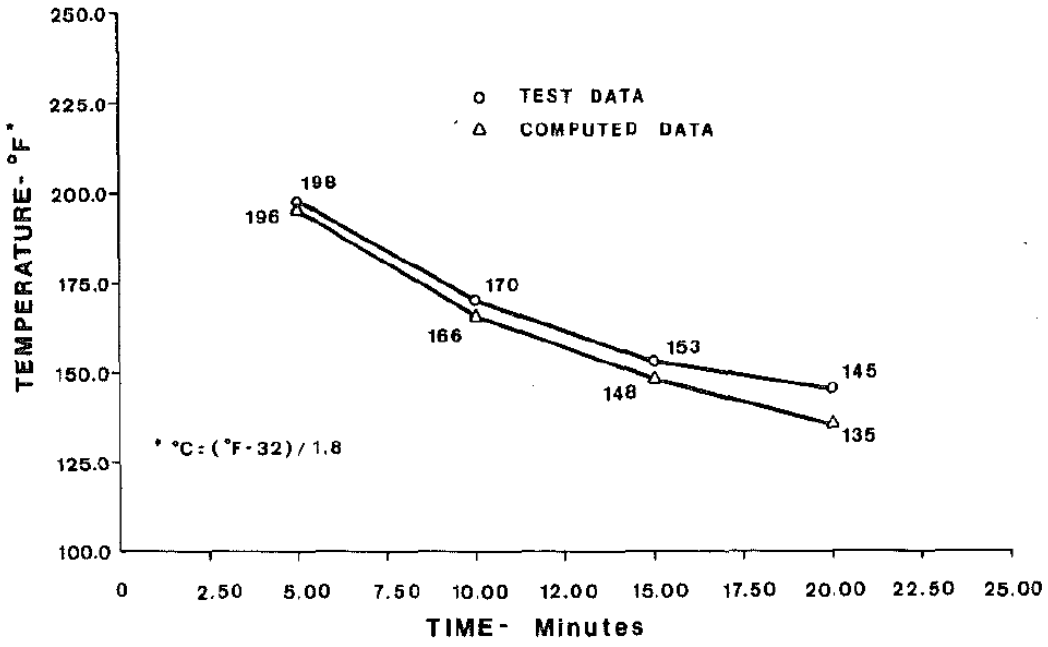

FIGURE 2.3 Measured and predicted cooling curves validated by Wolfe et al. (1983)

Based on a finite difference solution for the theoretical heat transfer of asphalt concrete, Chadbourn et al. (1998), with funding from the University of Minnesota and the Minnesota Department of Transportation, developed a numeric algorithm, known as PaveCool, which successfully simulated the cooling phenomenon on single lift asphalt pavements. The model was extended to a multi-layer solution by Timm et al. (Timm et al., 2001) under a project funded by the California Department of Transportation and the University of California Berkeley. The resulting computer software, initially named CalCool, was later renamed MultiCool. This software has been successfully validated on multiple occasions and is currently used by the American paving industry in the compaction planning and decision-making process in the field during construction

(NAPA, 2013). A more detailed description of the MultiCool model and its validation studies will be given in the next section.

As described by Bijleveld et al. (2012), Van Dee conducted a simultaneous research to model the cooling rate of asphalt, funded by Delft University of Technology in The Netherlands. This model allowed considering the combined effect of wind, moisture and rain to determine the compaction window. However, it was finally concluded that its use would depend on the acceptance of the tool by the paving community.

Wise and Lorio (2004) proposed a guide for estimating the time available for compaction for thin-layer HMA in South Africa. This practical guide consisted of two easy-to-use charts, shown in Figure 2.4, which allowed determining the compaction window for asphalt layers ranging between 25 mm and 40 mm. The first chart allowed establishing an initial compaction window, in minutes, as a function of the mat thickness and three different combinations of air/base temperature, while considering zero wind velocity and initial and cut-off temperatures of 150°C and 80°C, respectively. The second chart was used to reduce the previously obtained compaction time accounting for the wind speed. Two projects in Cape Town, South Africa were used to validate the method, revealing very positive results

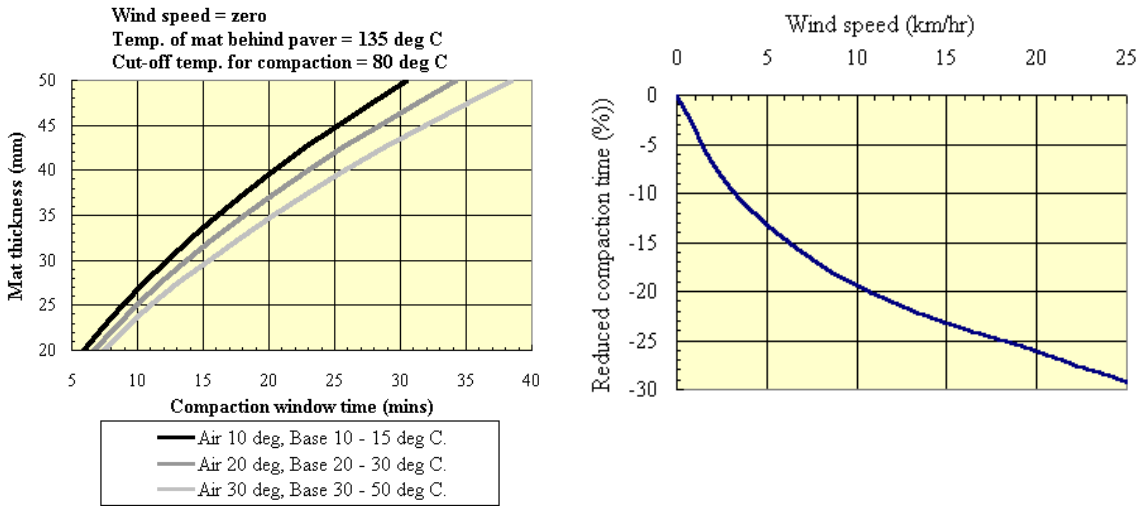

FIGURE 2.4 Guide for estimating the compaction window (Wise and Lorio, 2004)

Mieczkowski (2007) developed a complex heat transfer theoretical model for HMA compaction based on the concept that during compaction, the thickness of the mat changes constantly and a phenomenon of unstable thermal conduction occur. A number of calculations were executed for an HMA layer 5cm thick (on the surface, inside and bottom of the layer) with 3.5 m width, assuming that the side edges and the lower surface were insulated. Two different ambient temperatures were considered (0°C and 15°C), two wind velocities (0.2 m/s and 15m/s), a constant relative humidity (80%) and an HMA initial temperature of 135°C. The results of this theoretical case revealed that water contained in the pores of unbound layers may have a negative effect on the performance of HMA layers. In fact, the high heat consumption needed to convert water into steam tended to affect the momentary temperature drop at the bottom of the asphalt layer,

increasing the viscosity of the binder at the base-AC interface, while limiting the adhesion between the two layers and reducing the load capacity of the pavement.

More recently, proprietary computer programs have also been developed by certain equipment manufacturers and construction companies. Dynapac Road Construction Equipment, a paving equipment manufacturer developed a computer software named PaveComp® that provides accurate cooling time data, allowing to optimize the rolling patterns and amplitude settings for maximum compaction performance (Dynapac, 2013). Similarly, Eurovia, a subsidiary of Vinci Group and one of the world's leaders in transportation infrastructure construction and urban development, developed a comprehensive asphalt concrete temperature simulation tool called Gradius® (Eurovia, 2013). This software, based on transient heat conduction theory, has been designed to incorporate temperature losses during transport from the plant to the job site, waiting time in front of the paver, and during the compaction process, becoming a comprehensive solution for paving operations.

2.3.3 MultiCool Software and Previous Validation Studies

As mentioned before, the MultiCool software is commonly used by the American paving industry and is one of the main emphases of this research. It is therefore important to describe in greater detail the program and the concepts behind it that allow determining the cooling curves for asphalt concrete.

The MultiCool Model

The cooling rate of asphalt pavements modeled in MultiCool is based on one-dimensional heat transfer by conduction, convection and radiation (Chadbourn et al., 1998, Timm et

al., 2001, and Vargas-Nordbeck and Timm, 2011a). These three mechanisms, extensively described in previous sections, are combined to simulate special boundary conditions at the top of the pavement structure, while assuming the bottom of the pavement to be perfectly insulated. Figure 2.5 illustrates the heat transfer for a two layer pavement structure and Equations 14 and 15 represent the boundary conditions at the surface and bottom respectively.

$$q = h \times (T_a - T_s) - k_{ac} \cdot \frac{dT}{dz} + \alpha \times H_s + \varepsilon \times \sigma \times (T_s^4 - T_a^4) \quad (14)$$

$$q = 0 \quad (15)$$

Where:

q	=	Heat flux in the vertical direction (W/m^2)
h	=	Convection heat transfer coefficient ($W/m^2 \cdot K$)
T_s	=	Temperature of the pavement surface (K)
T_a	=	Meant air temperature (K)
k_{ac}	=	Thermal conductivity of asphalt concrete ($W/m \cdot K$)
$\frac{dT}{dz}$	=	Temperature gradient (change in temperature/change in depth)
α	=	Pavement absorptivity or absorptance (dimensionless)
H_s	=	Net solar flux calculated after Chadbourn et al. (1998)
ε	=	Pavement emissivity or emittance (dimensionless)
σ	=	Stefan-Boltzmann constant (5.669×10^{-8} $W/m^2 \cdot K^4$)

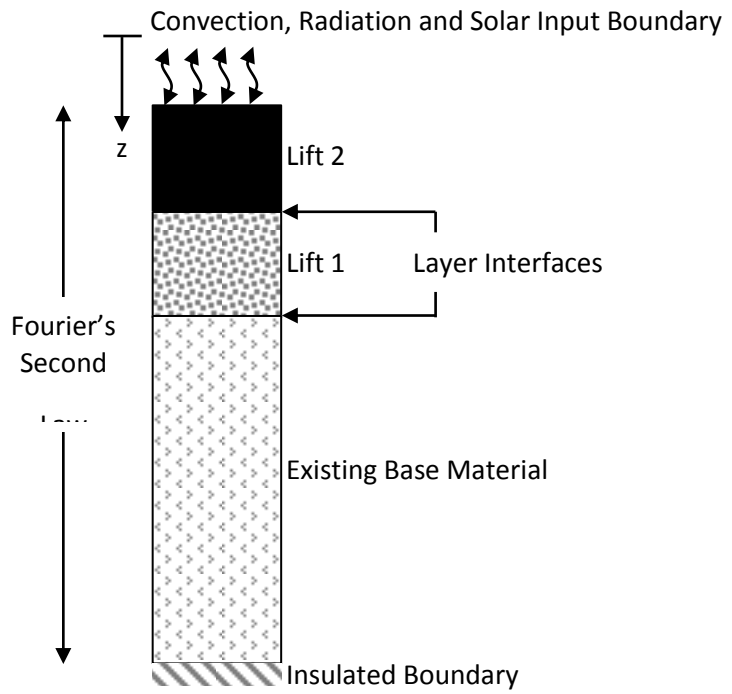

FIGURE 2.5 One-Dimensional Heat Transfer for the MultiCool Model (Timm et al, 2001)

As described by Timm et al. (2001), the program uses a finite difference method to solve the heat transfer equations. For this, the pavement structure is divided into finite control volumes, over which the numerical heat transfer solution may be applied, and a special node is located at the surface of the lift being paved to improve surface temperature predictions. In that way, the heat balance is expressed as the difference between the heat flowing from the top into a control volume and the heat flowing out of this control volume at the bottom. The heat transfer solution is then applied using a constant thermal conductivity for the asphalt layers and a specific thermal conductivity for the base depending on the moisture content, while using a geometric mean of the two conductivities for the asphalt-base interface.

As mentioned by Chadbourn et al. (1998), one of the main features of the MultiCool model is that it accounts for the effect of compaction on the heat transfer by utilizing a deformation space mesh, which allows considering the variation of the thermal properties as compaction occurs. The deformation is applied instantaneously at a specific moment in time, assuming that the rate of compaction is linear and uniform throughout the lift.

The program is meant as a pre-construction tool to aid designers and construction crews in predicting the rate of cooling and specifying an appropriate compaction rate (Timm et al., 2001). For that reason, all the computations previously described are performed automatically by the software, and the user only needs to provide certain inputs specific to the project without having to perform any difficult calculations.

Software Inputs

As mentioned before, the model takes into account mixture and layer parameters to predict the cooling rate of asphalt, based on one-dimensional heat transfer by conduction (asphalt – base), convection (asphalt – surrounding environment) and solar radiation. As shown in Figure 2.6, the inputs in the MultiCool program can be divided into four main categories; start time, environmental conditions, existing surface, and mix specifications.

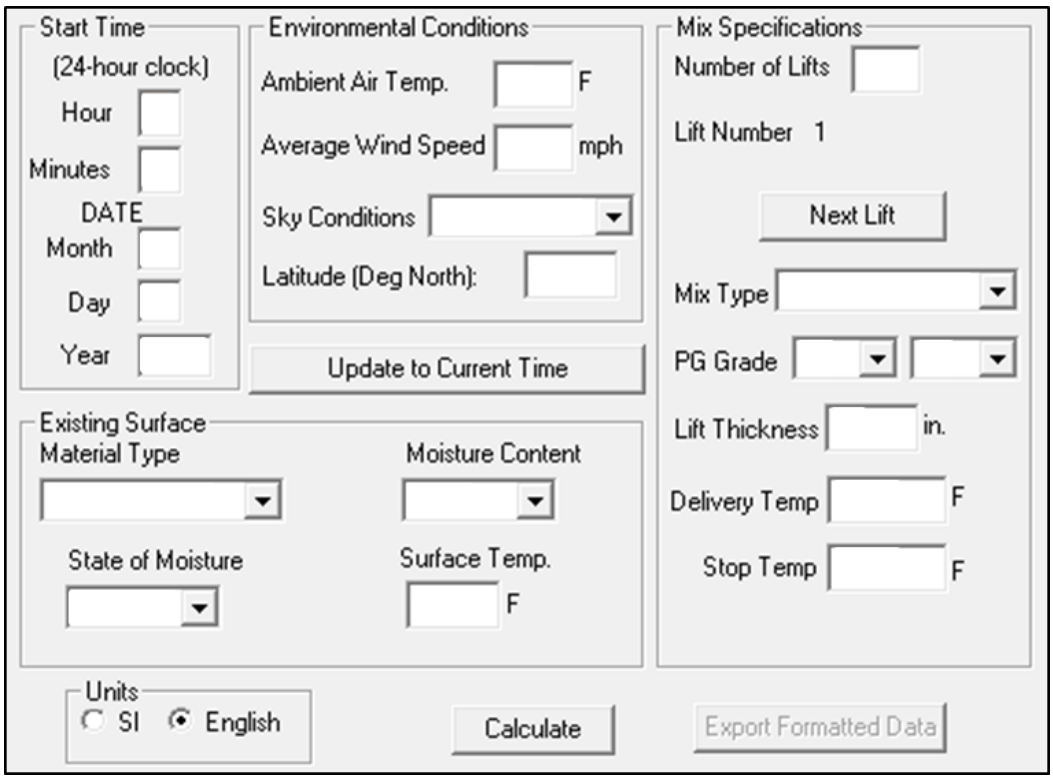

FIGURE 2.6 MultiCool Input Data Entry Window

Start Time. The specific time and date at the beginning of paving operations are used by the software to calculate the angle of the sun, and thus the incoming solar radiation. The time is updated automatically for the inclusion of additional pavement lifts.

Environmental Conditions. The average ambient air temperature, wind speed and sky conditions pertain directly to the surface boundary conditions and are assumed constant during the cooling of the lift. The latitude of the job site is used by the software to calculate the solar zenith angle during paving operations. This input is combined with the Start Time inputs to calculate the average solar flux at the surface of the pavement and the radiation heat flux.

Existing Surface. The software allows selecting from four types of base materials, including asphalt concrete, portland cement concrete, granular base, and subgrade soil. Additionally, two moisture content options (wet or dry) and two different states of moisture (frozen or unfrozen) may be selected. Specific combinations of the selected base material, moisture content and state of moisture automatically set research-based, default values for the thermal properties of the base material. Furthermore, the initial surface temperature allows establishing specific the boundaries for heat transfer at the bottom of the asphalt layer.

Mix Specifications. Being a multilayer solution for accelerated construction projects, the MultiCool software is capable of simulating a maximum of nine consecutive pavement lifts, assuming paving occurs in immediate succession. The mixture is specified as a function of the gradation (dense-graded, SMA, Superpave-fine, and Superpave-coarse) and the performance grade of the binder. While the binder grade is only intended as a label for the mixture, the gradation is used by the software to establish default thermal properties, determined by Chadbourn et al. (1998) for DG mixtures and SMA mixtures.

According to Timm et al. (2001), the thermal conductivity, specific heat and density of the base materials were determined based on previous studies by Kersten, Atkins, and Farouki. Similarly, the thermal properties of the asphalt concrete layers were based on research conducted by Chadbourn et al. (1996) and Chadbourn et al. (1998). The specific values used by the program are presented in Table 2.2.

TABLE 2.2 Thermal Properties Used in MultiCool

Material Type	Thermal Conductivity k_{ac} (W/m·K)	Heat Capacity c_p (J/kg^3·K)	Density ρ (kg/m^3)
Dense Graded Asphalt Concrete	2.00	1000.0	2000.0
Stone Matrix Asphalt (SMA)	1.50	1010.0	2010.0
Portland Cement Concrete	0.92	1090.0	2000.0
Granular Base – Dry/Unfrozen	1.16	963.0	2000.0
Granular Base – Dry/Frozen	2.00	858.0	2000.0
Granular Base – Wet/Unfrozen	1.22	1172.0	2000.0
Granular Base – Wet/Frozen	3.55	963.0	2000.0
Subgrade Soil – Dry/Unfrozen	1.35	1172.0	1800.0
Subgrade Soil – Dry/Frozen	1.40	963.0	1800.0
Subgrade Soil – Wet/Unfrozen	1.87	1591.0	1800.0
Subgrade Soil – Wet/Frozen	3.55	963.0	1800.0

Program Outputs

MultiCool uses these research-based default thermal properties and a finite difference approach, approximating the temperature at a certain point by computing the thermal conditions at neighboring points (Timm et al., 2001). The effect of compaction on heat transfer is accounted for by utilizing a deformation space mesh, and assuming that deformation is applied instantaneously and densification is continued at a constant, linear rate (Chadbourn et al., 1998). In that way, average lift temperatures are obtained by considering an initial node at the surface of the pavement layer and solving a system of simultaneous equations from the surface node to the bottom of the pavement layer. The result is a specific compaction time based on the cooling curve of each particular lift simulated, which can be shown in a tabular form and exported to Excel or as a graphical output, as shown in Figure 2.7.

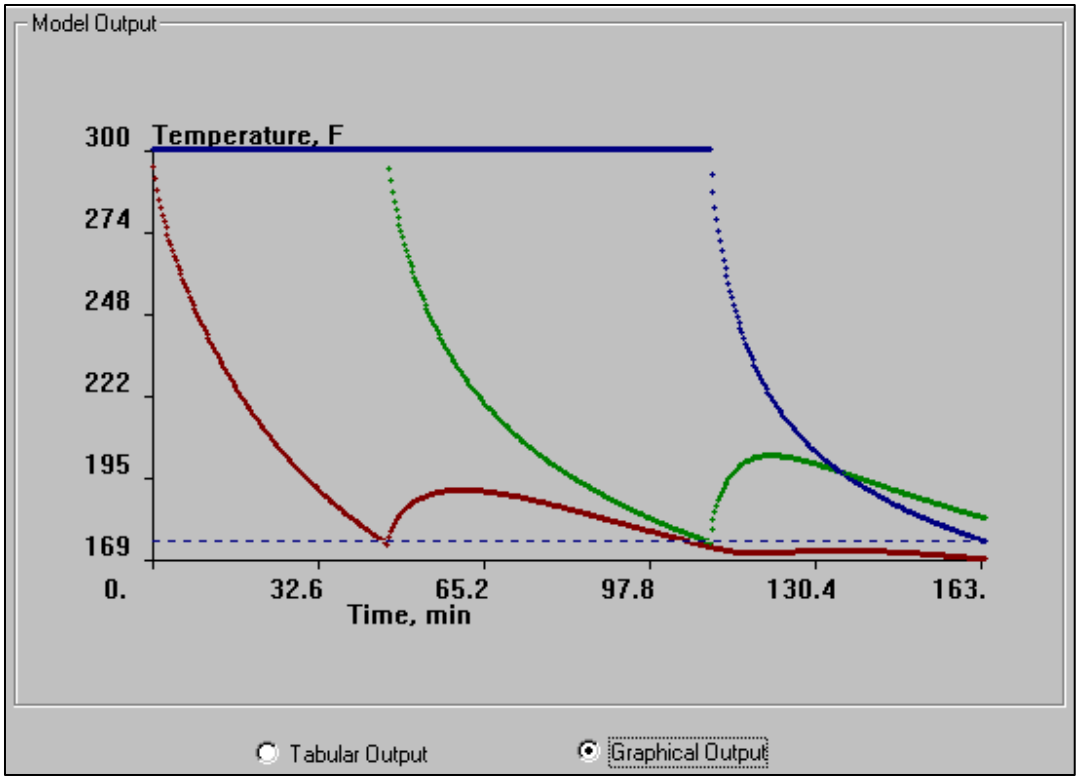

FIGURE 2.7 MultiCool Output Window

MultiCool Validation Studies

The MultiCool model has been successfully validated on multiple occasions. An initial validation of the original single-layer model was performed using temperature data from multiple thermocouples embedded in the asphalt layer on eight different projects in Minnesota between 1995 and 1997 (Chadbourn et al., 1998). In general, good agreement between measured and simulated cooling rates was obtained, as shown in Figure 2.8. Although this validation study only included material placed over existing asphalt layers, a tolerance of ± 18°F was recommended.

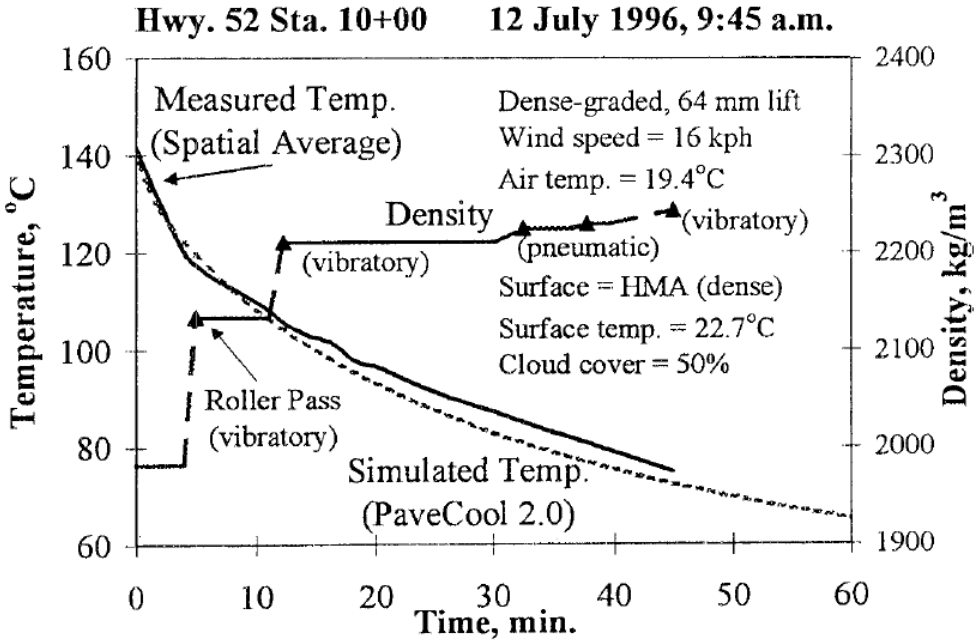

FIGURE 2.8 Field verification of the cooling model for Highway 52, Rosemount, MN (Chadbourn et al., 1998)

A subsequent validation of the multi-layer model was completed on two construction sites in California as part of the California Department of Transportation (CalTrans) report on asphalt constructability in 1999 and 2000. The validation was favorable in the case of single layer, but in the multi-layer analyses the model was found to under-predict the pavement temperature (Timm et al., 2001). An example of these observed differences for multiple layer paving operations is presented in Figure 2.9. The results from this study revealed that the ± 18°F tolerance recommended in the first validation was adequate and the authors recommended maintaining it.

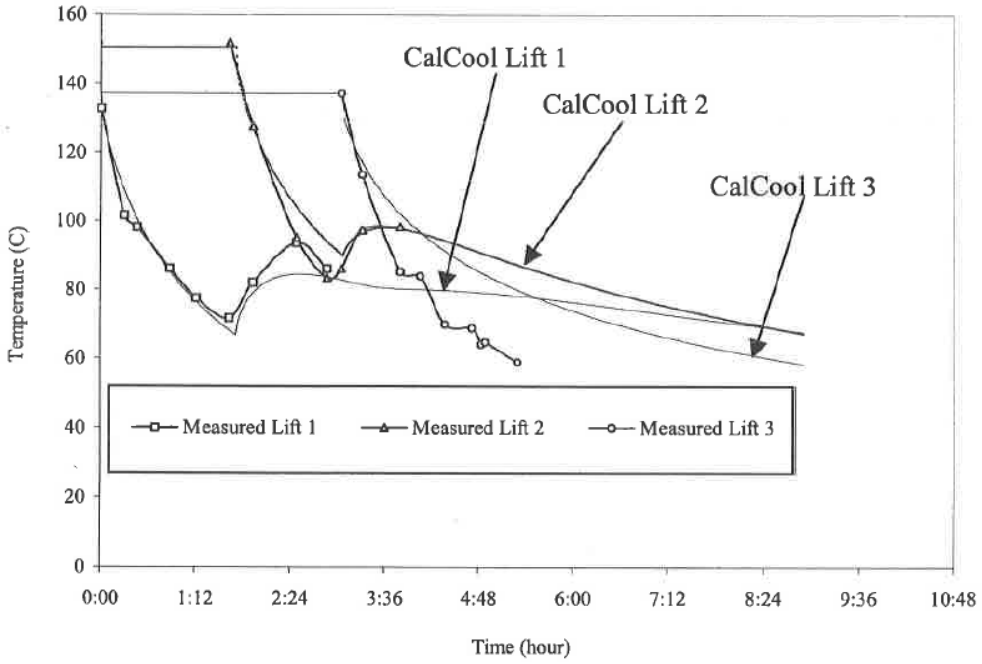

FIGURE 2.9 Field verification of the cooling model for Marina Blvd., San Leandro, CA (Timm et al., 2001)

A more recent validation study was performed at the NCAT, in Alabama, to evaluate the accuracy of MultiCool in predicting the cooling rate of warm mix asphalt (WMA), mixtures with high contents of reclaimed asphalt pavement (RAP), and polymer-modified asphalts (PMA). It was found that these materials had a statistically-significant effect on the accuracy of the model, but the differences between measured and simulated cooling rates were within the tolerance established in previous studies (Vargas-Nordcbeck and Timm, 2011a). Figure 2.10 shows the measured and predicted pavement temperatures for the control section in the study conducted at NCAT.

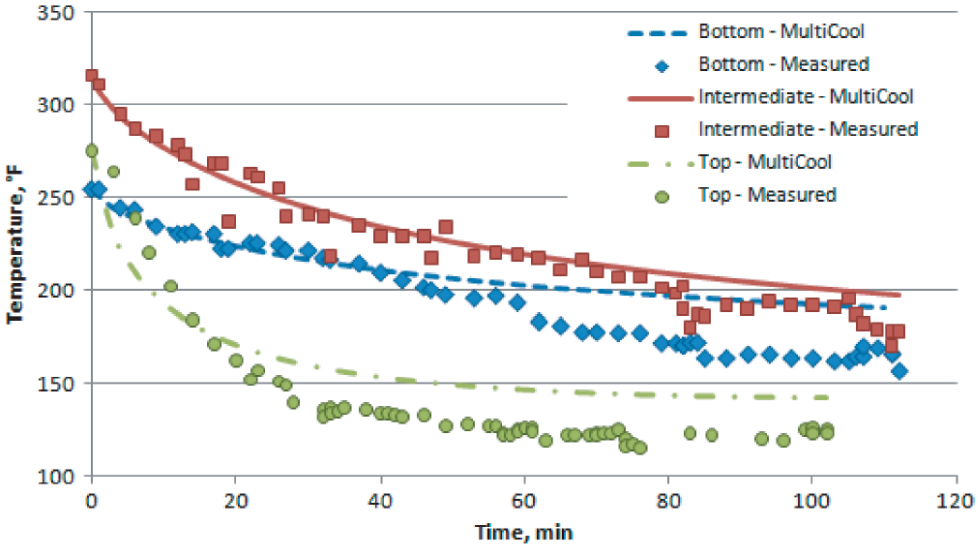

FIGURE 2.10 Field verification of the MultiCool model at the NCAT Test Track, AL (Vargas-Nordcbeck and Timm, 2011)

With the accelerated development of innovative sustainable technologies and methods for asphalt pavements arises an essential need for continued assessment of the constructability and compactability of such advances. A continued examination of the

cooling rate in the field of these new technologies would allow for a fast and accurate verification of the factors important for proper construction and performance. Although the precision of MultiCool has been previously validated on multiple occasions, the ever-increasing usage of recycled asphalt shingles (RAS), higher RAP contents, and ground tire rubber (GTR) modified binders, and the general growth in asphalt recycling and reclaiming technologies, denotes the need for further evaluating the MultiCool cooling model.

2.4 LONG-TERM THERMAL CYCLING

During the service life of a pavement, its surface is exposed to a great variety of environmental conditions, which directly influence its structural and functional performance. Of all the possible climatological conditions to which a pavement may be subjected, temperature, a compound climatological function, has been shown to contribute in many different ways to the development of distresses that lead to a premature failure of the structure (Williamson, 1972). Although external factors, such as rainfall and ambient temperature, are decisive aspects, the ultimate performance of an asphalt pavement is determined by its internal susceptibility to moisture and temperature changes (ARA Inc., 2004). Furthermore, the modulus of the asphalt concrete and the strains induced in the asphalt layers, are directly related to the temperature of the pavement. In fact, these temperature effects are one of the main considerations for mechanistic-empirical pavement design procedures, where the stresses and strains mechanistically calculated at different levels of a pavement structure are empirically correlated with its long term performance (ARA Inc., 2004; Priest and Timm, 2006).

The effect of temperature and solar radiation on pavements plays an important role in the urban heat island (UHI) effect. As discussed previously, asphalt concrete pavements absorb and emit radiation heat, which may cause the ambient temperatures to rise, especially in metropolitan areas. The UHI effect is then a result of the modification of land surface by urban development and the use of materials that effectively retain heat (Vargas-Nordcbeck and Timm, 2011b).

The following sections present a brief overview of heat transfer mechanisms that generate temperature cycling on asphalt pavements and its impact on the long-term structural performance of the pavement and the UHI effect.

2.4.1 Temperature Cycling on Asphalt Pavements

Based on the heat transfer mechanisms previously described, the temperature of a pavement is directly affected by the ambient temperature as well as precipitation, wind velocity, and solar radiation. Annual, seasonal and daily variations in the temperature of the surface layers have large influences on the structural response of a pavement, thus directly affecting its service life (Ongel and Harvey, 2004).

Effect of Temperature on Pavement Distresses

As mentioned before, the stiffness of the asphalt layers depends on the temperature of the pavement and the elastic and viscoelastic properties of the asphalt concrete are affected significantly by pavement temperature (Huang, 2004). Asphalt concrete tends to exhibit different characteristics at different temperatures, becoming stiffer at lower temperatures and softer at higher temperatures. This affects the stresses and strains induced in the

pavement structure, which explains the accelerated development of certain pavement distresses observed during the summer months (Priest and Timm, 2006). Therefore, thermal effects may be considered the major environmental factors influencing pavement distress modes as mixture rutting, fatigue cracking, and thermal cracking, although the latter mode is more likely to be a problem in lower temperature environments (Williamson, 1972).

Mixture Rutting. The results of accelerated pavement testing (APT) have demonstrated that the critical location for mixture rutting in a flexible pavement structure is within the top 100 mm of the asphalt pavement, where the temperatures tend to be the highest (Harvey et al., 2000). At higher temperatures, the asphalt concrete modulus decreases, the mixture becomes unstable and is incapable of resisting the shear stresses induced by the tires, resulting in mixture rutting in the wheelpath.

Fatigue Cracking. As described by Harvey et al. (2000), fatigue cracking develops from the bottom of the asphalt pavement and involves two phases, highly dependent on the temperature of the pavement. Crack initiation, the first mechanism, occurs at the bottom of the asphalt pavement as a result of repeated load damage. For pavement thicknesses of four inches or more, crack initiation takes place when the bottom of the AC layer is experiencing temperatures greater than 59°F. In the case of thinner pavements, where the asphalt layer thickness is less than three to four inches, crack initiation occurs at colder temperatures (Harvey et al., 2000). This explains the substantial increase in measured longitudinal tensile strains reported by Priest and Timm (2006).

Although the second mechanism in fatigue cracking, called crack propagation, may occur irrespective of the pavement temperature, it may be accelerated under colder temperatures. At this point, the asphalt becomes stiffer and more brittle, while at the same time the asphalt concrete contracts causing increased tensile strains to develop (Harvey et al., 2000). In general, warmer temperatures are more conducive to crack initiation, while colder conditions are more favorable for crack propagation.

Thermal Cracking. This phenomenon typically occurs in climates that have prolonged periods of freezing temperatures or extremely drastic temperature variations. When a flexible pavement is exposed to cold temperatures, the asphalt concrete becomes stiffer and more brittle and contracts, inducing increased tensile strains in the asphalt layer. Thermal cracking is primarily controlled by the selection of an appropriate asphalt binder capable of preserving relatively adequate viscous properties at lower temperatures. However, the rate of heat transfer in the asphalt concrete determines temperature variations in the asphalt layer, and thus plays an important role in thermal cracking.

Temperature Prediction Models

Extensive research has focused on developing prediction models to simulate the temperature fluctuations of asphalt concrete pavements as a function of the environmental conditions. Multiple models have been proposed, ranging from relatively simple equations based on measured conditions to sophisticated tools involving transient heat transfer theory and large amounts of data.

A simulation model, originally developed Schenck, was later modified by Williamson (1972) to predict the pavement temperatures using a finite difference solution, in South Africa. The program used transient heat transfer theory to calculate realistic theoretical temperature data, from three main inputs; climatological conditions, solar radiation, and the thermal properties of asphalt concrete.

Solaimanian and Kennedy (1993) proposed a relatively simple equation to calculate the maximum pavement temperature using the combined effect of ambient temperature and solar radiation. The suggested method is based on the heat transfer equations assuming a heat balance at the pavement surface which eventually results in thermal equilibrium of the asphalt layer. The proposed equation was found to be a fair predictor of the maximum pavement temperatures in a validation study consisting of 23 different sections in the United States and Canada. The pavement temperature was determined within a 3°C range in 83% of the cases. A comparison between the measured and calculated temperatures using this equation is presented in Figure 2.11.

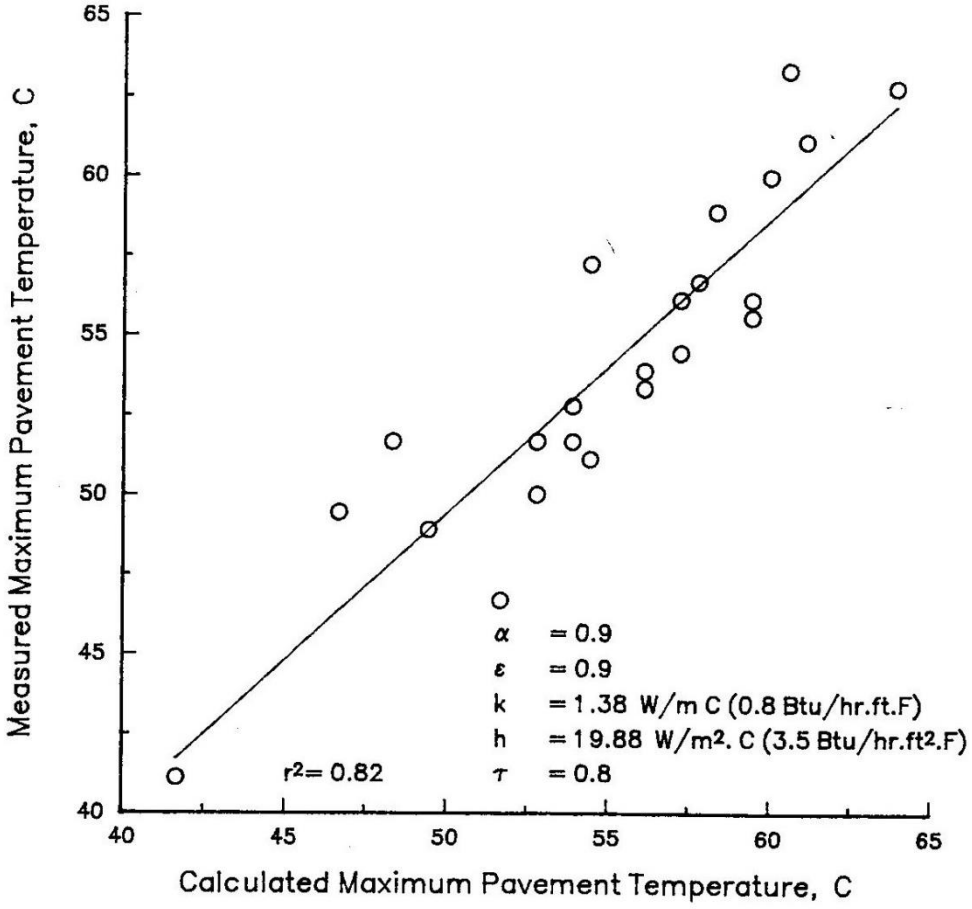

FIGURE 2.11 Comparison between measured and predicted pavement temperatures presented by Solaimanian and Kennedy (1993)

Hermansson (2000) proposed a simulation model to calculate the temperatures of asphalt concrete during the summer months, based on the heat transfer mechanisms describe in previous sections. Using hourly values for solar radiation, air temperature and wind velocity as inputs, the model calculated the pavement temperatures by means of finite difference approximation as the one used by Chadbourn et al. (1998). A subsequent validation of the model was performed using data from 12 different sections in the Long-Term Pavement Performance (LTPP) program, revealing good agreement between

temperatures predicted by the model and the field temperatures (Hermansson, 2001). Figure 2.12 shows an example of the accuracy of the Hermansson model for one of the sections in the LTPP program. A final recommendation was made to use the model to calculate maximum pavement temperatures to be used in combination with the Superpave mixture design methodology (Hermansson, 2000; Hermansson, 2001).

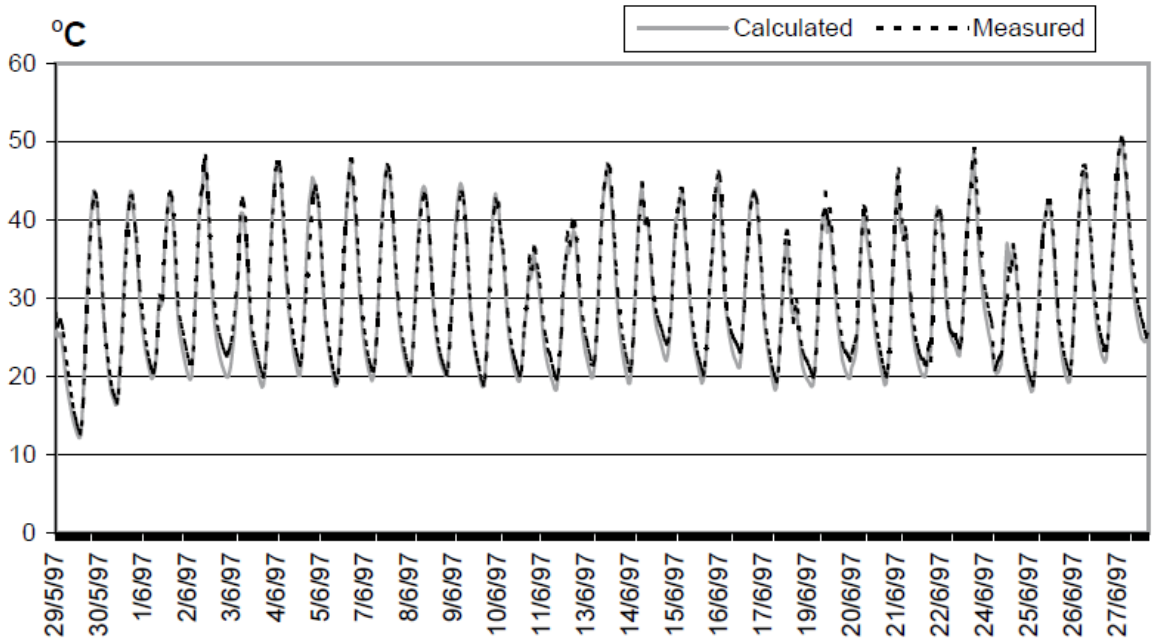

FIGURE 2.12 Validation of the Hermansson model for LTPP program, section 46-086, South Dakota (Hermansson, 2001)

A sophisticated temperature prediction model was included in the Mechanistic-Empirical Pavement Design Guide (MEPDG), as part of the Enhanced Integrated Climate Model (EICM). The EICM is a one-dimensional heat and moisture flow program that allows simulating the effects of the climatic conditions on the behavior and characteristics of the asphalt concrete and the unbound materials over several years of

operation (ARA Inc., 2004). The EICM model was based on the combination of three different models developed by the University of Illinois, the United States Army Cold Regions Research Engineering and Laboratory (CRREL), and Texas A&M University. These three independent models where coupled together by the Texas Transportation Institute to create the Integrated Climatic Model, which in time became the EICM. The final version of the EICM model, included in the MEPDG, predicts the temperature of the pavement, pore water pressure, water content, frost and thaw depths, frost heave, and drainage performance and computes specific resilient modulus adjustment factors, which can be used to predict the long-term pavement performance (ARA Inc., 2004).

The Climatic-Materials-Structural (CMS) model, developed at the University of Illinois, is responsible for the temperature predictions in the pavement system. It is a one-dimensional, forward finite difference heat transfer model that considers radiation, convection, conduction, and the effect of latent heat (ARA Inc., 2004). Specific pavement properties such as heat capacity, thermal conductivity, absorptivity, and emissivity are combined with environmental conditions such as wind velocity, ambient temperature, and incoming solar radiation, to determine the temperature distribution in the pavement. For the pavement layers, the CMS model assumes constant thermal properties, determined by the user.

A second model developed by CRREL allows determining the thermal properties of unbound materials as a function of the moisture and frost contents. The CRREL model simulates one-dimensional coupled heat and moisture flow in the subgrade soil at temperatures that are above, below and at the freezing temperatures of water, while predicting the depth of frost and thaw penetration (ARA Inc., 2004). In that way, the

temperature calculations of the ECIM are coupled with moisture predictions based on local weather conditions. Complex models such as the EICM are important part of the current structural design procedures (AASHTO, 2013).

2.4.2 Urban Heat Island Effect

The average temperatures in many urban and suburban areas may be elevated in comparison to their surrounding rural areas (EPA, 2010). The magnitude of these differences can be quite large depending on the weather conditions, thermophysical and geometrical characteristics, and anthropogenic moisture and heat sources present in the urban areas (Taha, 1997). Field studies have shown that the annual mean air temperature of a city with one million or more people can be 1.8°F to 5.4°F warmer than its surroundings, with potential for up to a 22°F difference on a clear, calm night (EPA, 2010). This phenomenon, known as the urban heat island (UHI) effect, has been recognized and documented since the early 1900's (Taha, 1997).

The United States Environmental Protection Agency (EPA) identifies two different types of urban heat islands, described as surface and atmospheric. While atmospheric UHI refers to the warmer air present in urban areas, surface UHI pertains to urban surfaces, such as pavements. Surface heat islands are mainly originated by the effect of solar radiation heat transfer at the surface of the pavement. For this reason, surface UHI tends to be stronger during the day, in presence of the sun, but may be present day and night. In fact, pavements tend to be denser than natural surface cover, thus absorb and retain more thermal energy which continues to be released even at night.

Heat is transferred to the pavement according to the heat transfer mechanisms discussed in previous sections. From the perspective of the UHI effect, the most important pavement properties affecting temperature fluctuations are solar reflectance or albedo and permeability, in addition to thermal properties such as thermal conductivity, thermal diffusivity, heat capacity, thermal emissivity, and thermal absorptivity.

Pavement albedo, or solar reflectance, is the property of the pavement that defines the percentage of solar energy reflected by its surface. Albedo values range between zero, for perfect absorbers, to one, for perfect reflectors. Higher albedo values indicate that a larger percentage of the direct solar energy is reflected by the pavement into the surrounding environment, allowing for less radiation heat to be absorbed and thus reducing the surface and subsurface temperature of the pavement (Gui et al., 2007). The permeability of the pavement, on the other hand, affects the amount of thermal energy that may be stored in the pavement layer. A permeable pavement allows rainwater and air to flow through the air voids, generating conduction and convection heat transfer and thus reducing the temperature of the pavement.

With funding of the Federal Highway Administration (FHWA), Iowa State University, in collaboration with the National Center for Asphalt Technology (NCAT), is currently conducting a nationwide study to quantify the pavement albedo of different pavement types. The study is an attempt to generate experimental data that will allow determining the real contribution of pavements to the UHI effect (NCAT, 2013; FHWA, 2013).

2.5 SUMMARY

High quality, smooth asphalt pavement surfaces are the result of many key factors, including proper materials selection, mixture design, production, placement and compaction. Ultimately, the long term performance of the pavement depends on using sound engineering that accounts for the effect of variations in environmental conditions.

In a pavement structure, thermal interactions occur based on one-dimensional heat transfer by conduction, convection and radiation. Thermal energy, or heat, is transferred by conduction from the asphalt layer to the base, by convection from the asphalt layer to the surrounding air, and by radiation directly applied at the surface of the asphalt layer. Heat conduction is described by Fourier's Law, assuming constant heat flux and uniform thermal conductivity throughout the entire asphalt layer. Convective heat transfer is very difficult to model due the complex fluid motion of air; however, it can be described as a function of the heat transfer coefficient and the temperature differential between the ambient and the asphalt layer. Similarly, heat transfer through radiation may also be simplified as a function of the pavement absorptance and the solar flux on one hand, and the pavement emmitance and the temperature variation on the other. Furthermore, a detailed summary of the thermal properties of asphalt concrete affecting these three heat transfer mechanisms was presented.

During construction, adequate control of the temperatures during compaction is the most important factor in achieving proper densification of asphalt concrete and deficient monitoring of rolling operations may cause densities below the specified thresholds, which detrimentally affects the long-term performance of the pavement. The shape, size, texture, porosity and gradation of the aggregates, as well as the binder

viscosity and the volumetric properties of the mixture have been found to have a direct effect on the compactability of the asphalt layers. Nonetheless, the temperature of the mixture probably has the greatest influence on compaction and densification of an asphalt concrete pavement. The mixture temperature at the time of compaction is affected by conditions at the asphalt plant, paving operations, thermal properties of the materials, thickness and gradual densification of the pavement layer, and environmental conditions, such as air temperature, wind velocity and solar radiation. Varying field conditions may cause the optimum compaction time frame to expand or compress, depending on the rate of cooling. For this reason, multiple one-dimensional solutions to the pavement cooling phenomenon have been developed in an attempt to model the rates of cooling. The original pavement cooling model developed Corlew and Dickson (1968) was expanded by Tageler and Dempsey (1973), Jordan and Thomas (1976), Daines (1985), and Hunter and McGuire (1986). In 1998, Chadbourn et al. developed a numeric algorithm, known as PaveCool, which successfully simulated the cooling phenomenon on single lift asphalt pavements (Chadbourn et al., 1998). The model was extended to a multi-layer solution by Timm et al. and the resulting computer software, initially named CalCool (Timm et al., 2001), was later renamed MultiCool. This software has been successfully validated on multiple occasions revealing good agreement between measured and simulated cooling rates, and is used by the paving industry in the compaction planning and decision-making process in the field during construction (NAPA, 2013).

During the service life of the pavement, thermal interactions control the structural and functional performance of the pavement. The modulus of the asphalt concrete and the strains induced in the asphalt layers, are directly related to the temperature of the

pavement. In fact, thermal effects may be considered the major environmental factor influencing pavement distress modes as mixture rutting, fatigue cracking, and thermal cracking, although the latter mode is more likely to be a problem in lower temperature environments. Furthermore, extensive research has focused on developing prediction models to simulate the temperature fluctuations of asphalt concrete pavements as a function of the environmental conditions and multiple models have been proposed, ranging from relatively simple equations based on measured conditions (Solaimanian and Kennedy, 1993) to sophisticated tools involving transient heat transfer theory and large amounts of data (ARA Inc., 2004). On the other hand, pavement temperature is also an important variable affecting the urban heat island effect (UHI). Since pavements tend to be denser than nature surface cover, they absorb and retain more thermal energy which continues to be released even at night, significantly increasing the ambient temperature in urban areas (Oke et al., 1997).

CHAPTER THREE

EXPERIMENTAL PLAN

3.1 INTRODUCTION

As part of the fifth research cycle at the NCAT Pavement Test Track, twenty new experimental pavement test sections were built, including seven instrumented test sections with the ability to measure the structural response of the pavement layers under traffic loading. Four sections included in this structural study constituted the "green group" experiment (GG), and three other sections were sponsored by the Virginia Department of Transportation (VDOT). Four agencies (Alabama DOT, Alabama Department of Environmental Management, North Carolina DOT, and South Carolina DOT) supported the GG experiment in an attempt to assess the effect of multiple combinations of sustainable technologies, such as recycled asphalt shingles (RAS), high reclaimed asphalt pavement (RAP) contents, and ground tire rubber (GTR) modified asphalt binders on the performance of asphalt pavements. The VDOT sections were designed to investigate 100% RAP foamed cold-mix (FCM) and cement treated base (CTB) as base layers. This chapter contains a detailed description of the test sections included in the 2012 structural study, the construction process, and the experimental plan followed for the study of the effect of these sustainable technologies on the thermal interactions of asphalt concrete pavements.

3.2 TEST FACILITY

The NCAT Pavement Test Track, operated by the National Center for Asphalt Technology (NCAT), is a 1.7 mile closed loop full-scale flexible pavement test facility located near Opelika, AL. This unique accelerated pavement testing (APT) facility combines real-world pavement construction with live heavy trafficking for rapid testing and analysis of asphalt pavements, allowing highway agencies to improve their mixture specifications, construction practices, and pavement design methods (West et al., 2012). Figure 3.1 shows an aerial photograph of the NCAT Pavement Test Track.

FIGURE 3.1 Aerial Photograph of the NCAT Test Track (West et al., 2012)

Consisting of forty-six individual two-hundred foot test sections, with twenty-six sections located on the two straight segments and twenty sections distributed amongst the two curves, the NCAT Pavement Test Track has been continuously sponsored during five different three-year research cycles. Over the multiple research cycles, select test sections

have been replaced and reconstructed, while certain test sections have been left in-place for continued traffic loading. During each research cycle, once reconstruction has been completed, all test sections were loaded with approximately ten-million equivalent single axle loads (ESALs) over a two-year period. Live traffic has been applied by means of special tractor trailer rigs manually operated at a target vehicle speed of 45 mph, on a daily basis (sixteen hours a day, five days a week). The trucks were composed of a 12,000-lb steer axle, a 40,000-lb tandem axle, and five 20,000-lb single axles.

During each trafficking phase, samples of the mixtures obtained during construction were tested and analyzed at the NCAT's state-of-the-art laboratory, located in Auburn, AL. Similarly, the performance of each test section was assessed through weekly performance measurements that include international roughness index (IRI), rut depth, and crack mapping. Additionally, the pavement structural response was measured weekly, for selected test sections containing embedded instrumentation, known as the structural sections.

The fifth research cycle began in 2012, with the reconstruction of twenty new experimental test sections between the months of August and September. Seven new sections constituted the 2012 structural study and contained a minimum of twelve asphalt strain gauges (ASG) located at the bottom of the asphalt layer and two earth pressure cells (EPC) located on top of the base and subgrade layers, respectively. Additionally, a minimum of four temperature probes were installed at various depths within the structure, to measure in-place temperatures of the asphalt layers.

3.3 TEST SECTIONS

The seven structural sections were used in the present study. As mentioned before, four sections constituted the "green group" experiment (GG), and three sections were sponsored by VDOT. The GG experiment consisted of one section in the north tangent (N5) and three sections in the south tangent (S5, S6, and S13), built in three separate lifts with individual asphalt mixtures including multiple combinations of post-consumer (PC) RAS, RAP, and GTR-modified binders. The three VDOT sections included sections N3 and N4 located in the north tangent, and section S12 in the south tangent. Section N3 consisted of three asphalt concrete layers placed over a fourth layer of plant-produced FCM containing 100% RAP. Similarly, sections N4 and S12 consisted of two asphalt concrete layers (top and bottom) placed over a third layer of the same FCM, with the exception that section S12 contained a CTB as base layer.

3.3.1 Pavement Cross-Sections

The pavements in the 2012 structural study were designed and constructed based on the individual needs and common practices of the sponsoring agencies. Figure 3.2 shows the average as-built thicknesses of the asphalt layers included in this study. To account for possible variability during the paving process, the as-built thicknesses were obtained as the average thickness measured at twelve random locations along the pavement sections and after each individual layer was paved. The accuracy of the measurements was optimized by using surveying equipment, such as a global positioning system (GPS) and a total station, to identify the exact random locations and make individual thickness measurements for every layer built.

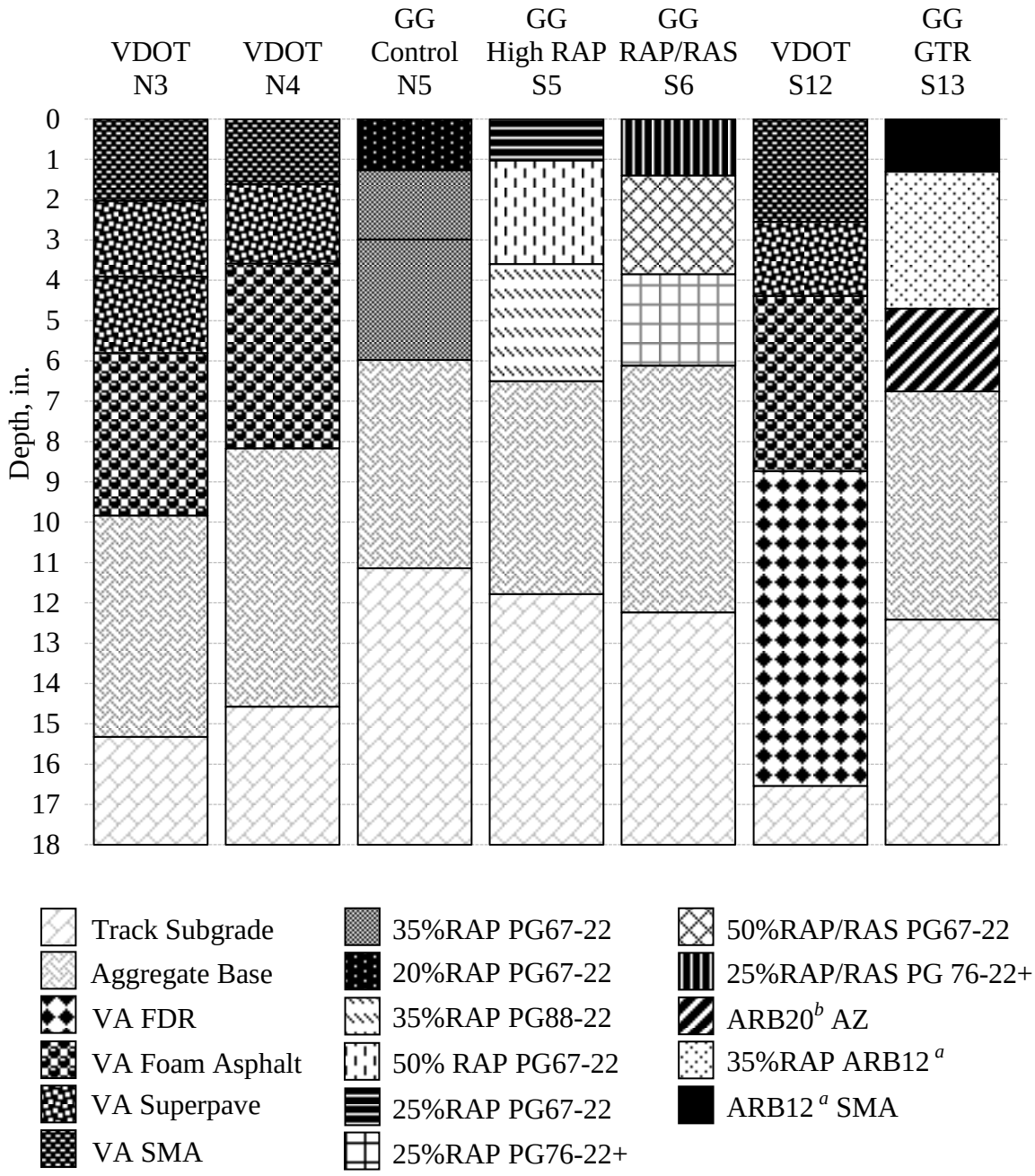

FIGURE 3.2 2012 Structural Experiment Cross-Sections

All test sections included in this study were built over a common subgrade material, referred to as "Track subgrade". This material, classified as an A-4(0) soil according to the AASHTO soil classification system, consisted of a metamorphosed

quartzite soil material obtained and excavated directly from the Test Track property, which has been used as a fill material during multiple research cycles (Taylor and Timm, 2009). Figure 3.3 shows the Track subgrade placed and compacted on one of the test sections at the NCAT Test Track.

FIGURE 3.3 Track Subgrade

The additional layer built on top of the subgrade varied depending on the needs and research objectives of each test sections. A description of the 2012 structural sections, including the materials, the mixture designs, and the construction process is presented below.

The four test sections included in the GG experiment were built over a granular base with an approximate thickness of 6 in. The material used consisted of a well-graded crushed granite aggregate supplied by Vulcan Materials, Inc. and manufactured in

Columbus, GA, and has been commonly used by the Alabama DOT for their construction projects (Taylor and Timm, 2009). Three individual asphalt layers, adding up to an average thickness of approximately 6 in, were built for every GG section. All the mixtures were produced at the same asphalt plant using warm-mix asphalt (WMA) technologies, consisting of either an additive or a foaming process, to assist in the compaction process. The asphalt mixtures used in the GG sections were specifically designed to include a particular sustainable technology, such as RAP, RAS or GTR-modified binders. The mixtures used in all bottom and intermediate lifts had a 19 mm nominal maximum aggregate size (NMAS), except for section S13 where the NMAS for the bottom lift was 12.5 mm. The top layer mixture in section N5, the control section for the GG experiment, was a dense-graded (DG) 9.5 mm Superpave mixture while the other GG sections were 9.5 mm SMA mixtures.

Section N5 was the control section for the GG experiment, using conventional RAP contents ranging between 20% and 35%. Section S5 included higher RAP contents, especially the intermediate layer which contained 30% coarse fractionated RAP and 20% fine fractionated RAP for a total of 50% RAP in the mixture. Section S6 was defined as the RAS section since its bottom and intermediate layers contained a combination 25% RAP and 5% RAS, while the top layer was produced with only 5% RAS. Finally, section S13 contained two different GTR-modified binders, including different particle sizes and only the intermediate section contained 35% RAP.

As mentioned before, the VDOT sections were designed to investigate foamed cold-mix (FCM) and a cement treated base (CTB) as base layers. Section N3 consisted of three asphalt concrete layers placed over a fourth layer of plant-produced FCM

containing 100% RAP on top of a granular base. Similarly, section N4 and S12 consisted of two asphalt concrete layers (top and bottom) placed over a third layer of the same FCM, with the exception that section S12 contained a CTB base layer, while section N4 was built over a granular base layer.

A summary of the mixtures used in each lift is presented in Table 3.1, specifying the mix gradation, binder type (virgin, polymer-modified or GTR-modified), production temperature, RAP content, PC RAS content, and lift thickness, respectively. Two different crumb rubber particle sizes and contents were used for section S13.

TABLE 3.1 Summary of Test Sections

Section	Mix Parameter	Top	Intermediate	Bottom
N3 (VDOT)	Mix Type:	SMA	DG	DG
	Binder Grade:	PG 76-22	PG 67-22	PG 67-22
	Plant Temp. (°F):	325	330	330
	RAP Content (%):	12.5%	30%	30%
	Thickness (in):	2.1	2.1	1.9
N4 (VDOT)	Mix Type:	SMA		DG
	Binder Grade:	PG 76-22	No	PG 67-22
	Plant Temp. (°F):	325	Intermediate	330
	RAP Content (%):	12.5%	Lift	30%
	Thickness (in):	2.0		1.9
N5 (GG Control)	Mix Type:	DG	DG	DG
	Binder Grade:	PG 67-22	PG 67-22	PG 67-22
	Plant Temp. (°F):	270	285	280
	RAP Content (%):	20%	35%	35%
	Thickness (in):	1.3	1.7	3.0
S5 (GG High RAP)	Mix Type:	SMA	DG	DG
	Binder Grade:	PG 67-22	PG 67-22	PG 88-22
	Plant Temp. (°F):	275	280	285
	RAP Content (%):	25%	50%	35%
	Thickness (in):	1.0	2.6	2.7
S6 (GG RAP/RAS)	Mix Type:	SMA	DG	DG
	Binder Grade:	PG 67-22	PG 67-22	PG 76-22
	Plant Temp. (°F):	275	280	280
	RAP Content (%):	0%	25%	25%
	RAS Content (%):	5%	5%	0%
	Thickness (in):	1.3	2.4	2.3
S12 (VDOT)	Mix Type:	SMA		DG
	Binder Grade:	PG 76-22	No	PG 67-22
	Plant Temp. (°F):	32	Intermediate	330
	RAP Content (%):	12.5%	Lift	30%
	Thickness (in):	2.0		1.9
S13 (GG GTR)	Mix Type:	SMA	DG	SMA
	Binder Grade:	ARB12 (-30)[a]	ARB12 (-30)[a]	AZ20 (-16)[b]
	Plant Temp. (°F):	275	280	300
	RAP Content (%):	0%	35 %	0%
	Thickness (in):	1.2 in.	3.2	2.0

[a] Asphalt rubber binder with 12% 30-mesh rubber particles
[b] Asphalt rubber binder with 20% 16-mesh rubber particles

3.3.2 Construction Process

The different pavement layers above the Track subgrade were built in accordance with common industry practices. Four individual processes were identified in the construction of the 2012 structural experiment. All sections contained a granular base, with the exception of section S12, which contained a CTB. Additionally, the VDOT sections contained a FCM layer on top of the base layer. Finally, although the asphalt mixtures were different for every layer and every section, paving and compaction operations were the same. These construction processes are described in the following sections.

Granular Base Layer

The granular base layer was transported and placed in the corresponding sections using dump trucks, where a loader assisted in spreading the material to the entire width of the section. As shown in Figure 3.4, a single drum vibratory sheep-foot roller, with operating weight of 8,000 kg, was used to compact the layer until optimum density was achieved.

FIGURE 3.4 Granular Base Material Being Compacted

Cement Treated Base

The CTB for section S12, in the VDOT experiment, was built using the Track subgrade material. For this, a cement truck was used to spread portland cement over the entire width of the pavement, as shown in Figure 3.5.

FIGURE 3.5 Portland Cement Being Spread on Section S12

The cement and the Track subgrade material were subsequently mixed using a cold recycler, with a working width of 2 m, connected to a water truck as shown in Figure 3.6.

FIGURE 3.6 Cold Recycler and Water Truck

A milling and mixing rotor, equipped with multiple cutting tools, provided a thorough and homogeneous mixture of the materials in the mixing chamber of the recycler. A set of water nozzles, contained inside the mixing chamber, injected and measured specific amounts of water, necessary to reach the optimum moisture content. Once the mixing of the CTB was completed, a single drum vibratory sheep-foot roller was used to compact the layer until optimum density was achieved, while a motor-grader was used to provide the final grade to the CTB layer.

Foamed Cold Mix

The foamed cold mix was produced using a mobile cold-recycling mixing plant. The RAP materials obtained from milling the test sections from the 2009 research cycle were fractionated at the NCAT Test Track using a mobile screen. The resulting materials were combined and mixed with foamed asphalt on-site, using the cold-recycling mixing plant shown in Figure 3.7.

FIGURE 3.7 Mobile Cold-Recycling Plant used at the NCAT Test Track

Pavement recycling using foamed asphalt constitutes an environmentally friendly and cost effective technique that allows reusing the existing structure as an enhanced foundation for a new pavement (Wirtgen Group, 2002). Originally perceived as a method for improving the quality of marginal aggregates, asphalt foaming has been found to produce good quality cold asphalt mixtures encouraging its use for road construction and rehabilitation (Jenkins and Van de Ven, 2001). Foamed asphalt, also known as "foamed bitumen" in Europe and Africa, has been effectively used as a recycling agent with a wide variety of materials ranging from marginal gravels with high plasticity to reclaimed asphalt pavements (RAP) (Asphalt Academy, 2009).

Foamed asphalt is the result of the spontaneous foaming produced by injecting water into hot liquid asphalt binder. The temperatures needed for a normal asphalt binder to become fluid are generally higher than the boiling temperature of water. For this reason, when a constant stream of water is introduced into hot asphalt binder, covalent bonds are formed in the thin film state, generating a visible expansion of the asphalt binder (Wirtgen Group, 2002). Asphalt foaming was extensively described by Jenkins (1999, 2001) as a physical–chemical process based on heat and energy transfer. As cold water droplets (at ambient temperature) make contact with heated binder (between 170°C and 180°C), the binder exchanges energy with the surface of the water droplet, heating it to a temperature above its boiling point, while simultaneously cooling the binder. This transferred energy exceeds the latent heat of steam resulting in explosive expansion and generation of steam bubbles. During this expansion, the surface tension of the asphalt film counteracts the ever-diminishing steam pressures until a state of equilibrium is reached. Due to the low thermal conductivity of asphalt binder and water, the steam

bubbles are capable of remaining stable for a certain period of time. However, as the colloidal mass cools at ambient temperatures, steam condenses causing bubbles to collapse and foam to decay, resulting in a product known as water-saturated bitumen (Van der Walt et al., 1998).

The foaming system used by the cold-recycling mixing plant used at the NCAT Test Track, described in Figure 3.8, consisted of relatively small thick-walled steel tubes where encapsulated steam was allowed to expand until the formation of a thin film of slightly cooler asphalt binder was capable of holding a foam bubble through surface tension. This foamed asphalt was then ejected through a spray nozzle to a mixing pugmill, where the provisional expansion of the effective surface of the binder, which caused a temporary state of reduced binder viscosity, allowed for optimum mixing of the binder with the fractionated RAP materials at ambient temperatures.

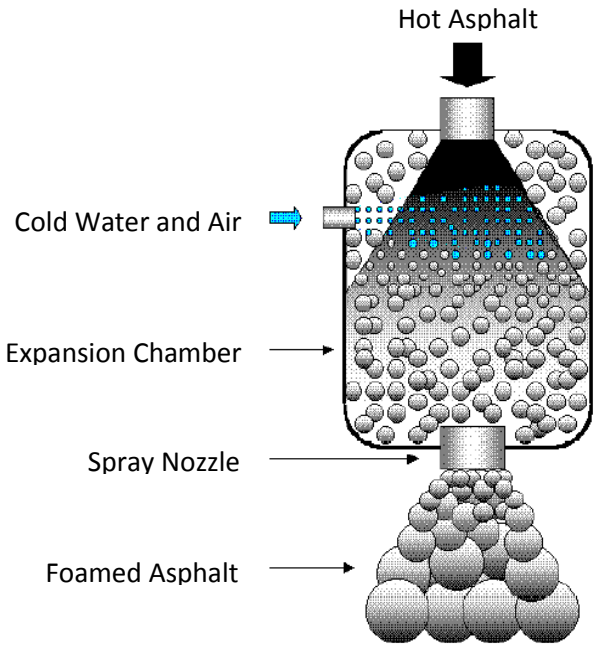

FIGURE 3.8 Asphalt Foaming (Jenkins and Van de Ven, 2001)

During the mixing process of a FCM, the foamed asphalt disperses throughout the aggregate by adhering to the finer particles to form a strong, homogeneous mastic that bonds the larger aggregate particles together (Asphalt Academy, 2009). Due to the rheological characteristics of the asphalt binder, this mastic acts as a thermal bridge between the larger particles enhancing the overall thermal conductivity of the FCM (Côté et al., 2013). Nonetheless, FCM is still a granular material in nature (Jenkins and Van de Ven, 2001) and its thermal conductivity remains lower than that of normal asphalt concrete.

Asphalt Pavements

One single crew was in charge of paving all the sections at the 2012 NCAT Test Track. Figure 3.9 shows a general view of the paving process at the Test Track, where a material transfer vehicle (MTV), a wheeled asphalt paver, a tandem vibratory roller, a pneumatic tire roller (not seen in the picture), and a steel wheel finish roller (not seen in the picture) were used to place and compact all asphalt layers.

FIGURE 3.9 Paving Process at the NCAT Test Track

A comprehensive quality control of the mixtures produced, field densities, and as-built lift thicknesses was performed as part of normal Test Track construction procedures. Individual rolling patterns were determined for each pavement layer in advance by monitoring the densities with a nuclear density gauge on individual test strips built at a nearby location. The compaction process was conducted in accordance with common practice, and included breakdown rolling with a tandem vibratory roller, intermediate rolling with a rubber tire roller, and finish rolling with a static steel wheel roller. Figure 3.10 shows the three rollers used for paving operations.

(a) **(b)** **(c)**

FIGURE 3.10 Rolling Operations Performed by (a) Tandem Vibratory, (b) Rubber Tire, and (c) Static Steel Wheel Rollers

As mentioned before, all the mixtures placed for the 2012 experiment were produced using a WMA technology, to assist during the compaction process. Sections S5-Bottom, S6-Intermediate, S13-Bottom, and S13-Top were produced using 0.5% Evotherm® Q1 additive, a chemistry package designed to enhance coating, adhesion, and workability at reduced temperatures (Prowell et al., 2011). The remaining layers were produced using Astec's Double Barrel Green® WMA system, which uses a multi-nozzle

foaming device to microscopically foam the asphalt particles, reducing production and compaction temperatures significantly (Prowell et al., 2011).

As mentioned before, the GG experiment mainly focused on three sustainable technologies; High-RAP contents, RAS, and GTR-modified binders. RAP and RAS materials were added to the mixtures directly at the asphalt plant, while crumb rubber particles were incorporated into the asphalt binder at the asphalt terminal by means of a "wet process". The use of these three materials, commonly sent to landfills, in asphalt pavements has gained popularity over recent years due to the multiple environmental and economic benefits they generate.

High RAP Contents. Although the use of RAP began in the 1970's, recent increases in production costs and limited availability of aggregates have encouraged the use of higher RAP contents. A high-RAP mixture, commonly defined as an asphalt mixture containing 25% or more RAP by weight of the total mixture (Copeland, 2011), has evident economic and environmental benefits. In fact, mixtures containing up to 50% RAP may generate estimated savings of up to 34% (Kandhal and Mallick, 1997), while conserving energy, reducing emissions, preserving natural resources, and reducing construction debris placed in landfills (Vargas-Nordcbeck, 2012).

Research results seem to indicate that only a small portion of the aged binder in RAP is actually mixed with the virgin binder, which creates a coating of stiff binder around RAP particles and makes them behave as "composite black rocks" (Huang et al., 2005). Additionally, the presence of a larger amount of aged binder may affect the

workability and compactability of high RAP mixtures, while also producing a blue, toxic smoke during paving operations (Vargas-Nordcbeck, 2012).

At the asphalt plant, the RAP materials were blended with super-heated virgin aggregates at the end part of the interior dryer drum of the Double Barrel Drum Mixer®. This allowed a transfer of heat between the superheated aggregates and the RAP, which in turn softened the aged binder and broke the RAP materials into smaller lumps. The resulting combination of RAP and virgin aggregates was then mixed with the asphalt binder at the mixing unit folded around the aggregate drier drum. The use of WMA technologies allowed producing the mixtures at lower temperatures than those required for higher RAP contents.

Recycled Asphalt Shingles. In general, post-consumer (PC) RAS is composed of high quality crushed aggregates, fibers, and may contain more than 30% asphalt binder with a high viscosity (Foo et al., 1999). All these materials are desirable in asphalt mixtures; therefore, the inclusion of PC RAS generates important economic and environmental benefits, by significantly reducing material costs, energy consumption, and emissions (Robinette and Epps, 2010).

Research results seem to indicate that the aged binder derived from RAS can cause a significant increase in the stiffness of the asphalt mixture. In fact, adding up to 5% RAS may cause the binder in the mixture to increase one PG grade (Foo et al., 1999). Furthermore, the use of RAS may improve the rutting resistance of the mixture, but may reduce the fatigue and low temperature cracking resistance. To avoid this, the use of softer virgin binders has been suggested (Foo et al., 1999).

PC RAS from Wedowee, AL was added at the asphalt plant in similar way as the RAP, by mixing the RAS with superheated aggregates at the end of the interior drum and subsequently mixing the combined materials with the asphalt binder. Once again, the use of WMA technologies allowed for lower production temperatures and energy savings during production.

GTR-Modified Binders. Recycled scrap tires are ground and reduced to small rubber particles aptly named ground tire rubber (GTR). These particles are blended with asphalt binder to produce GTR-modified binders, resulting in improved pavement performance and environmental benefits (Heitzman, 1992). Although several grinding methods have been used to produce GTR, they may be classified as ambient or cryogenic, depending on the temperature used in the process. The cryogenic process, which involves freezing the scrap tires with liquid nitrogen, tends to generate more angular GTR than the ambient process, conducted at warmer temperatures (Way et al., 2011).

The process of introducing GTR directly to the virgin binder at the asphalt terminal, is called the "wet process", as it refers to modifying the liquid, or wet, portion of the mixture (Way et al., 2012). During this blending process, the aromatic fraction of the asphalt binder is absorbed by the GTR, causing a physical expansion of the GTR particles to a variable extent, which increases the viscosity of the binder and improves the high temperature stiffness of the mixture (Putman, 2006). The aromatic fraction of the binder plays an important role in the modification process, thus asphalt binders must be carefully selected to satisfy the absorption demands of the GTR (Heitzman, 1992).

Three different asphalt mixtures, containing two different binders modified with individual GTR particle sizes, were used on section S13 at the 2012 Test Track. The top and intermediate layers were built with common SMA and DG asphalt mixtures, respectively. The mixture used for the bottom layer had a gap gradation, and is commonly known as Arizona rubber mixture or asphalt rubber asphalt concrete, ARAC (Kaloush et al., 2003). The use of GTR-modified binders did not affect the paving and compaction operations during the construction process.

3.4 TEMPERATURE MEASUREMENTS

In an attempt to study the thermal interactions of the sustainable asphalt pavements, described previously, field measurements of the temperature variations during the construction process and during the service life of the pavement were performed.

3.4.1 Cooling during Construction

During construction, an infrared hand-held temperature device was used to determine the temperatures at the surface during delivery, laydown, and compaction of each asphalt concrete layer. Four random locations were selected along the paving lane at an approximate distance of 3 ft from the edge of the pavement. An initial temperature measurement of the underlying material (existing pavement layer, granular base or FCM) was taken at each location as the paver approached, as shown in Figure 3.11(a). Once the new material was laid down, the temperature at the four locations was recorded behind the paver and every 3 minutes subsequently until the compaction process was completed,

as shown in Figure 3.11(b). Figure 3.12(a) shows the infrared temperature hand-held-device used for this study.

(a)

(b)

FIGURE 3.11 Measurement of the Temperature of (a) Underlying Materials and (b) Laid Asphalt Concrete

Additionally, a portable, hand-held weather tracker, shown in Figure 3.12 (b) was used to record the wind speed, ambient temperature and humidity three times during paving operations; after laydown of the mixture, during rolling of the layer, and once rolling was completed. Although only the average values were used in the analysis, multiple measurements were made in an attempt to account for any possible weather variation during the paving process. A visual estimation of the sky conditions was also made at the time of construction.

(a) **(b)**

FIGURE 3.12 Instruments Used to (a) Monitor Pavement Temperatures and (b) Weather Conditions during Construction

3.4.2 Long Term Temperature Cycling

A minimum of four temperature probes were installed on each structural section at the 2012 Test Track. Campbell-Scientific's model 108 thermistor temperature probes, with an accuracy of ± 0.3°C over the range of temperatures observed in the field, were chosen due to their continued success in previous research cycles (Timm, 2009). The temperature probes were custom built for each section in an arrangement similar to the one shown in Figure 3.13. Efforts were made to ensure each section contained at least one temperature probe at the top, middle and bottom of the composite asphalt layer. The GG sections contained one additional temperature probe located three inches into the underlying aggregate base. However, the VDOT sections contained three additional temperature probes located within the FCM. Table 3.2 lists the depths of the thermal probes in each section.

FIGURE 3.13 Custom Built Temperature Probes

TABLE 3.2 Temperature Probe Depths

Section	Depth of Probe, inches					
	Probe 1	**Probe 2**	**Probe 3**	**Probe 4**	**Probe 5**	**Probe 6**
N3 (VDOT)	0.0	2.9	5.8	7.8	9.8	12.8
N4 (VDOT)	0.0	1.8	3.6	5.9	8.2	11.2
N5 (GG Control)	0.0	3.0	6.0	9.0	-	-
S5 (GG High RAP)	0.0	3.3	6.5	9.5	-	-
S6 (GG RAP/RAS)	0.0	3.1	6.1	9.1	-	-
S12 (VDOT)	0.0	2.2	4.4	6.6	8.7	11.7
S13 (GG GTR)	0.0	3.2	6.5	9.5	-	-

These temperature probes allow recording hourly maximum, minimum, and average temperatures for each pavement layer during the entire research cycle. An on-site weather station located on the north tangent of the Test Track allowed recording hourly ambient temperatures, wind speed, and humidity conditions for further analysis.

FIGURE 3.14 On-site Weather Station

3.5 SUMMARY

Seven structural test sections were built at the NCAT Test Track as part of the fifth reconstruction cycle, in August and September, 2012. All the mixtures were produced at the same asphalt plant and all the sections were paved in two or three lifts by the same paving crew and equipment.

Four sections in this study constituted the "green group" experiment (GG), and three sections were sponsored by the Virginia Department of Transportation (VDOT). The GG sections were built in three separate lifts with individual asphalt mixtures consisting of multiple combinations of post-consumer (PC) RAS, RAP, and GTR-modified binders. A summary of the mixtures used in each lift was presented in Table 3.1, specifying the mix gradation, binder type (virgin, PMA or GTR-modified), production temperature, RAP content, PC RAS content, and lift thickness, respectively. A detailed description of the mixtures and the construction process was provided. Furthermore, all mixtures were produced using a specific warm mix asphalt (WMA) technology, consisting of either an additive or a foaming process.

The VDOT sections were designed to investigate foamed cold-mix (FCM) and full-depth reclamation (FDR) as base layers. Section N3 consisted of three asphalt concrete layers placed over a fourth layer of plant-produced FCM containing 100% RAP. Similarly, section N4 and S12 consisted of two asphalt concrete layers (top and bottom) placed over a third layer of the same FCM, with the exception that section S12 contained a CTB layer.

During construction, a hand-held temperature device was used to determine the temperature of all the asphalt materials every three minutes, while a portable weather tracker allowed determining and recording the environmental conditions. Additionally, a minimum of four temperature probes were installed in each pavement section, allowing to collect hourly temperatures within the pavement structure, while a local weather station allowed recording hourly ambient conditions during the entire research cycle.

CHAPTER FOUR

INFLUENCE OF SUSTAINABLE TECHNOLOGIES ON PAVEMENT CONSTRUCTION COOLING

4.1 INTRODUCTION

With the accelerated development of innovative sustainable technologies and methods for asphalt pavements arises an essential need for continued assessment of the constructability and compactability of such advances. As described before, once paving operations have begun, adequate control of the temperatures during compaction is the most important factor in achieving proper densification of asphalt concrete. Therefore, a constant examination of the cooling rate in the field of these new technologies would allow for a fast and accurate verification of the factors important for proper construction and performance. To evaluate the effect of innovative sustainable technologies on the cooling rate of asphalt pavement layers, a critical assessment of the accuracy of the MultiCool program in predicting the cooling rate of the mixtures used for the 2012 structural experiment at the Test Track was performed. Specific weather information, mixture characteristics and as-built properties were used as inputs to generate simulated cooling curves in MultiCool. A statistical analysis of the results was conducted to compare the simulated cooling curves to field measurements under controlled conditions.

4.2 MULTICOOL SIMULATIONS

The conditions documented during construction were used as inputs to perform pavement cooling simulations with MultiCool. As previously described, the model used by the software takes into account mixture and layer specifications to predict the cooling rate of asphalt, based on one-dimensional heat transfer by conduction (asphalt – base), convection (asphalt – surrounding environment) and solar radiation. In that way, the software inputs, divided in four main categories described previously, were estimated as described herein.

The first input (Start Time) referred to the specific time and date of the beginning of paving operations recorded during construction. This information is directly used by the software to calculate the solar declination and the solar hour angle, which are later used to determine the incoming solar radiation at the surface of the pavement (Chadbourn et al., 1998).

The second input in the software describes the *Environmental Conditions*. Average ambient air temperature, wind speed and sky conditions documented during paving operations were specified as inputs. These inputs pertain directly to the surface boundary conditions and are assumed constant during the cooling of the lift (Timm et al., 2001). Multiple measurements of the ambient air temperature and wind speed revealed a relatively low variability of the environmental conditions during paving, with standard deviations ranging between 0.5°F and 6.0°F, and 0.3 and 2.0 mph, respectively. Nonetheless, the cooling measurements were obtained during approximately one hour of paving, and certain variability was expected. The latitude of the site was projected as 33 degrees north in accordance with previous studies (Vargas-Nordcbeck and Timm, 2011).

This coordinate is used by the software to calculate the solar zenith angle during paving operations. Additionally, it is combined with the *Start Time* inputs, previously mentioned, to calculate the average solar flux at the surface of the pavement (Chadbourn et al., 1998).

The next input in the software refers to the *Existing Surface*. The material type was selected as asphalt concrete (AC) or granular base depending on the lift being analyzed. In the case of the FCM, multiple simulations were performed to determine which predetermined input ("AC" or "granular base") produced the lowest difference between measured and predicted temperatures. The moisture content was input as dry and the state of moisture was selected as unfrozen to simulate the existing conditions as close as possible. This combination of existing base material, moisture content and state of moisture automatically sets laboratory-determined default values from pre-existing studies for the thermal properties of the base materials (Timm et al., 2001). The average temperature of the existing surface, recorded during construction, is used by the program as an initial equilibrium condition and is assumed constant throughout the layer (Timm et al., 2001; Vargas-Nordcbeck and Timm, 2011).

The final input category concerns the *Mix Specifications*. As mentioned before, the MultiCool model generates a multi-layer solution allowing the simulation of a maximum of nine pavement lifts paved in immediate succession. The sections built at the Test Track were paved at least one day before the subsequent lift, allowing enough time for the mix to completely cool to an ambient condition. For this reason, each lift was modeled individually. The mixture used for each lift was described as a function of the gradation and binder grade, determined during plant production quality control. While the

binder grade is only intended as a label for the mixture, the gradation is used by the software to establish default thermal properties, determined by Chadbourn et al. (1998) for dense-graded (DG) mixtures and SMA mixtures. Although both gradations showed similar temperature trends, thermal conductivity of SMA was found to be significantly lower than that of DG mixtures. However, in the original calibration, these results were obtained using only a 120/150 penetration asphalt binder (Chadbourn et al., 1998). Therefore, the MultiCool model does not consider the possible effect of binder grade variation. Some of the potential error encountered in the simulations may be attributed to the assumption of these values.

Previous validation studies demonstrated a better agreement of the model when as-built rather than design lift thicknesses were used (Chadbourn et al, 1998; Timm et al., 2001). For this reason, as-built thicknesses obtained from surveying after construction, were used for the simulations in an effort to minimize possible errors. The delivery temperature, defined as the temperature of the mixture behind the paver, was measured directly behind the screed of the paver.

4.3 STATISTICAL ANALYSIS

The measured temperatures were compared to the predicted temperatures obtained from the MultiCool simulations. A direct comparison of the measured and predicted temperatures was performed to determine the relative accuracy of the MultiCool predictions. Similarly, the difference between the measured and predicted temperatures was calculated and an individual cumulative distribution function was obtained for each pavement layer. The accuracy of the model was determined by calculating the percentage

of data points within the ± 18°F (10°C) range found in previous validation studies (Chadbourn et al., 1998; Timm et al., 2001, Vargas-Nordcbeck and Timm, 2011). The average difference and standard deviation of each pavement layer were subsequently used to analyze the effect of different factors such as the amount of RAP and the use of GTR modified binders and RAS on the cooling rate of asphalt layers with different thicknesses. Pairwise and multiple statistical comparisons were performed among specific mixtures in an effort to provide a more clear explanation of the effect these sustainable technologies have on cooling rates.

Some basic analyses, conducted in previous validations of the model, were also performed as part of this study as a method of confirmation of previous findings. However, the temperature data included in this investigation allowed a more comprehensive analysis of the MultiCool model focusing on the effect of the aforementioned factors on the cooling rate.

4.4 COOLING CURVES

The cooling curves obtained using the MultiCool model presented a very similar trend to the temperatures measured in the field, with relatively rapid initial cooling leveling over time in a logarithmic form. These results were consistent with all previous validations (Chadbourn et al., 1998; Timm et al., 2001, Vargas-Nordcbeck and Timm, 2011). Figures 4.1 and 4.2 show an example of the measured and predicted cooling curves for two of the sections investigated. Section N5 is the control section, while section S5 is the increased RAP content section, both part of the GG experiment. In general, all measured and predicted cooling curves followed the same trend. However, certain layers (i.e. S5-

Bottom) presented relatively more scatter in the data than others (i.e. N5-Top), leading to the need for further verification of the acceptability and accuracy of the MultiCool model.

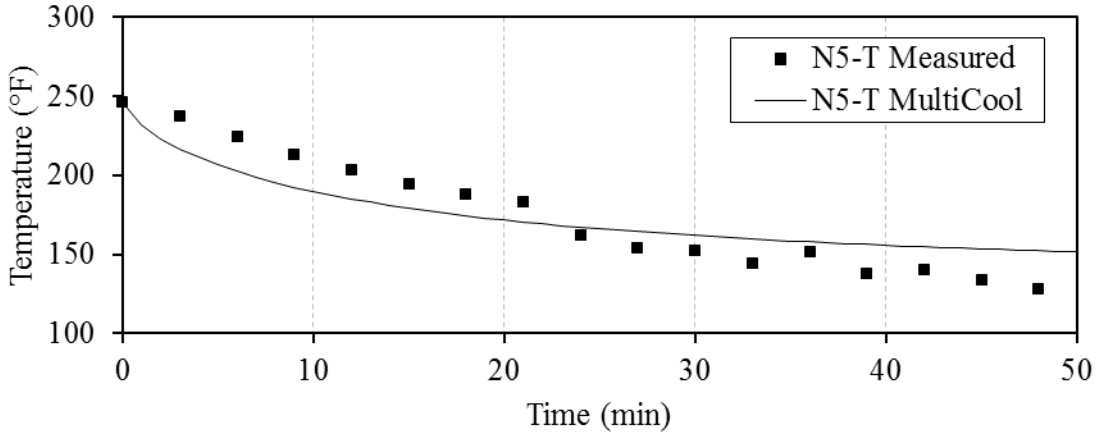

(a)

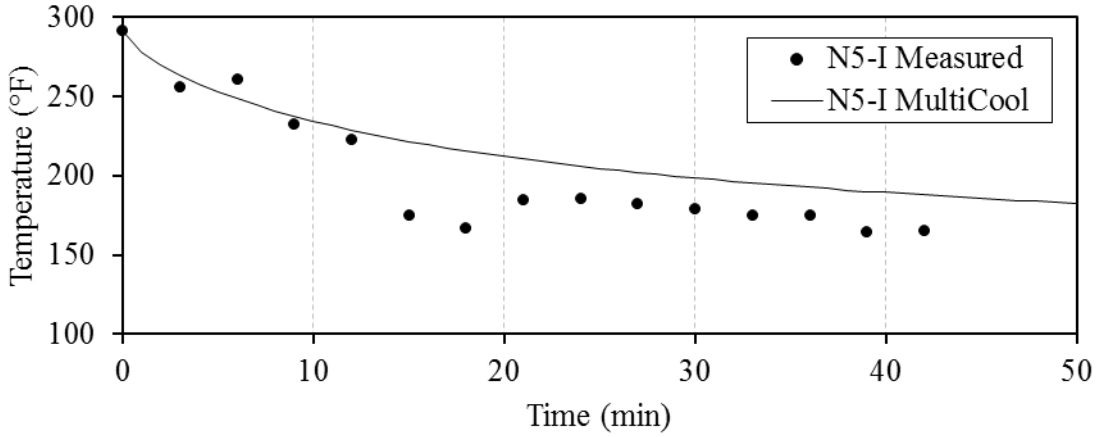

(b)

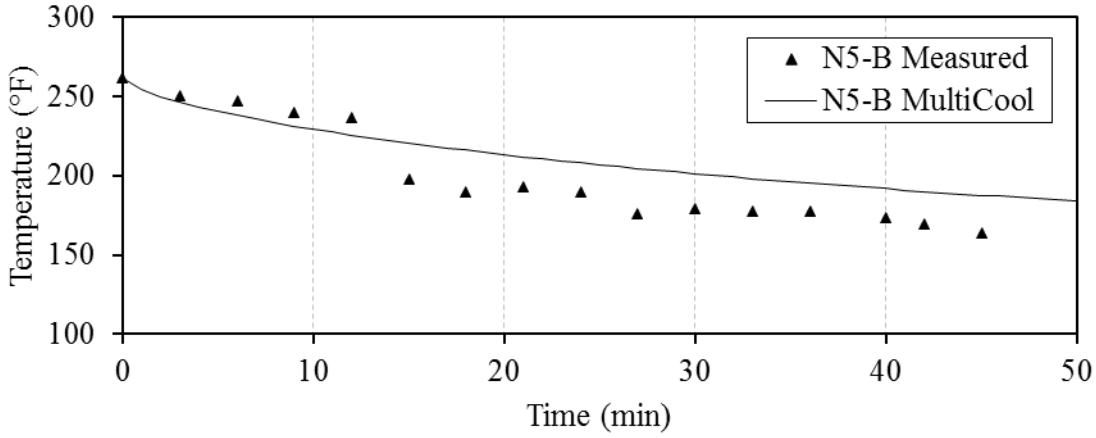

(c)

FIGURE 4.1 Cooling curves for lifts (a) N5-Top, (b) N5–Intermediate, (c) and N5–Bottom

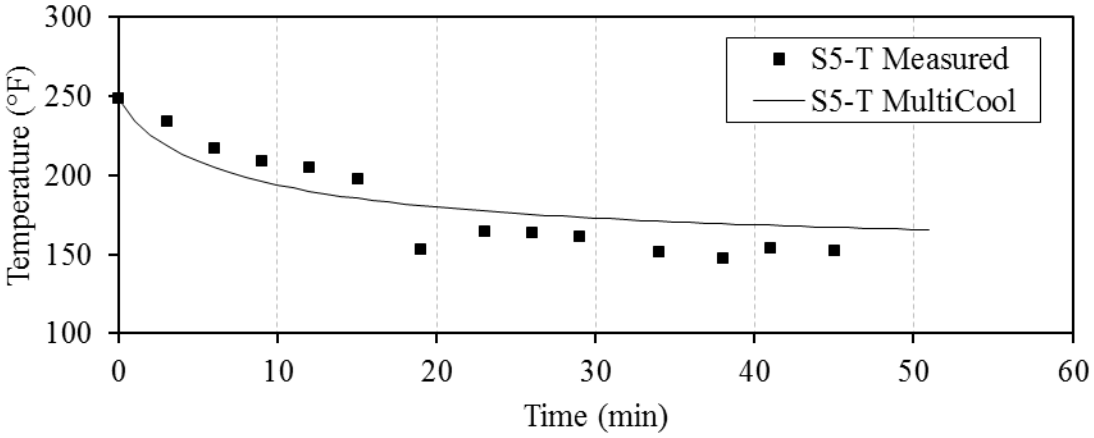

(a)

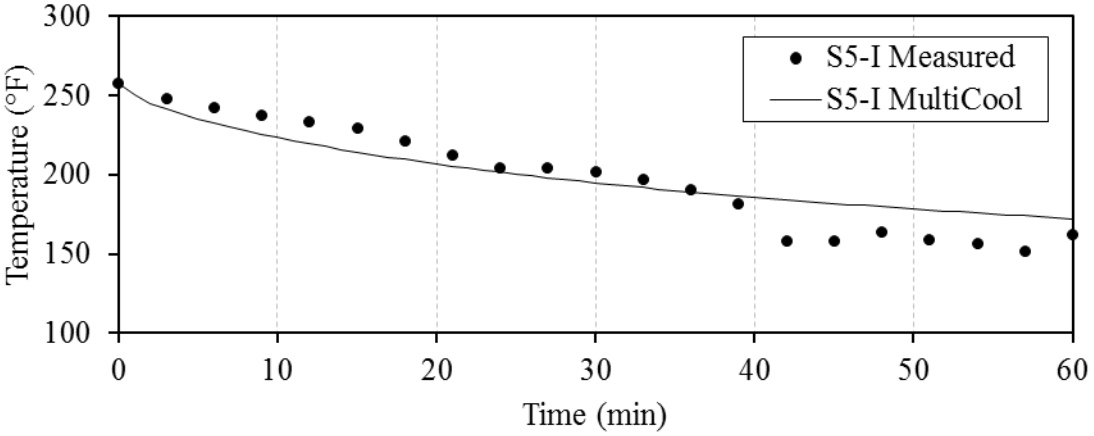

(b)

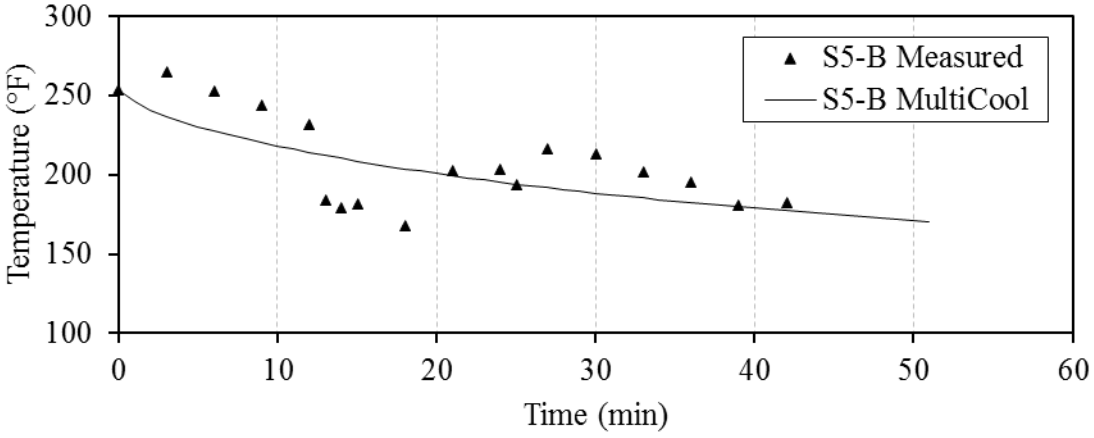

(c)

FIGURE 4.2 Cooling curves for lifts (a) S5-Top, (b) S5–Intermediate, (c) and S5–Bottom

As evident in the previous figures, the measured temperatures were scattered around the MultiCool prediction. These variations may be partially attributed to the combined effects of the compaction process and the measurements performed in the field. As described previously, measurements were made using a hand-held temperature device, which allows measuring the surface temperature of the pavement based on infrared signals and considers a specific area, defined by the distance and the inclination of the device when the measurement is taken. Although special care was taken to maintain the same distance and angle of the device for all measurements, sampling variations may have affected the measurements, causing the observed scatter of the temperature data. Additionally, the common paving practice of using water on the rollers to avoid the mixture adhering to the drum, as shown in Figure 4.3, may have caused some variations of the temperature readings.

FIGURE 4.3 Water Sprayed on the Drum of the Vibratory Roller

Figure 4.4 shows the effect of the roller passes for layer N5-Intermediate and S-6 Intermediate. The time lapse for each rolling stage (i.e. breakdown, intermediate, and finish) in the same place where measurements were taken is represented by an individual strip. As mentioned before, breakdown rolling was performed by a double drum vibratory roller, intermediate rolling was performed by a pneumatic tire roller, and finish rolling was performed by a static steel wheel roller. The trend for the measured temperatures seems to be affected by the rolling of the section. In fact, a slight discontinuity in the trend of the measured temperatures may be observed, especially for the breakdown rolling stage, while the MultiCool-predicted temperatures maintain a constant trend regardless of the rolling stage. The observed discontinuities may then be explained by two main conditions; the effect of the thin water film and the densifications of the mix. The elevated temperature of the mixture during compaction rapidly evaporates the thin water film created in each roller pass, transferring energy between the pavement and the environment, and thus accelerating the loss of heat by convection. On the other hand, breakdown rolling has been demonstrated to induce a greater increase in density than other rolling stages, during the compaction process (Chadbourn et al., 1998). This seems congruent with the observed results, where the largest discontinuity in measured temperatures was observed after the first pass of the breakdown roller. The MultiCool model considers constant densification of the layer, and therefore doesn't account for the individual passes of each roller. Nonetheless, predicting the exact time of the roller pass over the layer would be virtually impossible, and thus assuming a constant densification seems to be the most realistic approach available to model compaction in a program such as MultiCool.

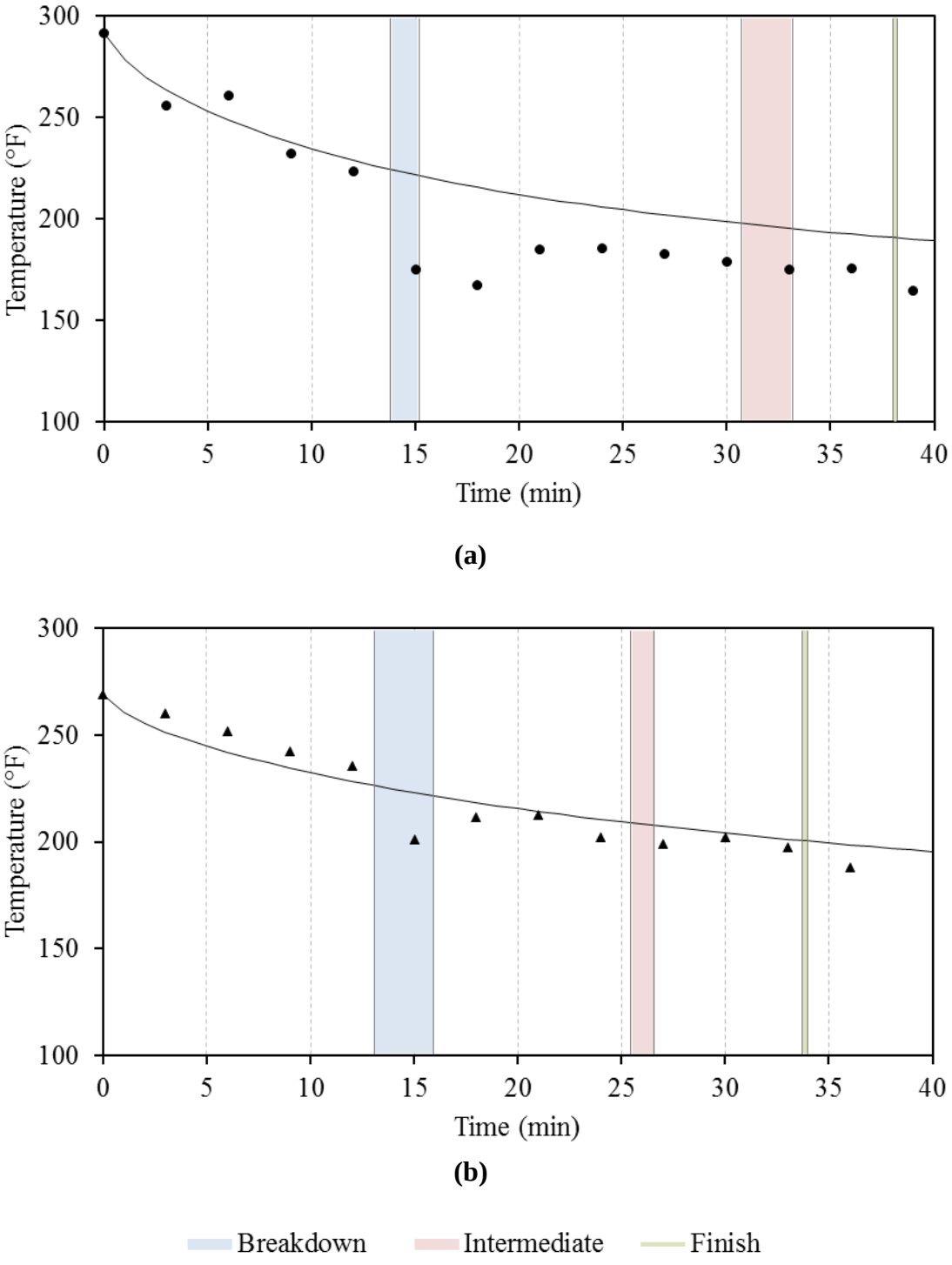

FIGURE 4.4 Roller Passes for (a) N5-Intermediate and (b) S6-Intermediate

4.5 ACCEPTABILITY OF THE MULTICOOL MODEL

To assess how close the model predicts the temperatures in the field, direct comparisons of measured and predicted temperatures were performed for each layer. Examples of these comparisons are presented in Figures 4.5 and 4.6, where the letters "T", "I" and "B refer to the top, intermediate and bottom layers, respectively. The relative scatter of the results, in reference to the line of equality (LOE), indicates the effectiveness of the MultiCool model in describing the temperatures measured in the field. Additionally, for each asphalt concrete layer, the best-fit linear trend line (LTL) was included in the figures to assist in visually comparing the trend of each layer with the LOE.

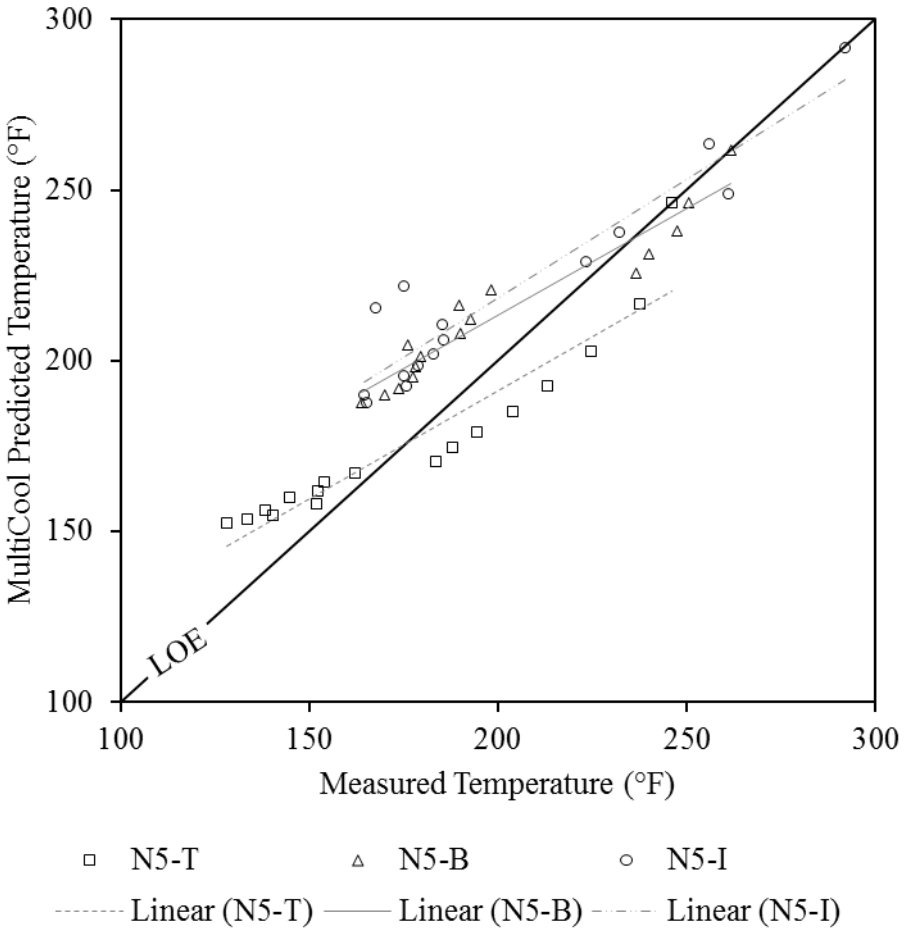

FIGURE 4.5 Measured versus predicted temperatures for section N5

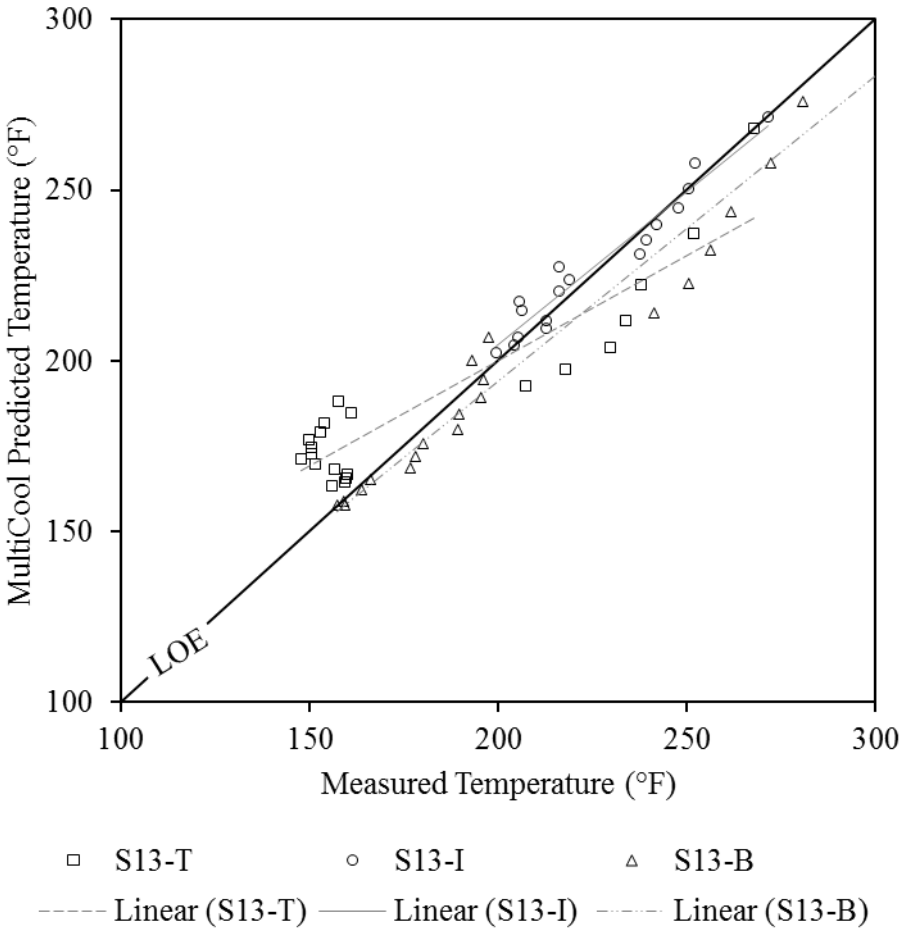

FIGURE 4.6 Measured versus predicted temperatures for section S13

In general, the data for all test sections followed a similar trend as that observed in Figures 4.5 and 4.6, where best fit trend-lines transect the equality line. This indicates that the cooling rate from the MultiCool model has a tendency to under-predict for higher temperatures and over-predict for lower temperatures in the analyzed sections. This may be attributed to the variability of the thermal conductivity of the mixture during rolling operations. As mentioned before, the MultiCool software uses default thermal conductivity values to perform the simulations. However, this property is directly affected by specific conditions of the mixture, such as density (Côté et al., 2013) and temperature (Chadbourn et al., 1998), and is not constant throughout the cooling process.

Although previous validation studies only analyzed general trends, similar results were reported with temperature under-predictions at the beginning of compaction operations (Chadbourn et al., 1998; Timm et al., 2001), and over-predictions over time (Vargas-Nordcbeck and Timm, 2011). The observed trends may also be caused by the difference between compaction process in the field and the densification considered in the model, as explained previously.

A more objective assessment of the precision of the MultiCool model was achieved by determining the estimated standard error (SE) of the predicted temperatures for each pavement layer, as shown in Equation 16. Figure 4.7 shows a graphical summary of the estimated standard errors obtained for all paved lifts, where lower SE values designate more precision of the model, thus better correlations between measured and predicted temperatures (Devore, 1995).

$$SE = \sqrt{\frac{SSE}{n-1}} \tag{16}$$

Where: SE = Estimated standard error of the prediction

SSE = Error sum of squares = $\sum\left(T_{measured\ i} - T_{predicted\ i}\right)^2$

n = Number of measurements performed for layer *i*

$T_{measured\ i}$ = Measured pavement temperature for layer *i*

$T_{predicted\ i}$ = MultiCool predicted pavement temperature for layer *i*

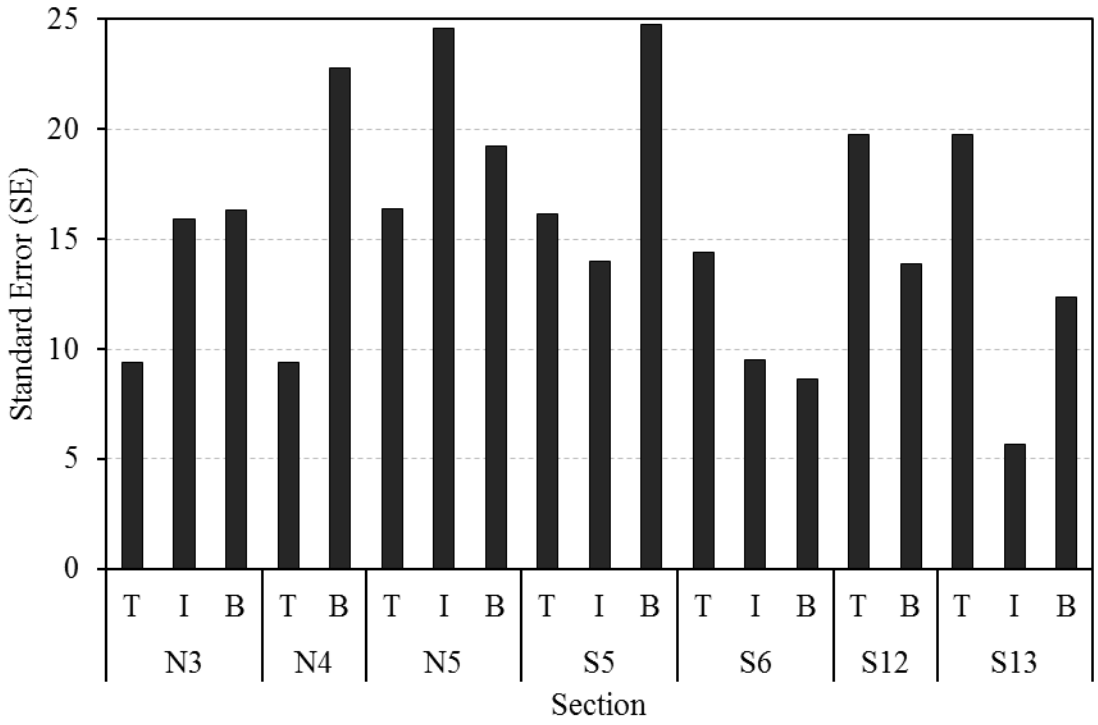

FIGURE 4.7 Standard error of the predictions from the MultiCool model

The bottom layer on section S5 and the intermediate layer on section N5 showed the highest SE values, which may be explained by a reduced slope and relative scatter of the data, as observed for each layer in Figures 4.5. Similarly, the lowest SE was obtained for the intermediate layer on section S13, in which the scatter of the data was very low and the slope of the LTL was very close to that of the LOE. In that way, SE values are significantly influenced by the scatter of the measured temperatures. To accomplish a more accurate comparison of the results; a normalized value was obtained by dividing the SE values by the standard deviation of the measured temperatures ($\sigma_{measured}$). This normalized standard error ratio (SE/ $\sigma_{measured}$) allowed evaluating the precision of the MultiCool model without the influence of the variability of the measurements. Figure 4.8 shows the calculated SE/$\sigma_{measured}$ values for the sections included in the study.

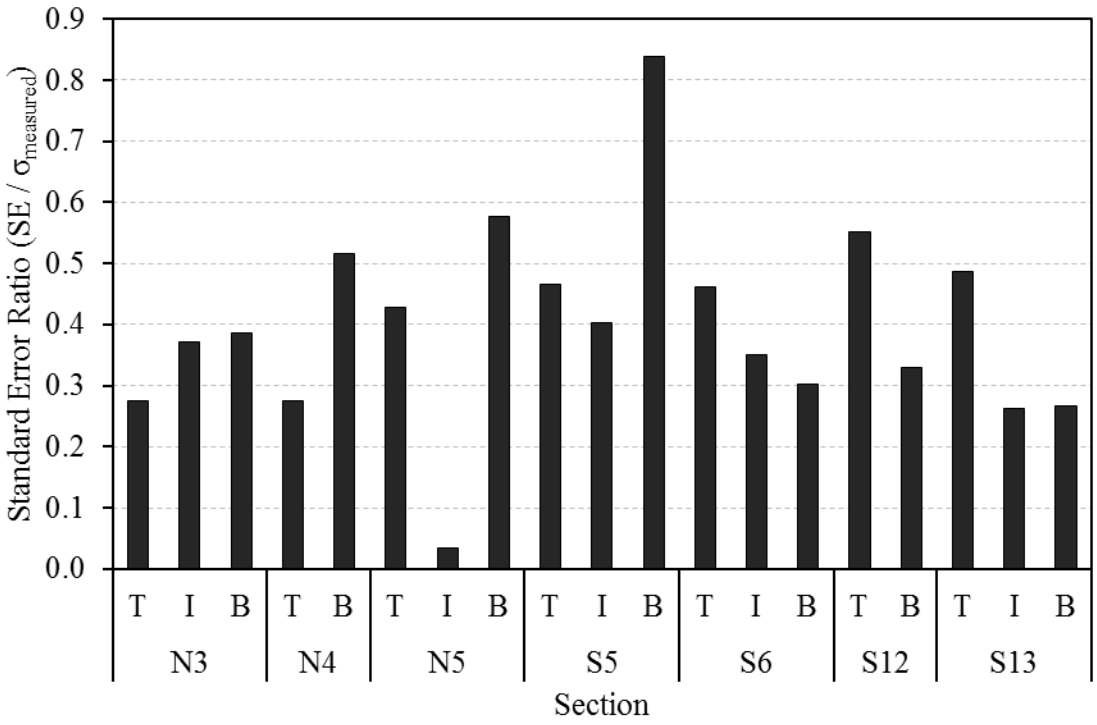

FIGURE 4.8 Precision of the MultiCool model

Once again, the bottom layer on section S5 shows the highest values, indicating the worst precision of the MultiCool model. This was evident in Figure 4.6, and may be attributed to measuring errors. In fact, the bottom layer on section N5 was the first paved lift of the structural experiment, and possible measurement errors made at this point due to the inexperience of the operator, were amended by focusing on the repeatability of the measurements in all other sections. Nonetheless, the results for all other sections are relatively lower, indicating that, in most cases, the MultiCool program tends to predict the pavement temperatures relatively well. Therefore, it is necessary to assess the level of accuracy of the model and the tolerance of the MultiCool software.

4.6 ACCURACY OF THE MULTICOOL MODEL

To assess how accurate the MultiCool model is in predicting the temperatures in the field, the difference between the measured and predicted temperatures was calculated and an individual cumulative distribution function was obtained for each pavement layer. Figure 4.9 shows the cumulative distribution function (CDF) plot for sections N5 and S6. Section N5 (control) had the highest variability suggesting that the observed deviations from the tolerance range may be also due to the inherent variability of the measurements and simulation processes.

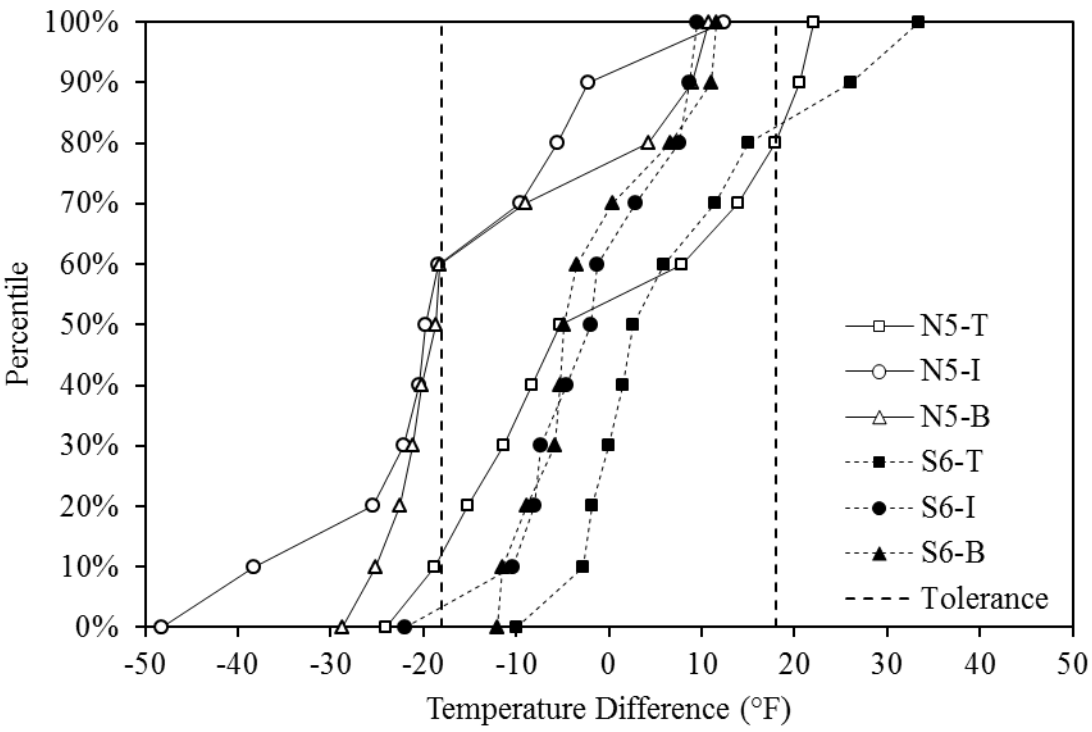

FIGURE 4.9 CDF plot for temperature differences for sections N5 and S6

Considering the ±18°F (10°C) tolerance, found in previous validations (Chadbourn et al., 1998; Timm et al., 2001; Vargas-Nordcbeck and Timm, 2011), the percent temperature differences detected within the allowable limits was calculated. A summary of the results obtained for each section is presented in Figure 4.10. While the analysis presented in the previous section addressed the statistical differences based on specific SE and $SE/\sigma_{measured}$ values, evaluating the percentage of the temperature difference within the tolerance evaluates the same concept from a more practical point of view. Certain sections, which had shown relatively high $SE/\sigma_{measured}$ values, presented a relatively higher percentage of the temperature differences within the tolerance. Such is the case of section S5-Bottom which presented the highest standard error ratio (0.84), but was found to have 76.9% of the values within the ±18°F (10°C) tolerance. This seems to indicate that even if, in some cases, the MultiCool model was not the best predictor of the temperatures in the field; the values reported by the software fall within the allowable tolerances and may be used in the field with sufficient confidence. In other words, even if the predictions of the MultiCool software are not entirely accurate, the calculated time available for compaction is acceptable for planning paving operations in the field. In that way, the results indicate that the MultiCool model may be used to predict the construction cooling of all asphalt concrete mixtures included in this study, with sufficient confidence.

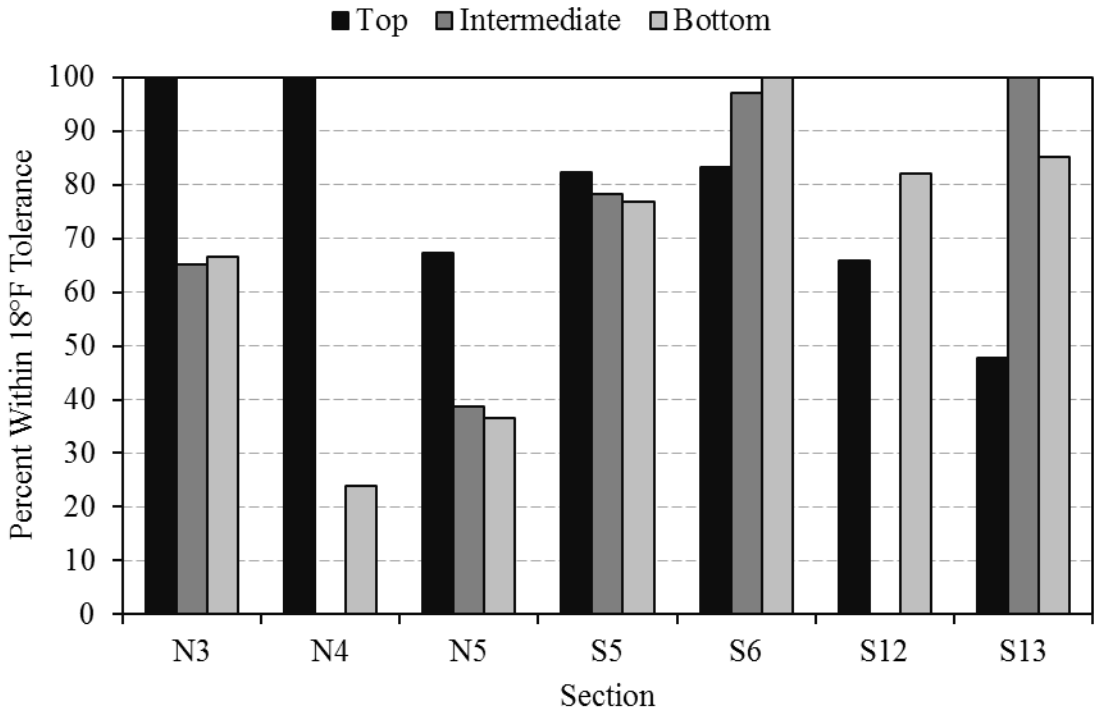

FIGURE 4.10 Percent within the 18°F tolerance by pavement lift

An Anderson-Darling test, performed on the temperature differences for all test sections revealed that only two layers, N4-Bottom and N5-Bottom, followed a non-normal distribution. To determine if the distribution for these two sections was significantly non-normal, an analysis of the skewness and the kurtosis was performed. By considering the differences between measured and predicted temperatures for each layer as individual data sets, the standard error of the skewness (SES) and the standard error of the kurtosis (SEK), were used to determine if the ranges of skewness and kurtosis values were within a reasonable tolerance. As proposed by Price (2013), if the values obtained by dividing the skewness by SES and the kurtosis by SEK were found to be within a ± 2 range, the data could be assumed to follow a sufficiently normal distribution. The results of this analysis indicated that even if the bottom layers on sections N4 and N5 followed a

non-normal distribution, the distribution could be assumed normal for subsequent statistical analyses.

Considering all layers followed a normal distribution, a hypothesis test could then be performed on the mean of the absolute value of the differences for each individual layer. This revealed that six of the nineteen lifts investigated exceeded 18°F. In fact, there seemed to be sufficient statistical evidence to demonstrate that layers N4-Bottom, N5-Intermediate, N5-Bottom, S5-Bottom, S12-Top, and S13-Top exceeded the allowable $\pm$18°F range at a 95% confidence level. These six sections also exhibited the highest variability (higher $SE/\sigma_{measured}$ values) in Figure 4.8. Furthermore, the intermediate layer in section S5 and the top layer in section S13 were of particular interest for the analysis. Layer S5-Intermediate contained an increased RAP content, while layer S13-Top consisted of an SMA mixture with a GTR-modified binder that was produced and placed at lower temperatures. This indicates that factors such as increased RAP contents, the mix gradation, and the presence of GTR or RAS, may have an effect on the precision of the MultiCool model. Each factor is discussed in greater detail in the following sections.

4.7 INCREASED RAP CONTENT

Figure 4.11 shows the effect of the amount of RAP in the prediction of pavement cooling from the MultiCool model. An individual level was assigned to the RAP contents of the analyzed mixtures. A multiple-comparison between all pairwise differences observed for each RAP content of the analyzed mixtures revealed a statistical difference, at a 95% confidence level, between the mixtures containing 35% RAP and the mixtures containing only virgin aggregates. However, all the mixtures containing 35% RAP (N5-Intermediate, N5-Bottom, and S5-Bottom) and one of the two mixtures with only virgin aggregates (S13-Top) correspond to the pavement lifts with the poorest MultiCool prediction, which may be adversely affecting the results.

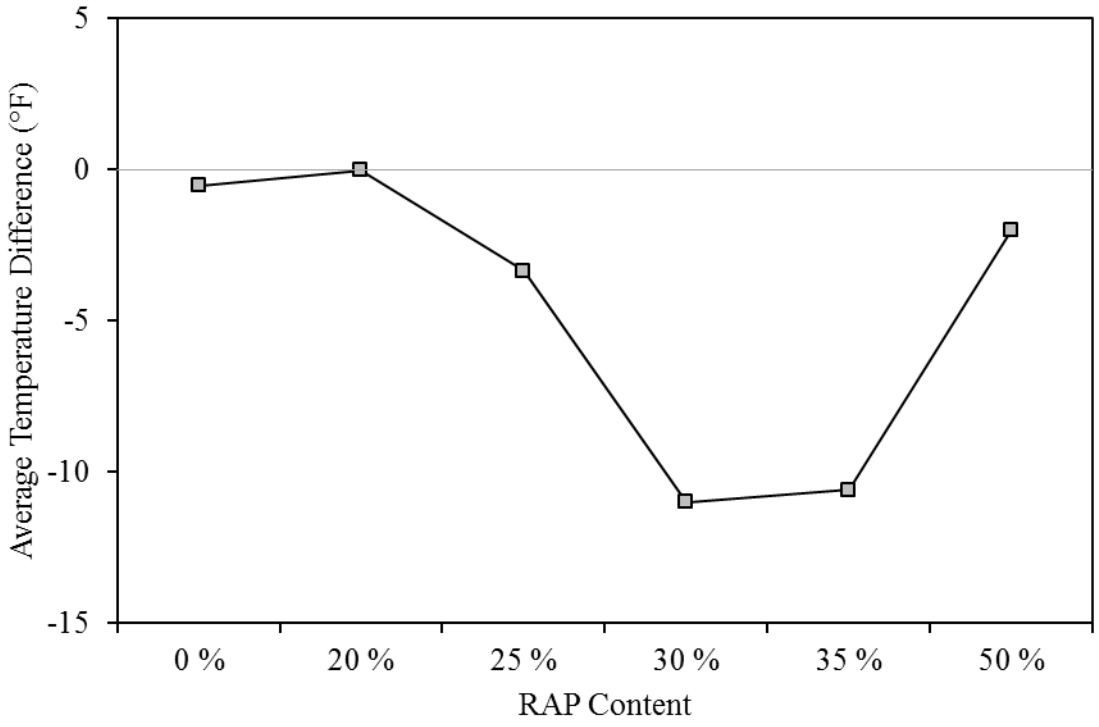

FIGURE 4.11 Main effects plot for RAP content

A better assessment of the true effect of increasing the RAP content on the cooling rate was accomplished by comparing layers N5-Top and S5-Intermediate, which had similar gradation, binder grade and laydown temperatures, but different RAP contents. This analysis demonstrated that there was no practical difference between the average cooling prediction of a mixture with 50% RAP (S5-Intermediate) and a mixture with only 20% RAP (N5-Top). Similar results were also found in a previous validation study (Vargas-Nordcbeck and Timm, 2011). The irregular results obtained for the mixtures containing 35% RAP may then be attributed to other mixture properties, or testing error, and not necessarily to the increased RAP content.

The two data sets were sufficiently normal and the average temperature was found to be statistically similar, differing by only 2.0°F. However, the variation of the temperature differences ranged between -24.1°F and 22.1°F for layer N5-Top, and from -26.3°F to 15.5°F for layer S5-Intermediate, as shown in Figure 4.12. This variation produced differences as high as 8.53°F for the 90^{th} percentile, which were not considered in a simple comparison of the mean temperature differences using a t-test.

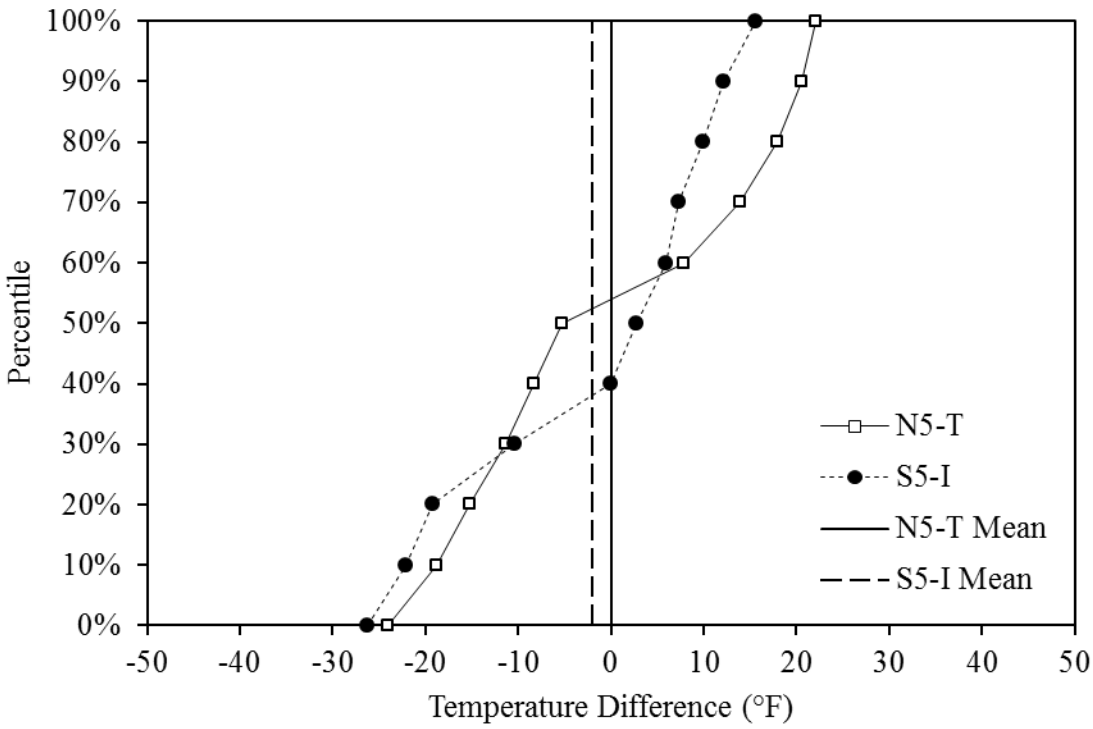

FIGURE 4.12 CDF plot for layers N5-Top and S5-Intermediate

A more robust analysis was then performed using the absolute temperature difference for the two layers. To statistically validate the similarities between the cumulative distributions for layers N5-Top and S5-Intermediate, a Kolmogorov-Smirnov (KS) test was performed. A KS test considers the relative distribution of two data sets and, unlike a t-test, checks for statistical differences in the entire distribution and not only in the mean. The D-statistic obtained from a KS-test represents the maximum vertical deviation between two cumulative fraction functions, revealing the maximum difference between the two data sets (Saint John's University, 2013). Figure 4.13 shows the cumulative fraction or empirical distribution function plots for the absolute values of the temperature differences obtained for layers N5-Top and S5-Intermediate. A KS-test revealed a maximum vertical deviation (D-statistic) of 0.3249, which indicates a relative

difference between the two data sets. However, no statistical difference (p=0.223) was detected, confirming the previous results found for the mean difference values. Therefore, it may be established, with sufficient certainty, that the presence of increased RAP contents doesn't have a significant effect on the cooling of asphalt concrete during construction.

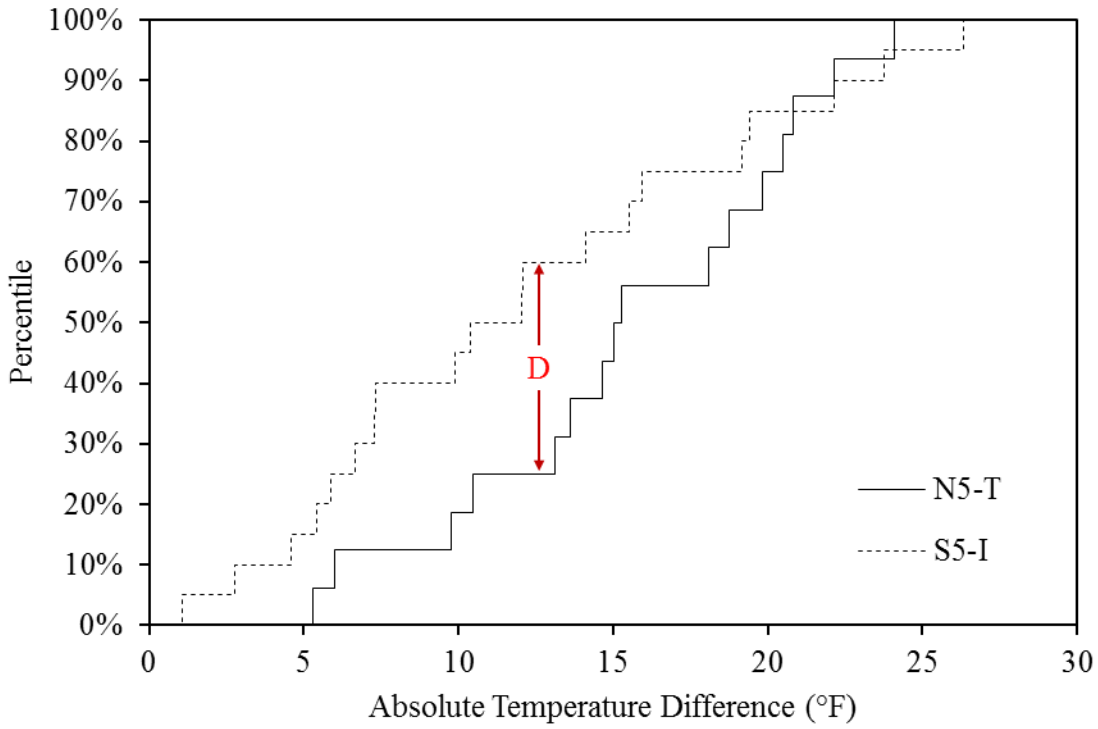

FIGURE 4.13 Cumulative fraction plot for the absolute temperature differences for layers N5-Top and S5-Intermediate

4.8 MIXTURE GRADATION

Seven of the nineteen paved lifts corresponded to gap graded mixtures, or more generally SMA gradations as specified in the software. As explained before, the original cooling model was based on a variation in the thermal properties of the material depending solely on the gradation of the mixture (Chadbourn et al., 1998). To assess the effect of the mixture gradation on the cooling rate prediction, a statistical comparison was performed between layers N5-Top and S5-Top, as shown in Figure 4.14. These two layers had similar binder grade, lift thickness, laydown temperature and RAP content, but different gradations. The analysis confirmed previous validation studies, showing that the difference between the predicted and measured temperatures was similar, at a 95% confidence level, for DG and SMA mixtures. These results support using the thermal properties already included in the MultiCool software.

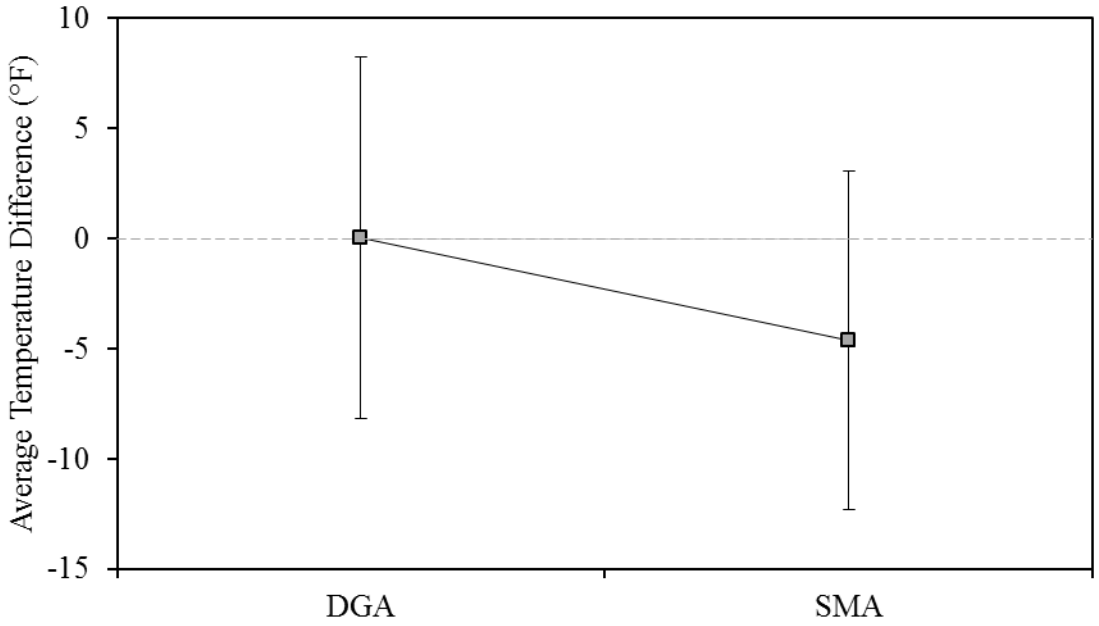

FIGURE 4.14 Main effects plot for mixture gradation

4.9 RECYCLED ASPHALT SHINGLES

The effect of RAS on the prediction of the mixture cooling rate is described in Figure 4.15. The steeper slope observed for the RAS mixtures, in contrast with the non-RAS mixtures, shows that the effect of RAS is governed by the gradation. A multiple comparison between all four conditions (RAS DG, RAS SMA, No-RAS DG, and No RAS-SMA) revealed that the SMA mixture containing RAS was only statistically different from the DG mixture without any RAS, at a 95% confidence level. Similarly, a KS-test performed between layers S6-Top, a SMA mixture containing RAS, and N5-Top, a DG mixture without any RAS, revealed a statistical difference (p=0.031) between the two conditions. This suggests that even if the MultiCool model is adequately predicting the pavement cooling of RAS mixtures, the presence of RAS may have a greater influence on the thermal properties of SMA mixtures than DG mixtures.

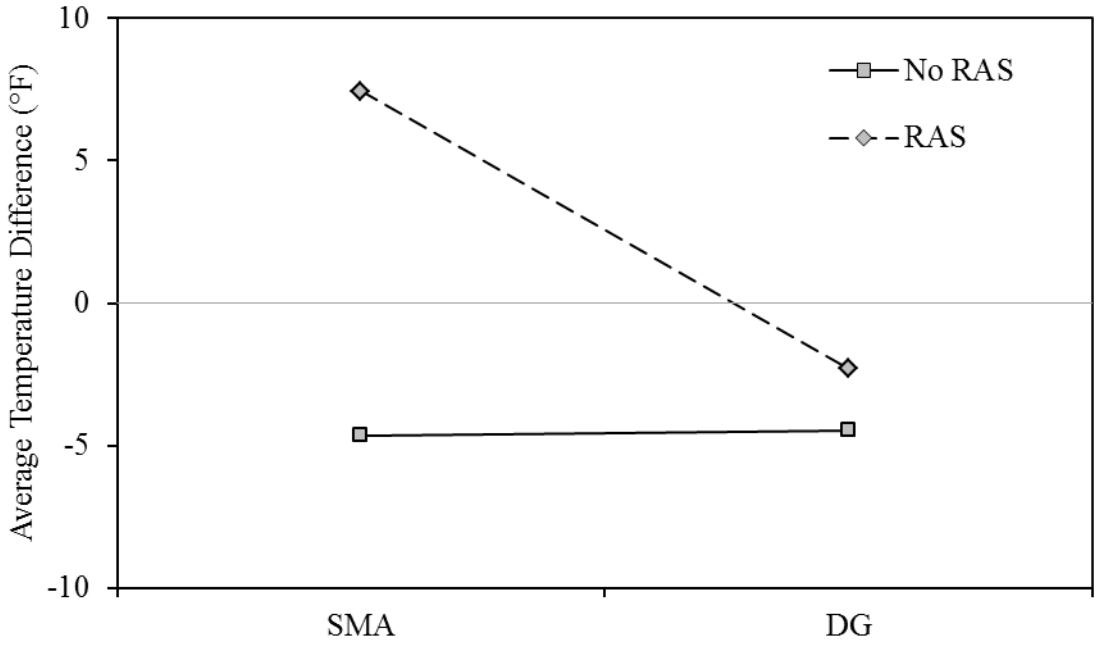

FIGURE 4.15 Interactions plot for RAS

4.10 GROUND TIRE RUBBER

The effect of GTR-modified binders on the prediction of the mixture cooling rate is explained in Figure 4.16, considering layers S13-Top and S13-Intermediate as the GTR mixtures with SMA and DG gradations, respectively. The different slopes observed for the GTR mixtures and the No-GTR mixtures show that the presence of GTR affects the MultiCool model, although it is difficult to estimate if the effect is over-predictive or under-predictive from these results. A multiple comparison between all four mixture types revealed that in all cases the average temperature difference was statistically similar, at a 95% confidence level. However, the effect of GTR on the temperature differences is evident, especially when analyzing Figure 4.17, where strong variations in the CDF plots seem to indicate differences between sections containing GTR-modified binders and sections containing virgin binders.

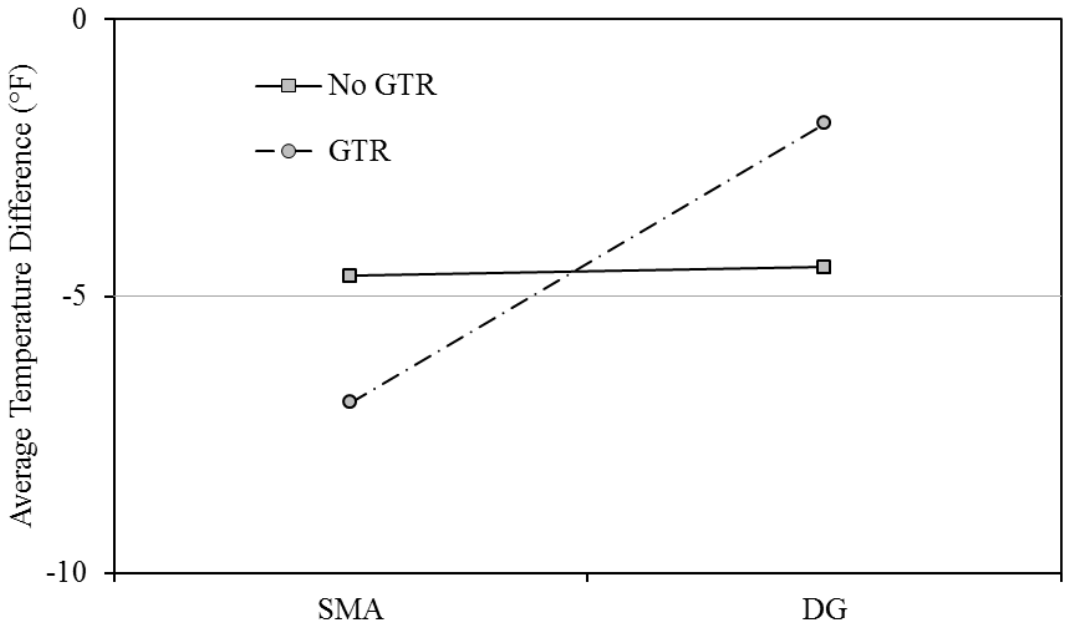

FIGURE 4.16 Interactions plot for GTR-modified binders

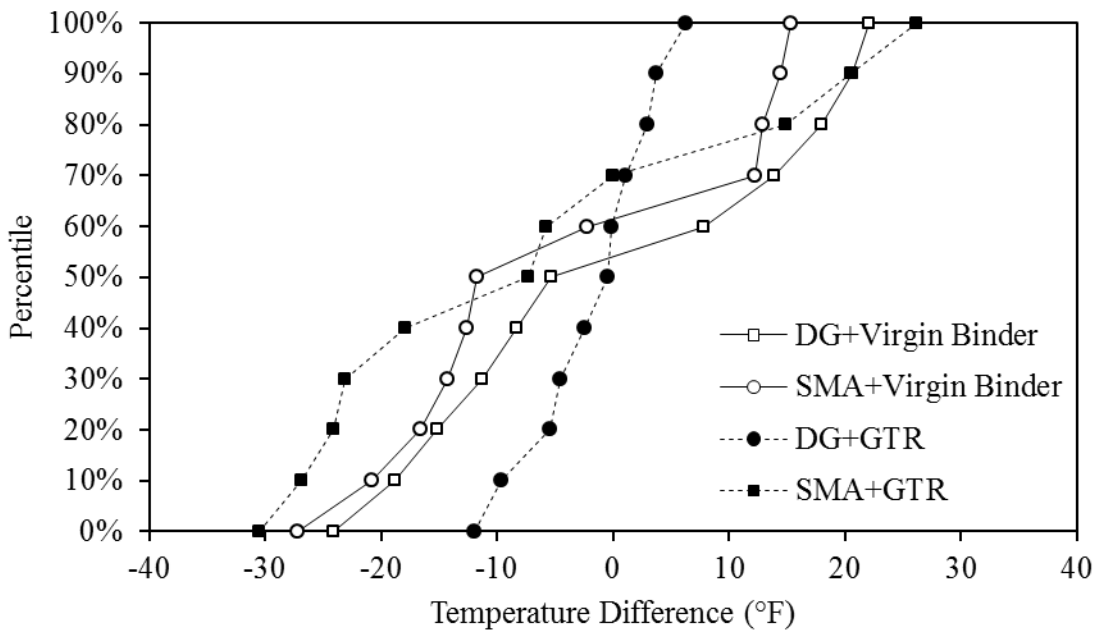

FIGURE 4.17 CDF plot for sections with GTR and virgin binders

A thorough analysis of the absolute temperature differences, based on the KS test, revealed clear statistical differences between the mixtures containing GTR-modified binders and those containing virgin binders. As shown in figure 4.18(a) for SMA mixtures, the use of GTR-modified binders seems to be affecting the predictions of the software, resulting in a maximum vertical difference of 40.5% (p=0.094) between the SMA mixtures containing different binders. Similarly, in the case of DG mixtures, shown in Figure 4.18(b), the maximum vertical difference was found to be 70.6% (p=0.000), suggesting a significant difference. A final case, considering two mixtures containing GTR-modified binders, revealed a substantial difference between DG and SMA mixtures (p=0.000), as shown in Figure 4.18(c). All this seems to indicate that, even if the MultiCool model continues to describe the cooling rate measured in the field reasonably well, the use of GTR-modified binders clearly affects the cooling predictions.

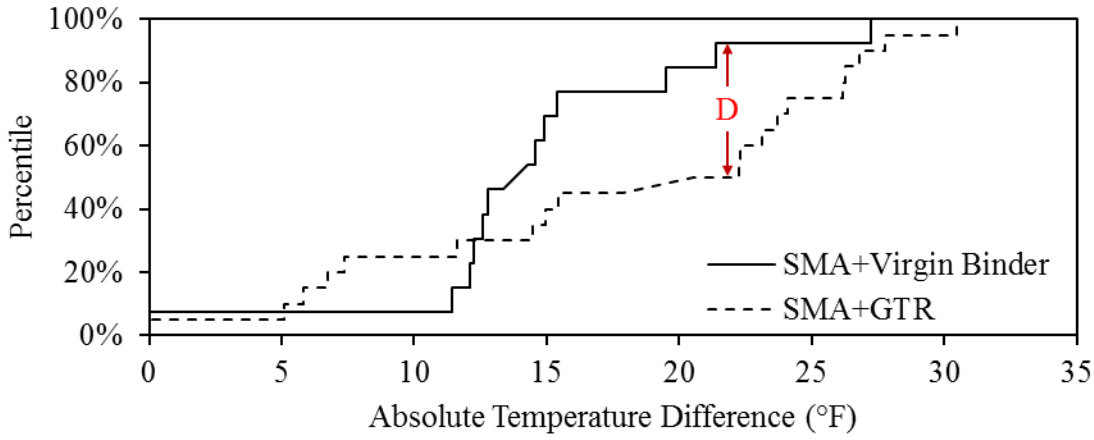

(a)

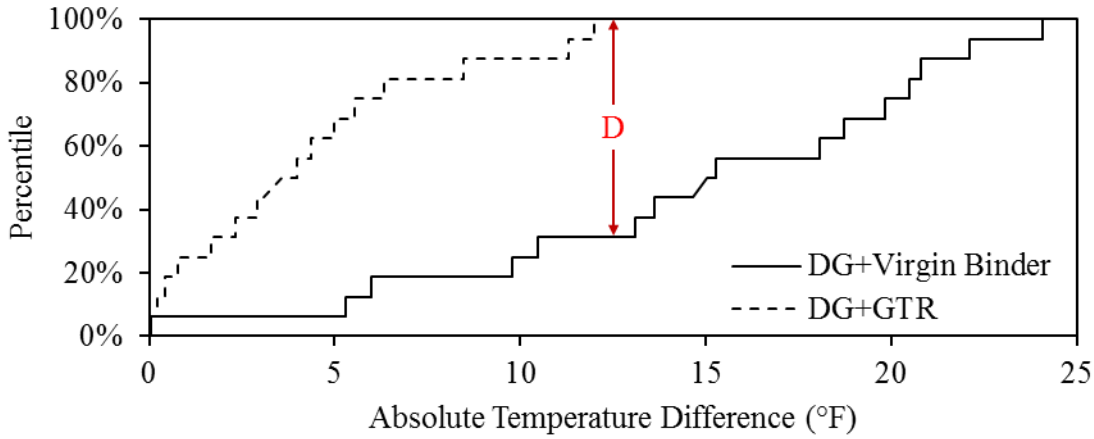

(b)

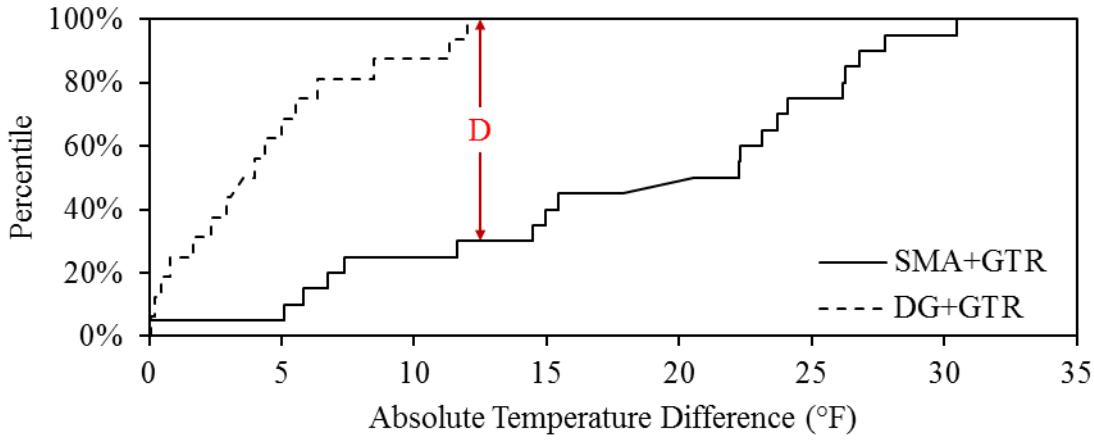

(c)

FIGURE 4.18 Cumulative fraction plot for the absolute temperature differences for layers (a) SMA, (b) DG, and (c) GTR-modified mixtures

As mentioned before, during the GTR blending process, the rubber particles absorb the aromatic fraction of the virgin binder. Aromatics, consisting of one or more stable six-carbon condensed, unsaturated ring structures, may be classified in two types, naphthene aromatics (NA) and polar aromatics (PA), when the adsorption-desorption method is used to fractionate the asphalt binder (NCAT, 2009). Naphthene aromatics are considered to be the softening component in asphalt binder, while polar aromatics have been related to the ductility of asphalt. In general, the aromatic fraction is responsible for the aging in asphalt binders. By absorbing this fraction, the rubber particles alter the chemical composition of the asphalt binder, affecting the temperature susceptibility of the binder and improving the high temperature stiffness of the mixture (Putman, 2006). This has a direct effect on the thermal properties of the binder and thus may be influencing the cooling of the mixture, which would explain the results obtained in this study.

In addition, the use of GTR to modify asphalt binder tends to increase the viscosity of the binder (Putman, 2006). This property has been found to affect the compactability of the asphalt layers and is commonly used to determine the mixing and compaction temperatures of asphalt mixtures (Asphalt Institute, 2007). It has been demonstrated that the use of polymers in asphalt binder tends to modify its viscosity and affects the thermal properties of the binder (Bahia et al., 2006). It's reasonable to consider that GTR may be having a similar effect on the mixtures considered in this study, which would contribute in explaining the observed differences.

The MultiCool software may continue to be used in the field when asphalt concrete mixtures containing GTR-modified binders are used. However, it must be noted that the presence of the rubber particles may be affecting the cooling rate of the mixture

and engineering judgment should prevail in the decision making process. A more detailed study on the thermal properties of asphalt GTR-modified binders would also be useful in improving the prediction of the MultiCool software.

4.11 FOAMED COLD-MIX BASE

For each pavement lift placed over a FCM base, an individual simulation was performed selecting each of the two options in the MultiCool software, granular base (GB) and asphalt concrete (AC). For each simulation, Figure 4.19(a) shows the statistical analysis of the temperature differences based on the standard error of the predictions, while Figure 4.19(b) shows the percent temperature differences within the $\pm$18°F tolerance. All three lifts consisted of the same mix and had the same layer thickness; therefore, the variability observed in the figures may be attributed to the effect of the FCM base. For both assumptions (AC and GB), section N4-Bottom showed the lowest correlation with the model, while section S12-Bottom showed the best correlation. However, in the first case, the best correlation was obtained when the FCM was modeled as an AC layer, and in the second case the best correlation was obtained when modeling it as a granular base. A more detailed analysis of the observed differences would generate more significant conclusions.

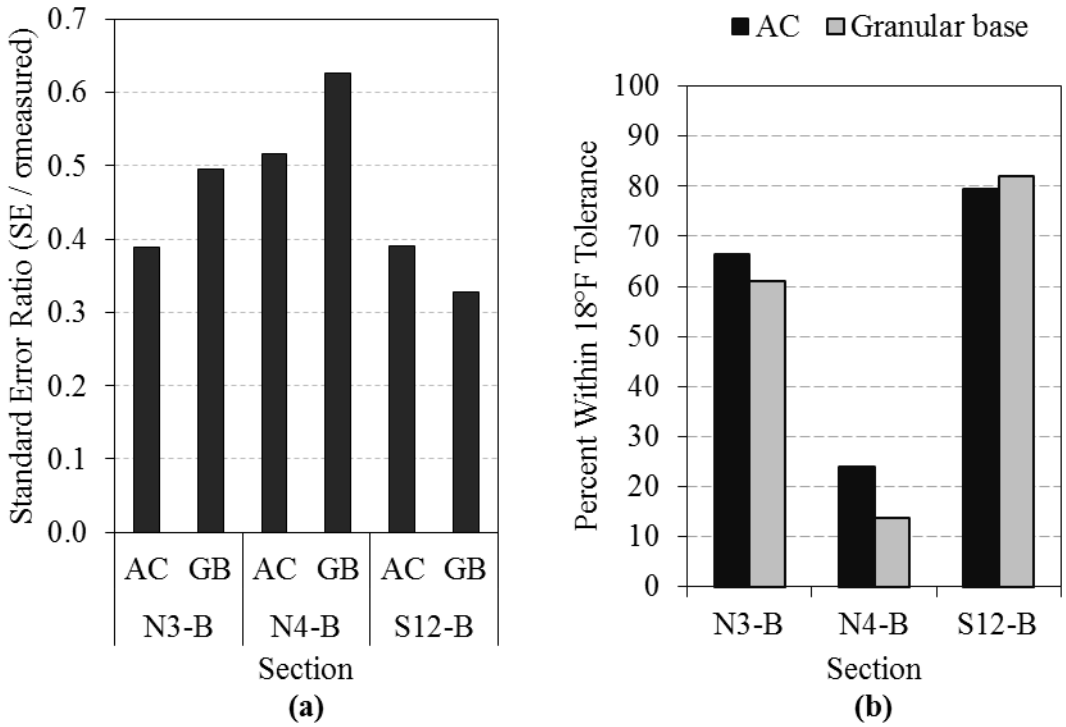

FIGURE 4.19 Effect of FCM base

A multiple-comparison between all pairwise temperature differences revealed a statistical difference in the cooling prediction, at a 95% confidence level, between section S12-Bottom and the other two sections. However, as shown in Figure 4.20, the cumulative distribution functions of each section/layer are clearly different, regardless of the simulation (i.e. AC or GB). A KS-test was performed to compare the same underlying material in all three layers, considering the absolute temperature difference. The results revealed strong differences in all cases (p ranging between 0.000 and 0.015), except for the simulations considering AC as underlying material for layers N3-Bottom and S12-Bottom (p=0.847). Furthermore, a significant difference was also found when comparing the absolute temperature difference for the two simulations, considering AC or GB, performed on layer N4-Bottom (p=0.038).

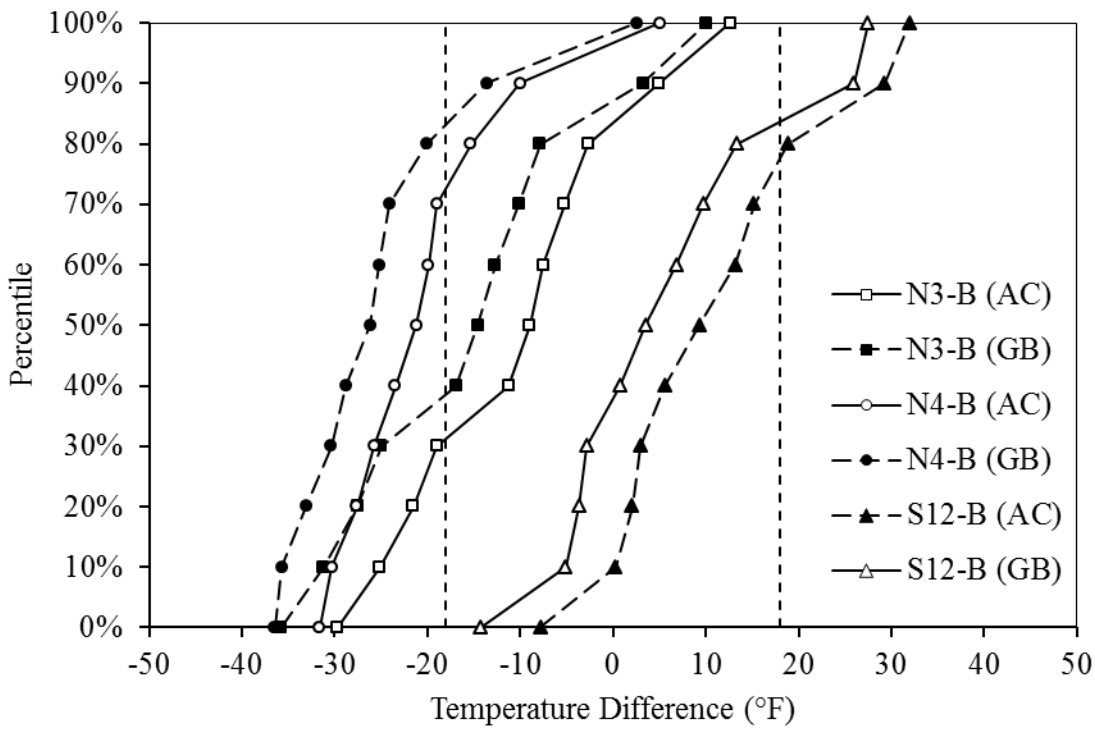

FIGURE 4.20 CDF plots for FCM base

Although it is hard to determine a specific trend, it is clear that the FCM base affects the predictions of the MultiCool model. Due to the rheological characteristics of the asphalt binder, FCM materials tend to be more temperature sensitive than granular materials (Asphalt Academy, 2009). During the mixing process of a FCM, the foamed asphalt disperses throughout the aggregate by adhering to the finer particles to form a strong, homogeneous mastic that bonds the larger aggregate particles together (Asphalt Academy, 2009). Due to the rheological characteristics of the asphalt binder, this mastic acts as a thermal bridge between the larger particles enhancing the overall thermal conductivity of the FCM (Côté et al., 2013). Nonetheless, FCM is still a granular material in nature (Jenkins et al., 2001) and its thermal conductivity remains lower than that of

normal asphalt concrete. In that way, the thermal properties of FCM materials may fall somewhere between those of conventional granular materials and asphalt concrete, and may be different than the default values included in the MultiCool software, which in turn may be affecting the predictions.

A more detailed study of the thermal properties of FCM materials in the laboratory may allow for improving the predictions of the software. However, for practical purposes, the MultiCool model may be used to predict the cooling of asphalt materials when a FCM base is used. A potential approach would be to perform two individual simulations, one considering the FCM as AC, and another considering it as a granular base. Considering these two resulting times available for compaction, a compaction window may be selected based on engineering judgment, as the shortest cooling period.

4.12 SUMMARY

A validation of the asphalt cooling rate model used in the MultiCool software was performed for select sustainable technologies (RAP, RAS, GTR-modified binders, and FCM base) used during the construction of the fifth research cycle at the NCAT Test Track. It was found that, in general, the MultiCool model is a fair predictor of the measured temperatures. However, a direct comparison between measured and predicted temperatures revealed that the model may tend to under-predict for higher temperatures and over-predict for lower temperatures. A statistical analysis established that six of the nineteen analyzed pavement layers exceeded the ±18°F tolerance level established in the

original validation of the model. While 68% of the lifts investigated were within the tolerance, these six cases warranted further investigation.

The use of sustainable technologies such as increased RAP contents, RAS, GTR-modified binders, and FCM bases has a significant effect on the MultiCool model fit. Even if the model appeared to adequately predict the pavement cooling in the majority of lifts evaluated, clear differences were found in certain cases, indicating that some of these technologies may be affecting the cooling of asphalt concrete during construction.

While the use of increased RAP contents doesn't seem to have a significant effect on the construction cooling of asphalt concrete, sufficient evidence was found indicating that the use of RAS tends to affect the cooling prediction, for SMA mixtures only.

Similarly, relative variability was observed for the cooling prediction in mixtures containing GTR-modified binders. The presence of GTR may be affecting the chemical composition of the asphalt binder, which in turn may be affecting the thermal properties of the mixture.

Lastly, the use of a FCM base considerably affected the predictions of the MultiCool model. The relative difference in the results obtained seems to indicate that the thermal properties of FCM materials may fall somewhere between conventional granular materials and asphalt concrete. Nonetheless, the MultiCool model may continue to be used in such cases by simply taking an alternate approach and performing two individual simulations, considering the FCM base as a AC layer and as granular base respectively. The time available for compaction may be selected based on the case with the fastest predicted cooling, considering the ±18°F tolerance.

CHAPTER FIVE

INFLUENCE OF SUSTAINABLE TECHNOLOGIES ON IN-PLACE THERMAL PROPERTIES OF ASPHALT PAVEMENTS

5.1 INTRODUCTION

The thermal interactions of asphalt concrete with the environment have been demonstrated to affect the development of distresses, defining the long-term performance or failure of asphalt pavements. To determine the contribution of modern sustainable technologies on the thermal response of asphalt pavements, a study was conducted to analyze energy storing and thermal conduction capacities of pavement sections built as part of the 2012 structural experiment at the Test Track. The study was based on average hourly pavement temperature measurements taken between January 1st and June 19th, 2013. Hourly measurements of the ambient air temperature, wind velocity and solar radiation, made by the on-site weather station, were also used to estimate the energy stored by the pavement and the heat conducted through the asphalt layer. A statistical analysis of the results allowed comparing the sections included in the GG experiment to analyze the possible effect of high RAP contents, RAS, and GTR-modified binders on the thermal properties of asphalt concrete pavements.

5.2 TEMPERATURE VARIATIONS

In general, the temperature of all pavement sections fluctuated throughout the entire analysis period. The minimum pavement temperatures were observed for the month of January while the highest temperatures were reached in June. This behavior was in agreement with the average daily ambient temperatures, which reached daily maximum and minimum values, as shown in Figure 5.1.

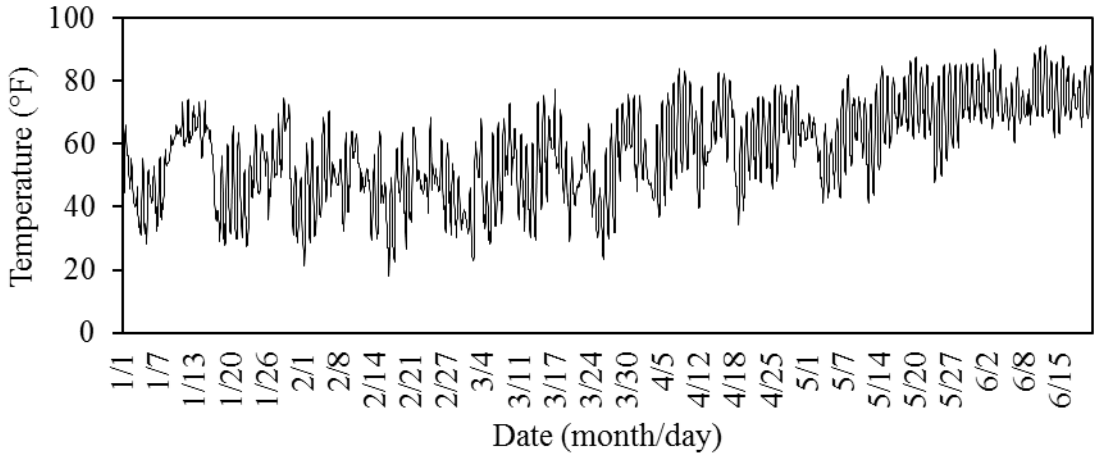

FIGURE 5.1 Average daily ambient air temperatures

Figure 5.2 shows the pavement temperature fluctuations for section N5 (Control). An analysis of the average pavement temperatures at the surface, mid-depth, and bottom of the asphalt layer revealed similar daily variations for all three depths. Nearly parallel trends, with lower temperatures in the morning and higher temperatures in the afternoon, were observed in all cases.

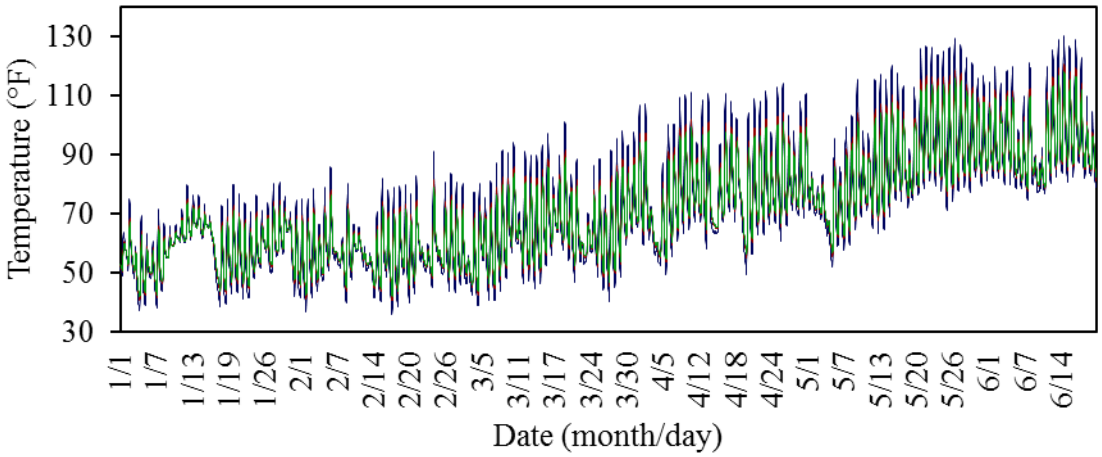

(a)

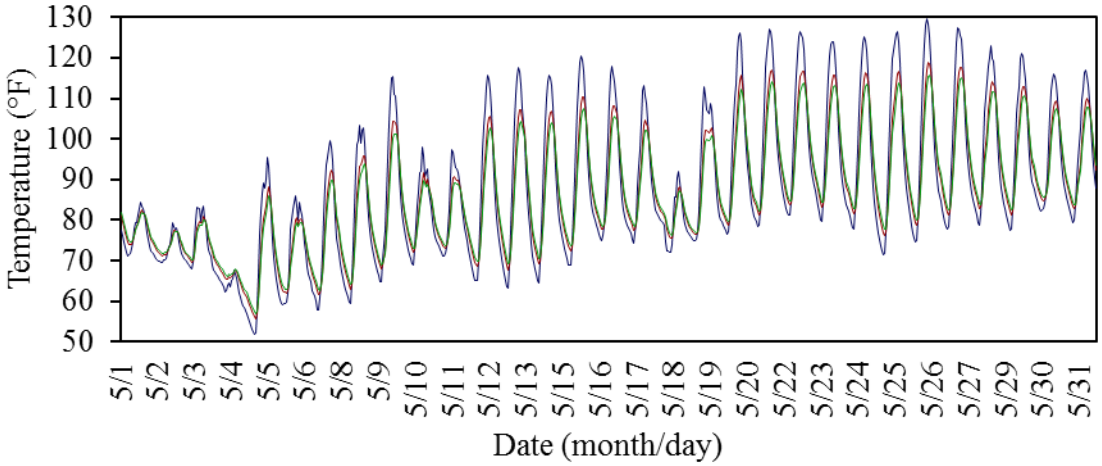

(b)

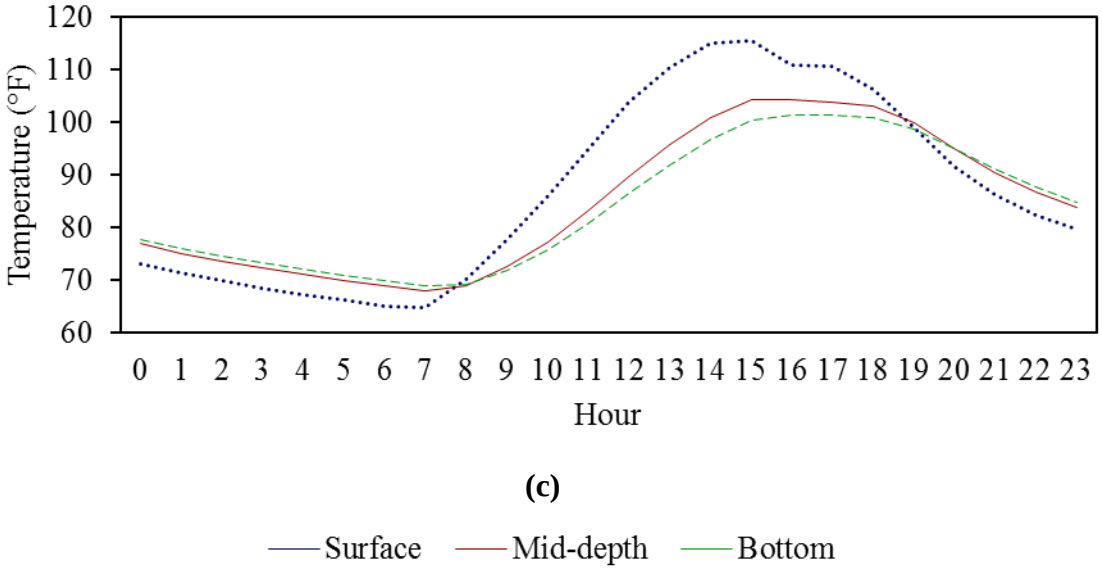

(c)

FIGURE 5.2 Variations in (a) monthly, (b) daily, and (c) hourly average pavement temperature for section N5

The pavement temperature seemed to decrease with depth during the day, and increase with depth at night, as shown in Figure 5.2(c). This is consistent with the heat transfer mechanisms previously described, where energy is lost by convection at night and gained by radiation during the day. Figure 5.3 shows the temperature for different depths within the pavement layer for two specific moments in a day, noon and midnight, making more evident the previously mentioned variation of temperature with depth. At midnight the temperature increases with increasing depth, while an opposite trend is observed at noon. The trend was not linear indicating that the nature of heat transfer is transient.

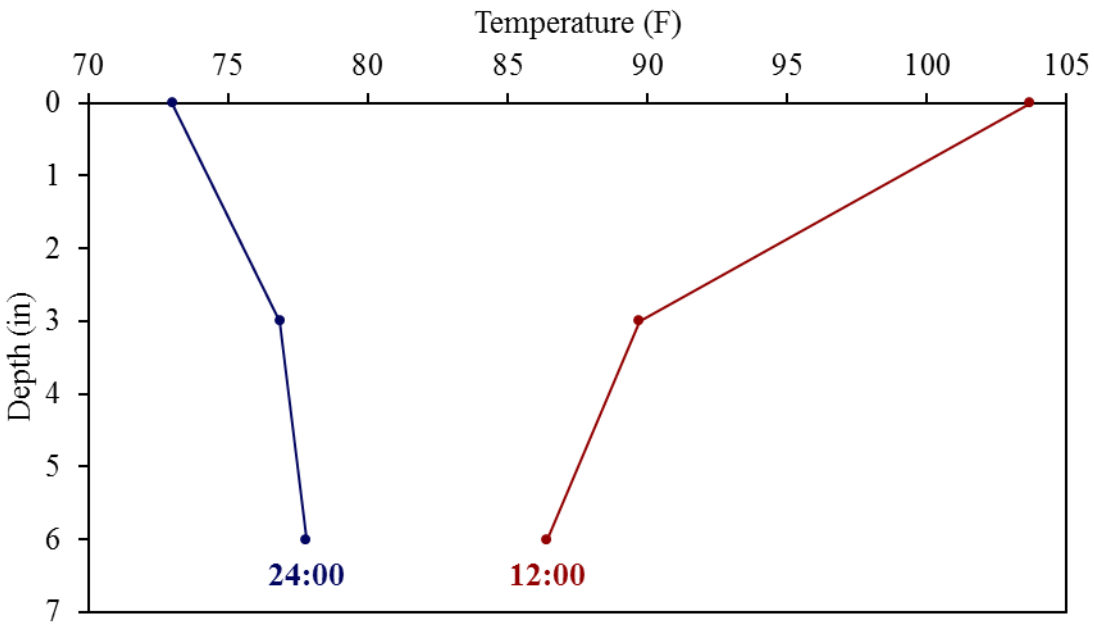

FIGURE 5.3 Temperature variations within the pavement for section N5

A closer examination of the daily trends, shown in Figure 5.2, revealed that temperature fluctuations were also related to the depth of the pavement layer. The temperature at the surface of the pavement seemed to be more susceptible to the daily

temperature changes, presented the highest maximum temperatures during the day and the lowest minimum temperatures at night. A contrasting trend was observed for the temperature at the bottom of the asphalt layer, with higher minimum temperatures at night and lower maximum temperatures during the day. The mid-depth temperature seemed to remain relatively more constant with average maximum and minimum values. Mid-depth pavement temperature has been directly correlated to the stiffness of the pavement and has been successfully used to predict pavement performance (Priest and Timm, 2006). This temperature, measured at the midpoint of the asphalt layer, could then be considered as an adequate predictor of the average temperature of the entire layer, even if surface and bottom temperatures showed more variation.

As shown in Figure 5.2(c), the temperatures throughout the entire asphalt layer seemed to simultaneously balance at two specific moments every day, once in the morning hours, approximately at 8:00 a.m., and once in the evening hours, approximately at 7:00 p.m. This phenomenon could be explained as a change in the direction of heat transfer, marked by a momentary state with an insignificant temperature gradient. In that way, heat is transferred from the surface towards the bottom of the pavement during the day and from the bottom to the surface at night. In other words, the pavement sections were storing energy during the day, and releasing it at night. This concept explains the contribution of pavement layers to the UHI effect, previously described.

5.3 ENERGY STORED BY THE PAVEMENT

As mentioned before, an asphalt pavement may be modeled as a large plane with one-dimensional heat transfer. Considering the mid-depth pavement temperature, the energy stored by the pavement during the day may be expressed as a function of the daily temperature differential, according to Equation 17.

$$\Delta E = c_p \cdot \rho \cdot h \cdot (T_{max} - T_{min}) \quad (17)$$

Where:
- ΔE = Energy content of the pavement (J/m^2)
- c_p = Specific heat at constant pressure ($J/kg \cdot K$)
- ρ = Pavement layer density (kg/m^3)
- h = Pavement layer thickness (m)
- T_{max} = Maximum mid-depth temperature in one day (K)
- T_{min} = Minimum mid-depth temperature in one day (K)

A direct measurement of the specific heat of the asphalt materials would require extensive and costly laboratory testing, and was beyond the scope of this study. However, the relatively low variation of asphalt concrete heat capacity found in the available literature and shown in Table 2.1 seems to suggest that specific heat could be assumed to have constant value for all the analyzed sections. In that way, a relative value of the energy stored in the pavement may be defined as shown in Equation 18.

$$\frac{\Delta E}{c_p} = \rho \cdot h \cdot (T_{max} - T_{min}) \quad (18)$$

Using the as-built thicknesses, the density of the all the asphalt layers was calculated based on the field densities measured during construction and the material properties obtained as part of the quality control testing at the Test Track, as shown in Equation 19. An individual, daily relative energy (ΔRE) was calculated for each section as shown in Figure 5.4.

$$\rho = \frac{h_1 + h_2 + h_3}{\frac{h_1}{\rho_1} + \frac{h_2}{\rho_2} + \frac{h_3}{\rho_3}} \tag{19}$$

Where: ρ = Pavement density (kg/ m^3)

ρ_i = Layer *i* density (kg/ m^3)

h_i = Layer *i* thickness (m)

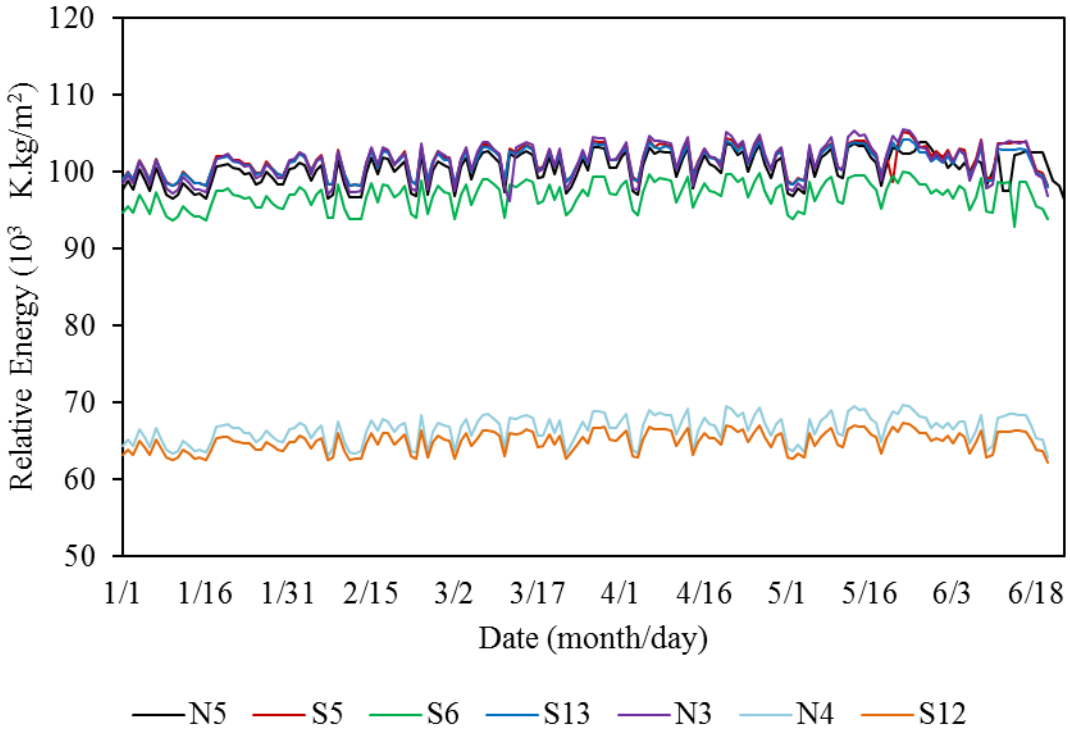

FIGURE 5.4 Daily relative energy stored by the pavement

Sections N4 and S12 clearly stored less energy than the rest of the sections included in the study. However, these two sections are significantly thinner, with a total thickness of 10 cm, nearly two thirds the total thickness of most sections in the GG experiment. The stored energy, as defined for this study, is a direct function of the pavement thickness (h), which would explain the significantly lower values obtained for the thinner sections. A simple analysis of all seven test sections revealed that the correlation between the relative energy stored by the pavement and the total thickness of the asphalt layer is relatively linear, as shown in Figure 5.5. Although the coefficient of determination (R^2) appears to be high (97.1%), the data are limited and relatively scattered, restraining the certainty of any possible inference on the effect of energy storing capacity of the sustainable technologies. Nonetheless, it would seem that the thickness of the asphalt layers, rather than the materials used in the mixture, have a greater effect on the energy stored and released by the pavement.

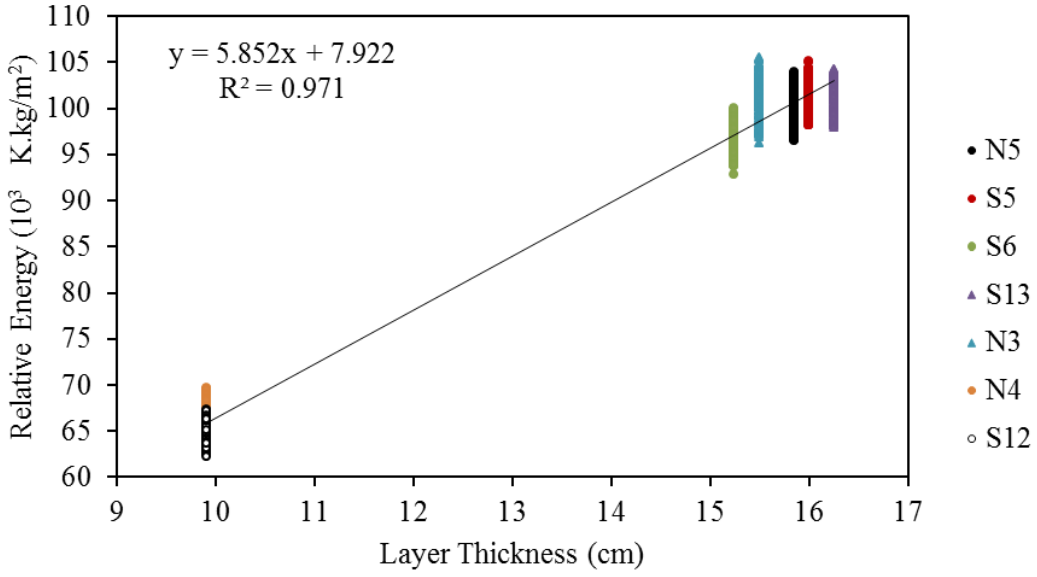

FIGURE 5.5 Relative energy versus pavement thickness

A direct comparison between the energy stored by the individual pavement sections may lead to misinterpretations if the effect of the pavement thickness is not considered. Certain sections, such as S13 (GTR) and S5 (High RAP), seemed to store more energy than others, such as N5 (Control), as shown in Figure 5.5. However, this may be due to the fact that section N5 is barely thinner than the other two sections, and thus implying that GTR-modified binders or higher RAP contents may increase the energy storing capacity, would be incorrect. A more direct comparison of the sections was performed by normalizing the stored energy in reference to the pavement thickness. These new daily parameters, referred to as normalized relative energies (ΔRE_n) are presented in Figure 5.6.

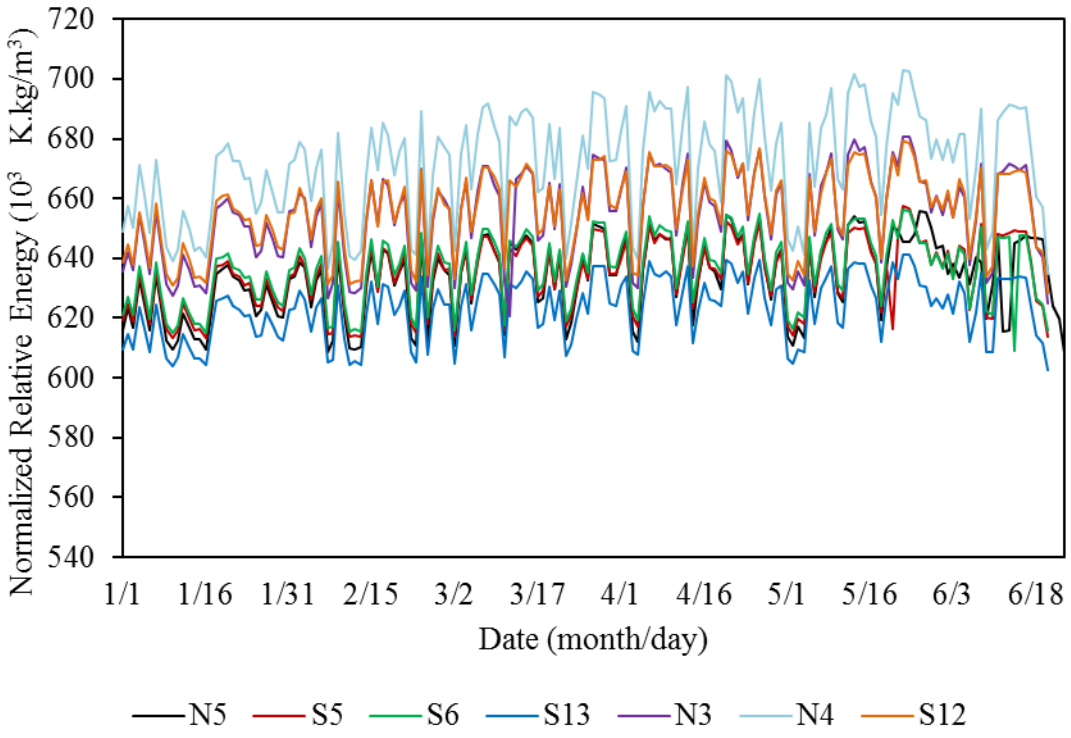

FIGURE 5.6 Daily normalized relative energy

A multiple-comparison using a Tukey-Kramer test between the average normalized relative energies for all test sections, revealed statistical similarities at a significance level (α) of 0.05, between sections N5 (Control), S5 (Higher RAP), and S6 (RAP+RAS) and between sections S12 and N3. As shown in Figure 5.7, sections N4 and S13 were statistically different from all other sections. Moreover, the average normalized energy absorbed by section N4 was significantly different from that absorbed by sections N3 and S12. This was particularly interesting because the three sections consisted of similar asphalt materials, but had different layer thicknesses. Even if the presence of a cement treated base (CTB) in section S12 may be affecting the heat conduction between the asphalt and unbound layers, a similar difference was also observed between sections N3 and N4 which consisted of the same mixture, but different thickness. This suggests that the CTB did not have a direct effect on the average relative energy absorbed by the pavement.

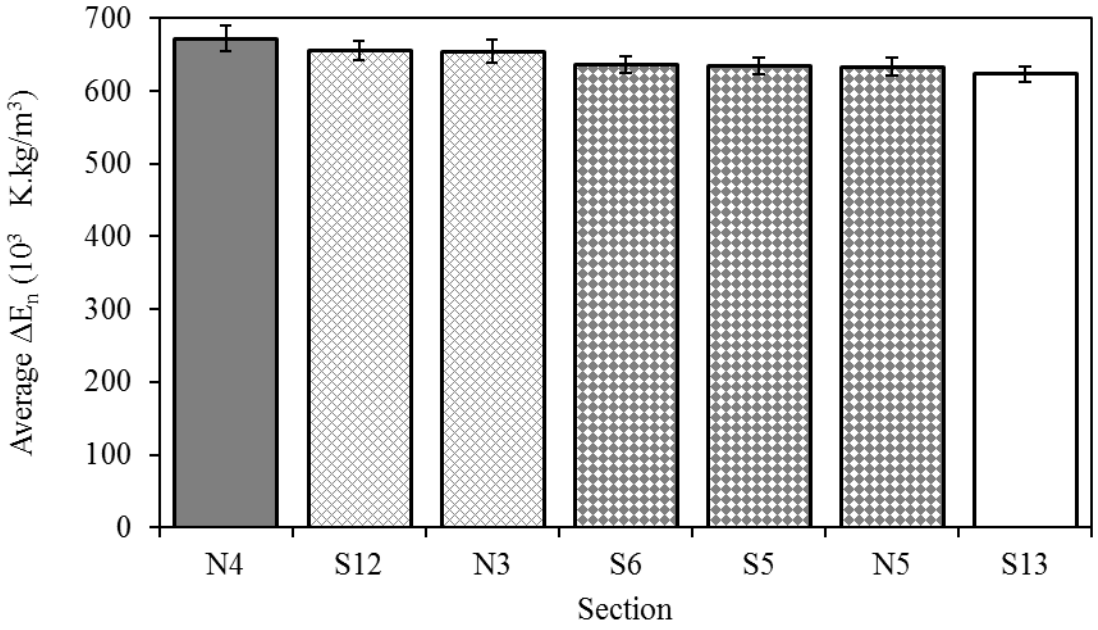

FIGURE 5.7 Normalized relative energies for all sections (different colors denote statistically significant differences)

Even if the energy absorbed by section N4 was statistically different from that absorbed by sections N3 and S12, the numerical difference between the average absorbed energy was less than 3%. Therefore, the difference can be overlooked for practical purposes and the energy absorbed by the three VDOT sections may be assumed to be the same. In that way, the CTB may be considered to have no substantial effect on the amount of energy absorbed by the asphalt layers.

The statistical difference observed for section S13 may be attributed to the use of GTR-modified binders. As mentioned before, the rubber particles may have a direct effect on the thermal properties of the asphalt binder, which in turn affects the heat transfer within the asphalt layer. A more thorough study of the heat transfer within the GG sections would allow a more reliable assessment of the effect of GTR-modified

binders. An alternative approach to compare the effect of RAP, RAS and GTR-modified binders on the thermal properties of asphalt pavements is presented in the following sections.

5.4 ANALYSIS OF THE THERMAL CONDUCTIVITY IN THE FIELD

Transient heat transfer theory was used to assign a numeric value to the thermal conductivity of the pavement, based on the conditions measured in the field and theoretical boundary conditions. Even if the pavement sections considered in the study consisted of at least two individual lifts with particular mixtures, the asphalt pavement was assumed to behave as a homogeneous material throughout its entire thickness. In that way, the thermal properties were considered to be consistent for the asphalt layer, even if the study of pavement cooling during construction suggested possible differences. The total thickness of asphalt concrete would then be subjected to one dimensional heat transfer with only two boundaries where heat transfer occurred, the surface and the asphalt–base interface. Conveniently, a temperature probe was located at each of these interfaces, which allowed having frequent, location-specific temperature measurements. Figure 5.8 shows a general representation of the asphalt pavement and its temperature probes, specifying the heat transfer mechanisms in the two boundary conditions.

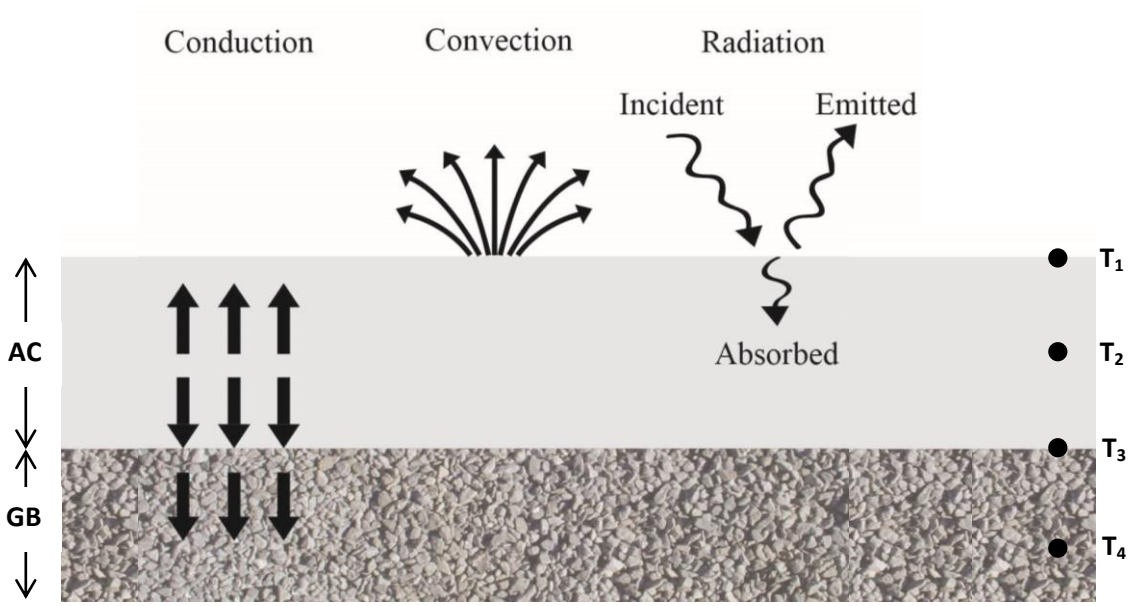

FIGURE 5.8 Relative energy versus pavement thickness

A preliminary analysis of the heat transfer within the asphalt layer was performed considering the temperature variations for a specific moment in time. The hourly temperature measurements taken by the three temperature probes (T_1, T_2, and T_3) embedded in the asphalt layer at varying thicknesses (z_1, z_2, and z_3) were used to calculate an absolute hourly temperature gradient, defined as the ratio of the absolute value of the change in temperature over the change in depth. Absolute values were used in order to only account for the difference in temperatures without the effect of the direction of the heat transfer. Three conditions were considered to calculate the temperature gradient between the surface and mid-depth temperatures (ΔT_{12}), mid-depth and bottom temperatures (ΔT_{23}), and surface and bottom temperatures (ΔT_{13}). The cumulative distribution of the resulting temperature gradients for section N5 (Control) is presented in Figure 5.9. Very similar plots were obtained for all other sections, revealing statistical differences between all three conditions. Nonetheless, it seems that the

temperature gradient between the surface and the bottom of the pavement (ΔT_{13}) provides an average value of the temperature variation, and may be used to reasonably describe the temperature variation within the entire layer, for practical purposes.

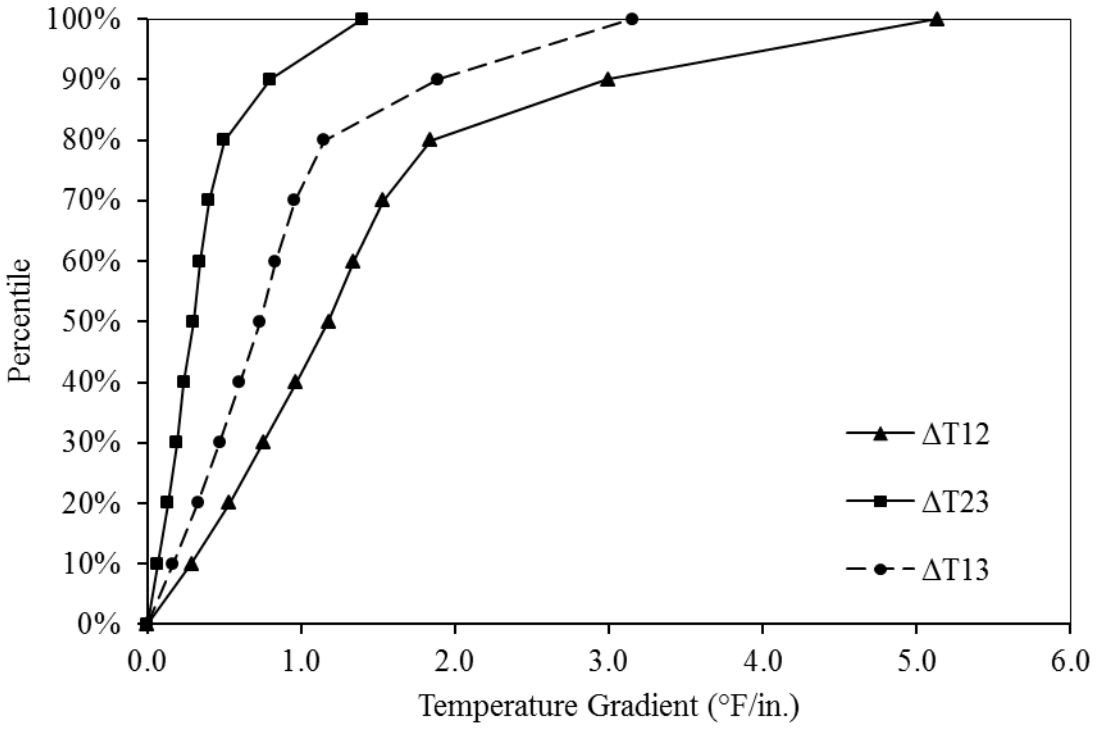

FIGURE 5.9 CDF plot for absolute temperature gradients in section N5

5.4.1 Field Thermal Conductivity Equations

At the surface boundary (z_1), heat transfer occurs by convection and radiation. Furthermore, it may be assumed that the net heat flux reaches equilibrium exactly at the interface between the pavement surface and the surrounding environment. At a specific time, the heat transferred by conduction through the pavement is equal to the heat flux due to convection and radiation. Considering the pavement temperatures at the bottom and top of the asphalt layer provide a sufficient description of the average temperature

variation within the pavement, this thermal equilibrium may be described by equation 20. In its most general form, this equation coincides with the surface boundary conditions considered in the MultiCool model and presented in equation 14. Although a finite difference solution would be ideal to model the heat transfer within the asphalt layer, a practical simplification was made considering a constant temperature gradient throughout the entire asphalt layer.

$$k_{ac} \cdot \frac{T_3 - T_1}{z_3 - z_1} = h \times (T_a - T_1) + \alpha \times H_s + \varepsilon \times \sigma \times (T_1^4 - T_a^4) \quad (20)$$

Where:

k_{ac}	=	Thermal conductivity of asphalt concrete (W/m·K)
T_3	=	Temperature measured at the bottom of the pavement (K)
T_1	=	Temperature measured at the surface of the pavement (K)
z_3	=	Depth to the probe at the bottom of the pavement (m)
z_1	=	Depth to the probe at the surface of the pavement [0.0 m]
h	=	Convection heat transfer coefficient calculated after Chadbourn et al (1998) as $7.4 + 6.39 \cdot w^{0.75}$ (W/m^2·K)
w	=	Wind velocity (m/s)
T_a	=	Mean air temperature (K)
α	=	Pavement absorptivity (0.90 according to available literature)
H_s	=	Measured solar radiation (W/m^2)
ε	=	Pavement emissivity (0.80 according to available literature)
σ	=	Stefan-Boltzmann constant (5.669×10^{-8} W/m^2·K^4)

Similarly, at the asphalt-base interface, heat transfer may be assumed to occur simply by conduction between the two media. Once again, the net heat flux at this point may be considered to reach equilibrium at a specific moment in time. Considering the temperature T_4 is measured within the granular base, the heat transfer at this bottom interface can be described by equation 21.

$$k_{ac} \cdot \frac{T_3 - T_1}{z_3 - z_1} = k_{gb} \cdot \frac{T_4 - T_3}{z_4 - z_3} \quad (21)$$

Where:
- k_{ac} = Thermal conductivity of asphalt concrete (W/m·K)
- T_3 = Temperature measured at the bottom of the pavement (K)
- T_1 = Temperature measured at the surface of the pavement (K)
- k_{gb} = Thermal conductivity of the granular base assumed as 1.16 W/m·K according to Timm et al. (2001)
- T_4 = Base temperature (K)

This approach does not account for the daily temperature fluctuations and considers steady heat transfer to occur. However, if a sufficiently small time frame (i.e. measurements for one specific hour during the day) is used, the obtained values may be considered as an approximation of the thermal conductivity of the material. For this reason, the average temperatures measured by the individual temperature probes specifically at noon (12:00 p.m.), were used to calculate two different thermal conductivity values for every day in the analysis period, according to equations 22 and 23. Furthermore, individual average values for the wind speed, ambient temperature, and solar radiation were obtained from the weather station, for the same time frame.

$$k_{ac1} = \frac{z_3 - z_1}{T_3 - T_1}[(7.4 + 6.39 \cdot w^{0.75}) \times (T_a - T_1) + 0.9 \times H_s + 0.8 \times (5.669 \times 10 - 8\ W/m^2 \cdot K^4) \times (T_1^4 - T_a^4)] \quad (22)$$

$$k_{ac2} = \frac{z_3 - z_1}{T_3 - T_1} \times (1.16\ W/m \cdot K) \times \frac{T_4 - T_3}{z_4 - z_3} \quad (23)$$

These "field thermal conductivity" values are explicitly different from the actual thermal conductivity of the mixture, measured in the laboratory under steady heat transfer conditions. However, they may be considered as fair indicators of the thermal properties of the pavement in the field, for practically comparing the pavement sections included in the study.

5.4.2 Daily Field Thermal Conductivity Values

Noteworthy variability was observed for the calculated field thermal conductivities. Figure 5.10 shows the thermal conductivity values calculated using each of the two equations for the analysis period. Greater variability was obtained when considering the surface boundary, shown in Figure 5.10(a), in comparison with the asphalt-base interface, shown in Figure 5.10(b). The equation derived for the surface boundary contains more variables, including individual values for wind speed, ambient temperature, and solar radiation, explaining the relative scatter observed in the results. However, in both cases the peaks corresponding to the highest and lowest field thermal conductivity values were very limited and erratically distributed throughout the analysis period. Since both equations considered inverse temperature gradients ΔT_{13}, relatively small temperature

variations in temperatures T_1 and T_3 caused extreme peaks in the calculated values, resulting in extreme field thermal conductivity values. To guarantee results sufficiently consistent, the field thermal conductivity values were adjusted by only considering the values lower than the 90^{th} percentile and higher than the 10^{th} percentile of the initial calculations. These adjusted values, shown by the blue-discontinuous line in the figure, excluded the influence of extreme, incoherent field thermal conductivity values without affecting the mean field thermal conductivity.

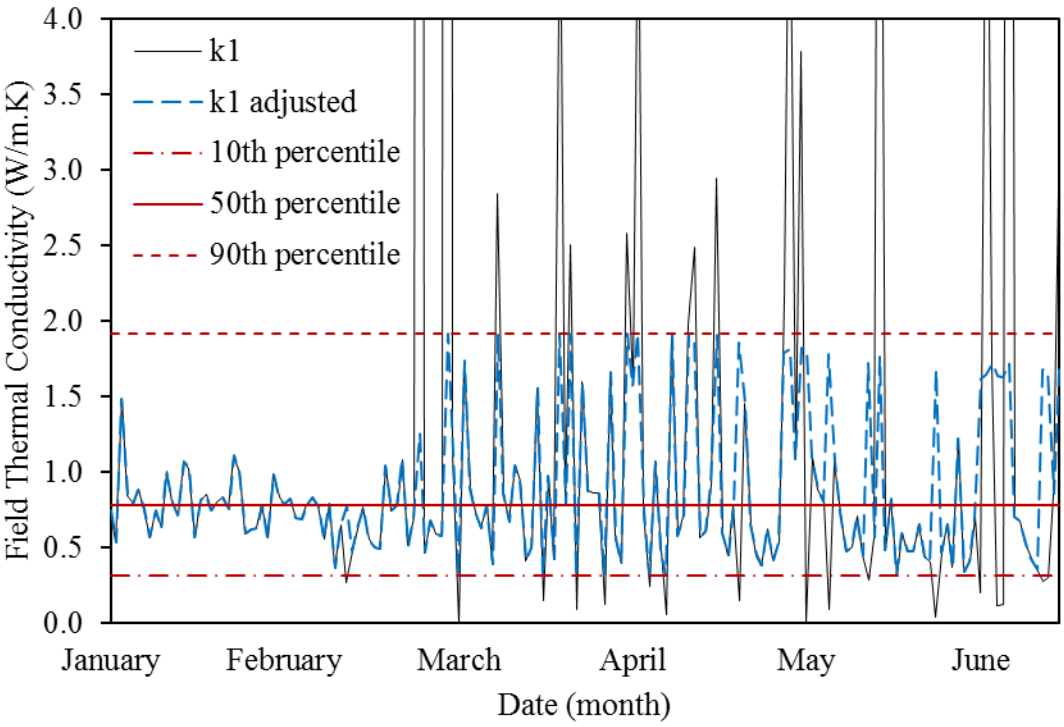

(a)

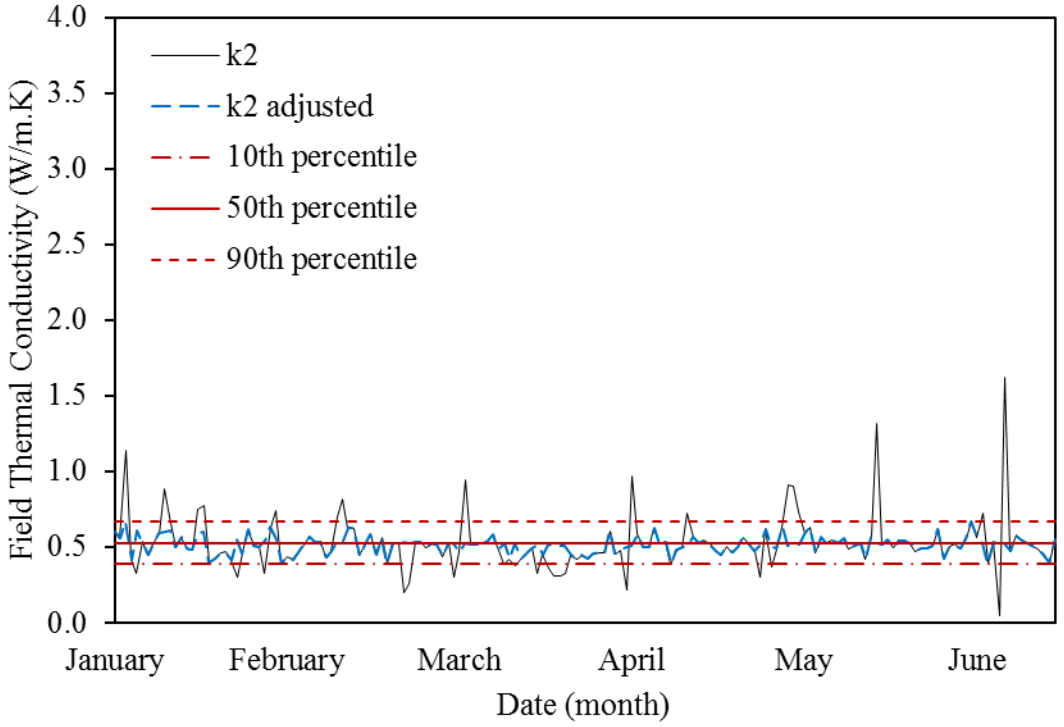

(b)

FIGURE 5.10 Field thermal conductivity values for (a) surface boundary and (b) asphalt-base interface in section N5

Even if the adjusted field thermal conductivities appeared to fall within the ranges found in the literature for the thermal conductivity of asphalt concrete, these two parameters should not be confused. The thermal conductivity reported in the literature and included in the MultiCool software is the result of controlled measurements under steady heat transfer conditions in the laboratory. The proposed field thermal conductivity, on the other hand, may be considered as a property of the material that accounts for the conditions in the field. Due to this difference, these two properties should not be compared. However, the values calculated for the surface boundary conditions seemed to fall within the lower end of the range found in the literature (0.6 W/m·K - 2.88 W/m·K), while the field thermal conductivity values calculated considering the asphalt-base interface usually ranged below the lower thermal conductivity values reported in the literature. Furthermore, both field thermal conductivity values calculated were clearly lower than the thermal conductivity values used by the MultiCool software, ranging between 1.50 W/m·K for dense graded mixtures and 2.00 W/m·K for SMA mixtures. Even if the calculated field thermal conductivity values were different from the values found in the literature and used in cooling prediction programs, they allow for performing practical comparisons between the different test sections, assuming they were exposed to similar ambient conditions in the field due to their relative proximity.

Two values of daily field thermal conductivity were calculated for each section, one considering the surface boundary, identified as (k_{ac1}), and another considering the asphalt-base interface, identified as (k_{ac2}). As shown in Figure 5.11, the values obtained for k_{ac1} were relatively higher and showed more variability than the values obtained for k_{ac2}.

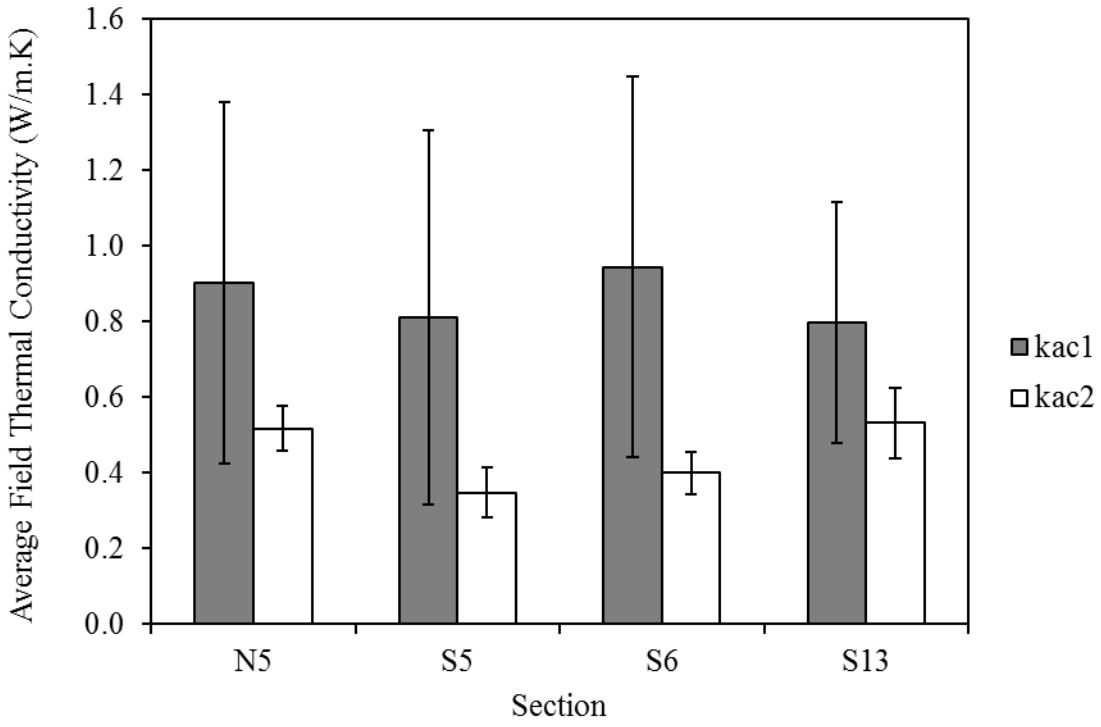

FIGURE 5.11 Average field thermal conductivity values for the GG sections

The two field thermal conductivity values calculated were used independently in an attempt to assess the effect of increased RAP contents, RAS, and GTR-modified binders. To guarantee the consistency of the results, two comparisons were performed in each case, considering the two boundary conditions, k_{ac1} and k_{ac2}. The individual comparisons are discussed in greater detail in the following sections.

5.5 INCREASED RAP CONTENT

The effect of increased RAP contents on the field thermal properties of asphalt concrete was evaluated by comparing section N5 (Control) and S5 (High-RAP). An individual cumulative distribution function (CDF) plot was developed to compare each of the two field thermal conductivity values, k_{ac1} and k_{ac2}, as shown in Figure 5.12. The effect of RAP on the thermal properties of asphalt materials was previously studied by Vargas-Nordcbeck and Timm (2011b). Using sections S9 (virgin mixture) and N10 (50%RAP) from the 2009 NCAT Test Track structural experiment, the authors determined the effects of RAP on the energy stored by the asphalt pavements. The results revealed that the presence of RAP may have changed the thermophysical properties of the asphalt layer and consequently affected the amount of stored energy by RAP mixtures in comparison with virgin mixtures. The results presented in Figure 5.12 may be viewed as an extension of the study conducted by Vargas-Nordcbeck and Timm (2011b), considering more recent data from a subsequent research cycle at the Test Track.

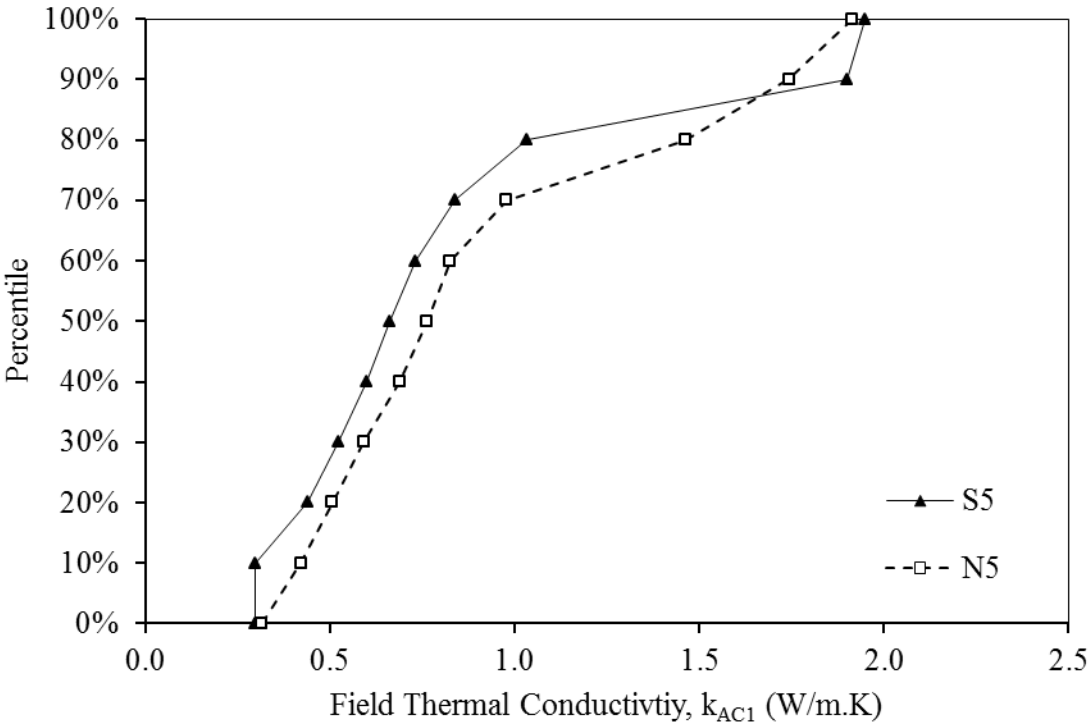

(a)

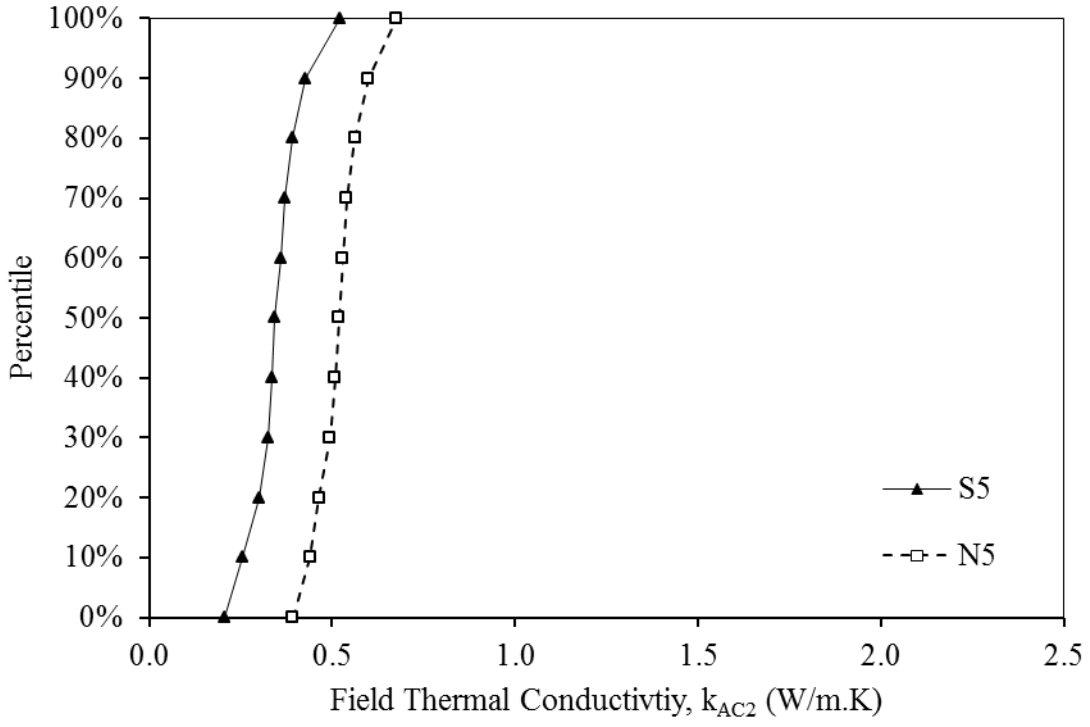

(b)

FIGURE 5.12 Effect of increased RAP content on field thermal conductivity values for (a) surface boundary and (b) asphalt-base interface

A comprehensive analysis of the field thermal conductivity values revealed that in both cases, the two sections were statistically different. Even if the results of a pairwise comparison of the mean field thermal conductivity values showed an estimate difference of 0.0921 (t=-1.73, p=0.084) for k_{ac1}, in the case of k_{ac2} a 0.1690 statistical difference (t=25.05, p=0.000) was estimated at a level of significance of 0.05. Furthermore, a KS test revealed significant differences amongst the two distributions, with maximum vertical deviations of 0.1631 (p=0.020) for $k_{ac1,}$ and 0.8294 (p=0.000) for k_{ac2}.

There seems to be sufficient statistical evidence indicating that increased RAP contents may decrease the thermal conductivity of asphalt concrete, for the analyzed data. Although determining an accurate value for this reduction would be difficult from these results, the field thermal conductivity calculated for both boundary conditions was statistically lower for section S5, which contained increased RAP contents. Overall, it can be inferred that the presence of larger amounts of aged binder in the asphalt concrete may be affecting the thermal properties of the layer by causing a reduction in the thermal conductivity of the material. Additionally, the presence of different aggregates from relatively unknown sources in the RAP, may also be affecting the thermal properties of the mixture. Similar effects were observed by Mrawira and Luca (2006) who attributed the variability of the thermal properties of asphalt mixtures to the variability in the properties of the aggregates.

Similar results were observed during the construction cooling of these sections. The comparisons previously shown in Figures 4.11 and 4.12 revealed that the average temperature difference between measured and predicted cooling temperatures was slightly lower for the sections with increased RAP contents. The cooling process in these

layers was slower than that in sections with reduced RAP contents, indicating a possible reduction of the thermal conductivity. A laboratory study of the thermal conductivity of the mixtures used in section S5 would allow describing the effect of increased RAP contents on the thermal properties of asphalt concrete.

5.6 RECYCLED ASPHALT SHINGLES

The effect of RAS on the thermal properties of asphalt concrete was evaluated by comparing sections N5 (Control) and section S6 (RAP+RAS). Cumulative distribution function plots were used to compare the field thermal conductivity at each boundary, as shown in Figure 5.13. Although a difference was obvious for the asphalt-base boundary condition, a simple observation of Figure 5.13(a) revealed less difference for the surface boundary condition. Although the effect of RAS on the field thermal conductivity of asphalt concrete was less evident than the effect of increased RAP contents, a pairwise comparison of the mean field thermal conductivity values revealed certain statistical differences, at a level of significance of 0.05. In the case of k_{ac1} no statistical difference was observed between the means, with a relatively low estimate difference of 0.0408 (t=0.77, p=0.444). However, in the case of k_{ac2} the difference was estimated as 0.05203 (t=7.94, p=0.000). A KS-test revealed strong differences amongst the two distributions, with maximum vertical deviations of 0.1412 (p=0.061) for $k_{ac1,}$ and 0.7353 (p=0.000) for k_{ac2}. In that way, there seems to be sufficient statistical evidence demonstrating a difference in the heat transfer in sections N5 and S6. This allows inferring that, in the same way as RAP, the presence of the aged binder and aggregates from different sources in the RAS may be decreasing the thermal conductivity of the asphalt mixture.

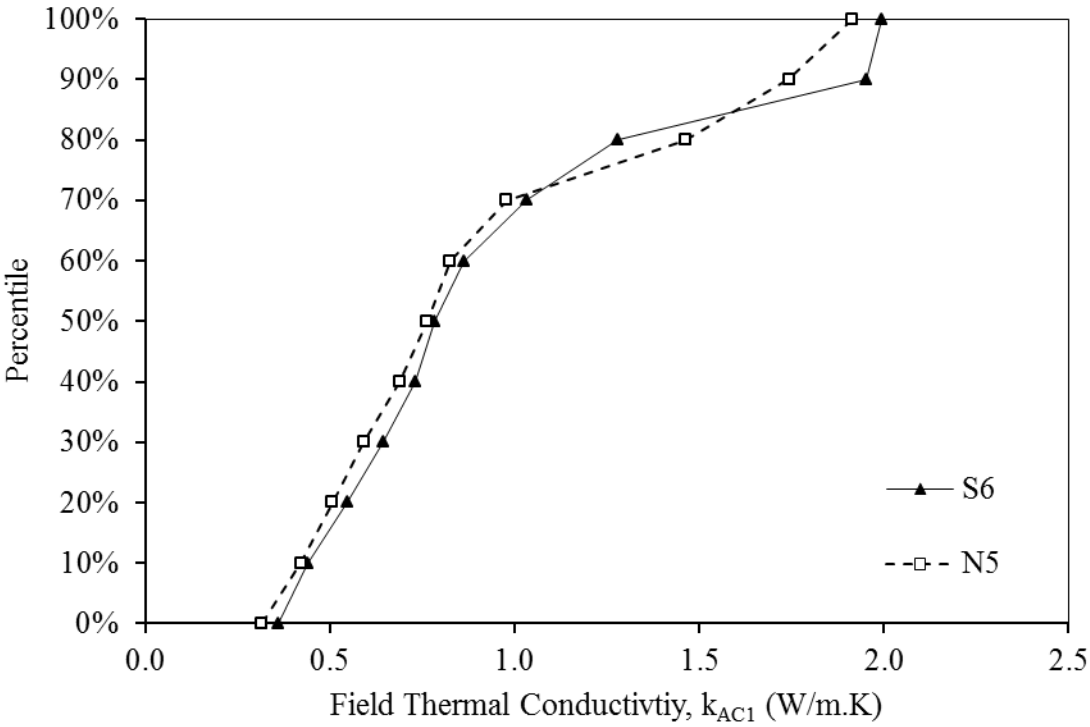

(a)

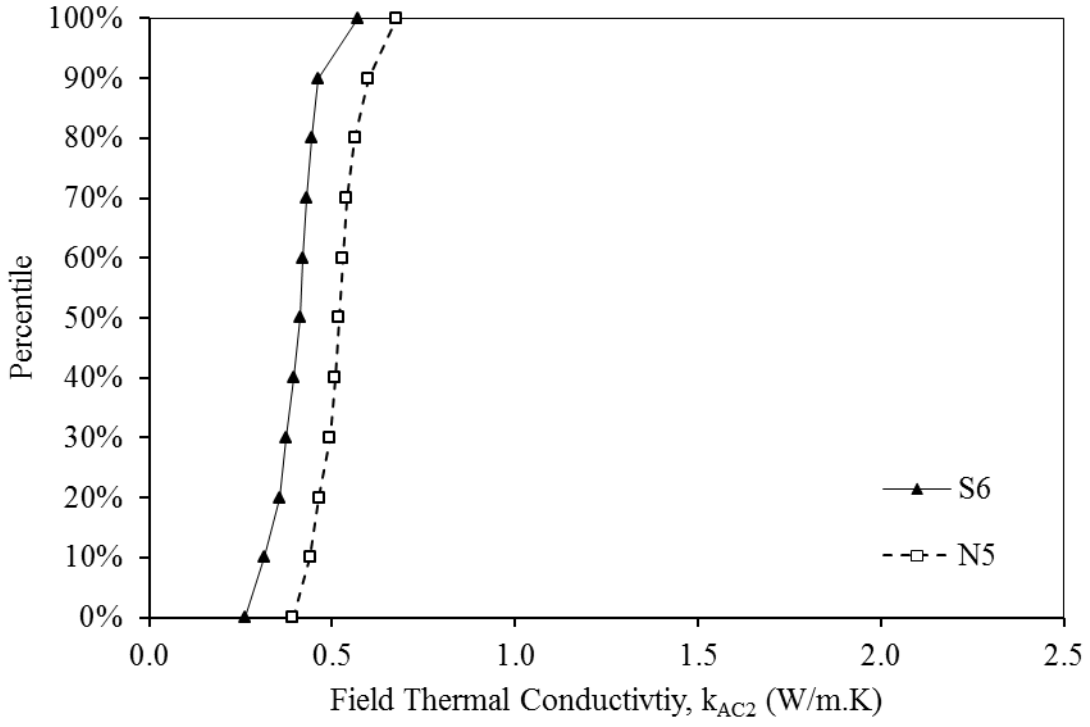

(b)

FIGURE 5.13 Effect of RAS on field thermal conductivity values for (a) surface boundary and (b) asphalt-base interface

Comparable results were observed for the analysis of the cooling during construction, where the average difference between the measured and MultiCool-predicted temperatures, was higher for the mixtures containing RAS in comparison with virgin mixtures. Although the presence of RAS showed a more significant effect in the case of SMA mixtures, the results were consistent with the analysis of the long-term thermal cycling. Therefore, it can be stated, with sufficient certainty, that the presence of RAS may be reducing the thermal conductivity of asphalt concrete. However, a laboratory determination of the thermal conductivity of the mixtures used in section S6 would allow a more systematic definition of the true effect of RAS on the thermal properties of asphalt concrete.

5.7 GTR-MODIFIED BINDERS

The effect of GTR-modified asphalt binders was assessed by directly comparing sections N5 (Control) and S13 (GTR). Once again, cumulative distribution function plots allowed visually comparing the field thermal conductivities for both sections. Figure 5.13(a), shows the CDF plot for the field thermal conductivity calculated for the surface boundary condition, while Figure 5.13(b) displays the same plot for the asphalt-base interface. Unlike the two previous cases, the cumulative distribution plots for the field thermal conductivities considering the asphalt-base interface (k_{ac2}) transected, as shown in Figure 5.14(b). The use of the GTR-modified binder seems to be affecting the thermal conductivity of the mixture to a much lesser degree. In fact, the trend could not be visualized as clearly as in the two previous cases of RAP and RAS. However, an effect is evident and warrants further analysis.

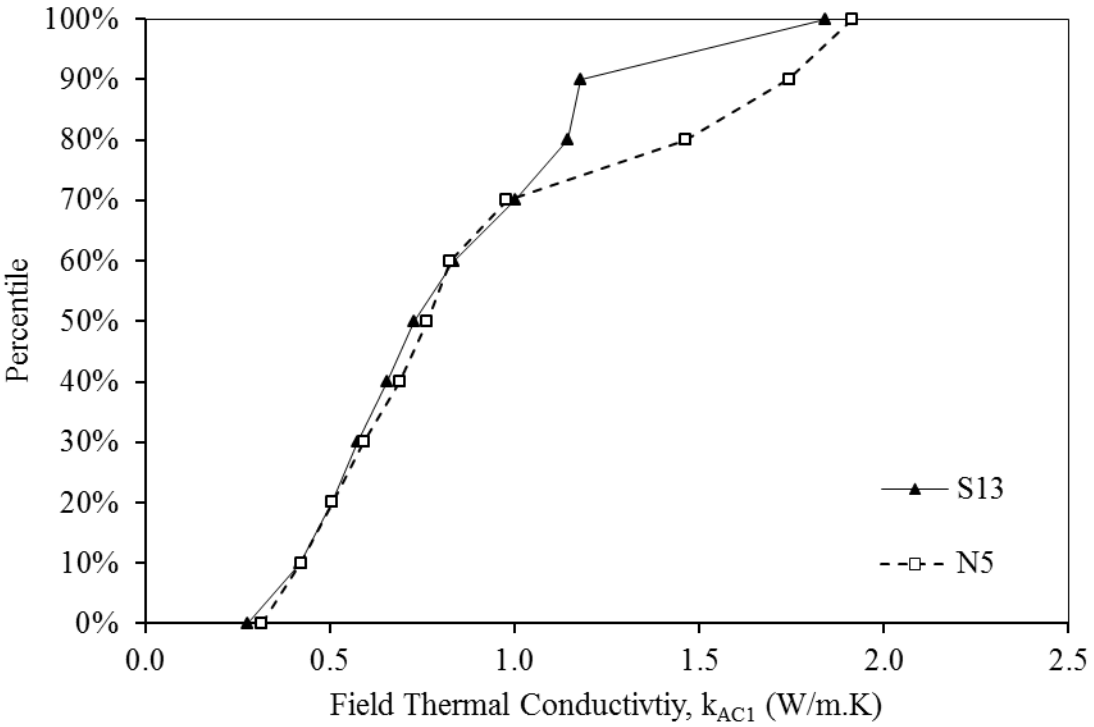

(a)

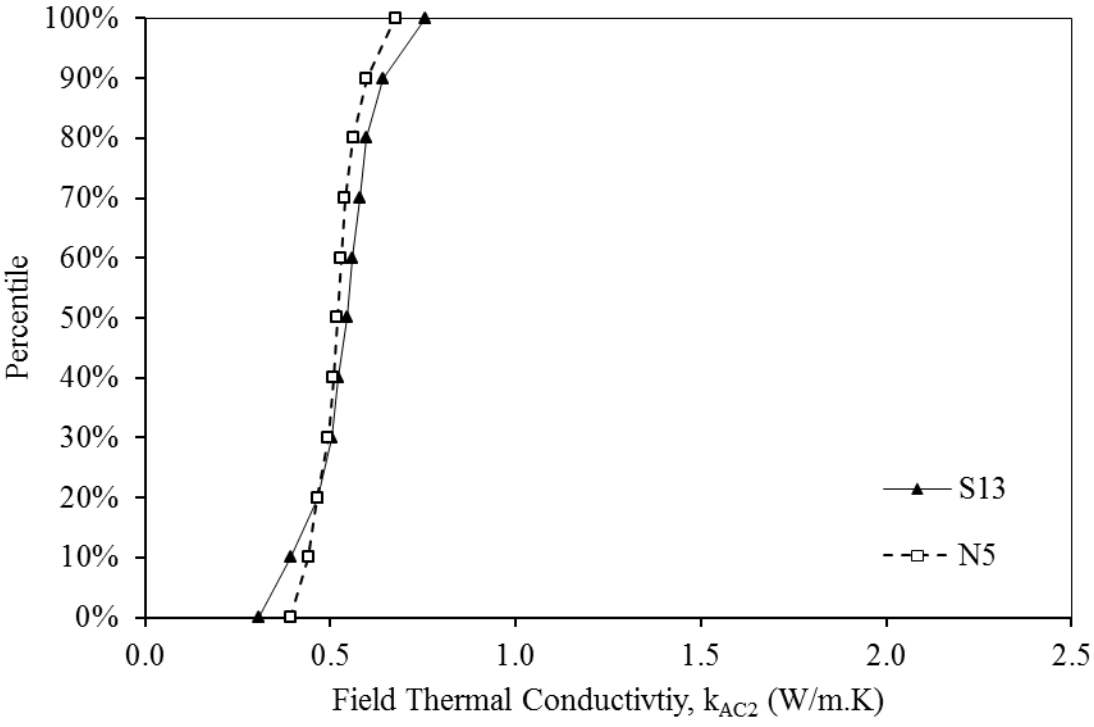

(b)

FIGURE 5.14 Effect of GTR-modified binders on field thermal conductivity values for (a) surface boundary and (b) asphalt-base interface

A pairwise comparison of the mean field thermal conductivity values revealed that in both cases, the two sections were statistically different, at a 95% confidence level. In the case of k_{ac1} an estimate difference of 0.1057 was found (t=-2.39, p=0.017), while in the case of k_{ac2} the difference was estimated as 0.1839 (t=20.89, p=0.000). Similarly, a KS test revealed strong differences amongst the two distributions, with maximum vertical deviations of 0.1765 (p=0.009) for $k_{ac1,}$ and 0.2588 (p=0.000) for k_{ac2}. In that way, the results seem to indicate that GTR-modified asphalt binders have a statistically significant influence on the thermal conductivity of asphalt concrete, for the analyzed data.

As mentioned before, during the modification process the aromatic fraction of the asphalt binder is absorbed by the GTR, causing a physical expansion of the GTR particles to a variable extent (Putman, 2006). Although this phenomenon has been demonstrated to increase the viscosity of the binder and improve the high temperature stiffness of the mixture, the presence of enlarged rubber particles may also be affecting the thermal properties of the binder. However, the results are not clear on whether the rubber particles are increasing or decreasing the thermal conductivity of the mixture. As shown in Figure 5.13(b), the average field thermal conductivity considering the asphalt-base interface was slightly higher for section S13 in comparison to section N5, indicating that GTR-modified binders may have increased the thermal conductivity of the mixture. However, further verification of the effect of GTR on the thermal properties of asphalt mixtures in the laboratory is warranted.

5.8 SUMMARY

An analysis of the thermal properties of select sustainable test sections (RAP, RAS, and GTR-modified binders) built as part of the fifth research cycle at the NCAT Test Track. It was found that, in general, the pavement sections analyzed stored thermal energy during the day and released it at night, as expected. Additionally, even if the contribution of sustainable technologies to the UHI effect was unclear, the thermal energy stored by the pavement seemed to be more affected by the total thickness of the asphalt layers, rather than the materials used.

Based on one-dimensional heat transfer mechanisms on a large plane wall, practical equations were developed to calculate the field thermal conductivity of the pavement based on internal layer temperatures and environmental conditions. Two different values of the field thermal conductivity, based on boundary conditions at the surface of the pavement and at the asphalt-base interface, were obtained daily for each section, over a 170 days analysis period. A statistical analysis established that the use of sustainable technologies such as increased RAP contents, RAS, and GTR-modified binders has a significant effect on the thermal properties of asphalt concrete pavements.

Sufficient statistical evidence pointed to the fact that the use of increased RAP contents may decrease the thermal conductivity of the pavement. From the results, it can be inferred that the presence of larger amounts of aged binder and aggregates from different sources contained in the RAP may be affecting the thermal properties of the layer by causing a reduction in the thermal conductivity of the asphalt mixture. Furthermore, the results obtained for sections S5 and N5 seem to indicate that higher RAP contents generate more significant decreases in the thermal conductivity. However,

only a more detailed laboratory study of the thermal conductivity of the mixtures used in section S5 would allow quantifying this effect with sufficient certainty.

Similarly, the aged binder contained in RAS seemed to reduce the thermal conductivity of the mixture affecting the conduction heat transfer within the asphalt layers. As mentioned before, a portion of the aged binder is mixed with the virgin binder, creating a coating of stiff binder around the RAP and/or RAS particles. The presence of this binder has been shown to affect the compactability and workability of asphalt concrete causing it to become stiffer than virgin mixtures. It may be inferred that this stiffening effect is also modifying the thermal conductivity of the material and affecting the heat transfer throughout the asphalt layers.

The effect of GTR-modified binders on the thermal conductivity of the asphalt mixture was less evident. Nonetheless, the results from this study seemed to indicate that the use of GTR-modified binders may have slightly increased the thermal conductivity of asphalt concrete. The presence of enlarged rubber particles within the asphalt binder phase of the mixture may be having an effect on the thermal properties of the GTR section. However, further laboratory verification is needed to more precisely determine the effect on the heat transfer within the asphalt layer.

CHAPTER SIX

CONCLUSIONS AND RECOMMENDATIONS

6.1 SUMMARY

A study of the thermal interactions of select sustainable technologies (RAP, RAS, GTR-modified binders, and FCM base) was performed using the structural sections built as part of the fifth research cycle at the NCAT Test Track. An initial analysis of the effect of such technologies on the initial construction cooling rate was presented in Chapter Four. For this, the MultiCool software was used to perform cooling simulations based on specific weather information, mixture characteristics and as-built properties. The resulting cooling curves were compared to field measurements performed during construction at the Test Track. A second analysis was performed to evaluate the effect of sustainable technologies on the long-term thermal response of asphalt pavements. For this, two individual analyses were conducted; one studying the heat energy absorbed by the pavement sections, and another investigating the thermal properties of the pavements in the field. For the latter, an unconventional parameter, developed based on heat transfer theory and named as “field thermal conductivity”, was used to compare the thermal conductivity of the pavement sections included in the study. The most relevant findings from this study are summarized in the following section. Similarly, certain recommendations for future research are included in the final section of this chapter.

6.2 CONCLUSIONS

6.2.1 Influence of Sustainable Pavement Technologies on Construction Cooling

The cooling curves obtained using the MultiCool model presented a very similar trend to the temperatures measured in the field, with relatively rapid initial cooling leveling over time in a logarithmic form. Even if some variations were observed between the cooling predictions and the measured temperatures, the results indicate that the MultiCool model may be used to predict the construction cooling of all asphalt concrete mixtures included in this study, with sufficient confidence. Nonetheless, additional laboratory measurements of the thermal properties of asphalt concrete would allow improving the predictions.

For the layers included in this study, the cooling trend for the measured temperatures seemed to be affected by the rolling operations. A slight discontinuity in the trend of the measured temperatures was observed, especially for the breakdown rolling stage, while the MultiCool-predicted temperatures maintain a constant trend regardless of the rolling stage. These discontinuities may be explained by two main conditions; the effect of the thin water film from the drums of the roller and the densifications of the mix.

A direct comparison between measured and predicted temperatures revealed that the MultiCool model may tend to under-predict for higher temperatures and over-predict for lower temperatures. A statistical analysis of the practical differences between the measured and predicted temperatures revealed that six of the nineteen analyzed pavement layers exceeded the ±18°F tolerance level established in the original validation of the model. While 68% of the lifts investigated were within the tolerance, these six cases warranted further investigation.

The use of sustainable technologies such as high RAP contents, RAS, GTR-modified binders, and FCM bases were found to have a significant effect on the fit of the MultiCool model. Even if the model appeared to predict the pavement cooling with sufficient precision for the majority of the lifts evaluated, clear differences were found in certain specific cases. These differences seemed to indicate that some of these technologies affected the cooling of asphalt concrete during construction.

Although some significant differences were found between the layers containing RAP, the results indicated that high RAP contents didn't have a significant effect on the cooling of asphalt concrete during construction.

Even if the MultiCool model is adequately predicting the pavement cooling of RAS mixtures, sufficient statistical evidence was found indicating that the use of RAS tends to significantly affect the predictions, particularly in the case of SMA mixtures. However, the MultiCool software continues to predict the time available for compaction with sufficient accuracy for practical purposes. In any case, to achieve optimum density, the compaction process should be carried as soon as the mixture is stable enough to withstand the weight of the rollers, especially in the case of SMA mixtures with RAS.

Relative variability was observed for the cooling prediction in the analysis of mixtures containing GTR-modified binders. Even if the MultiCool model continued to describe the cooling rate measured in the field reasonably well, the use of GTR-modified binders clearly affects the cooling predictions. It was suggested that the presence of GTR may be affecting the chemical composition of the asphalt binder, which in turn may be affecting the thermal properties of the mixture. Nonetheless, the MultiCool software provided a sufficiently precise prediction of the time available to compact the GTR

mixtures, and may be used to plan paving operations in the field with sufficient confidence. In the same way as for RAS mixtures, to achieve optimum density in the field, the compaction process should be carried as soon as the mixture is stable enough to withstand the weight of the roller.

The use of a FCM base considerably affected the predictions of the MultiCool model. The relative difference observed in the results seemed to indicate that the thermal properties of FCM materials may differ from those of granular materials or asphalt concrete. An alternative approach, considering the average between the times available for compaction for a granular base and for an asphalt concrete as the compaction window for a FCM, was proposed for practicality in the use of the MultiCool software. Nonetheless, a more detailed study of the of the heat transfer in FCM materials would allow a more accurate determination of the thermal behavior, and proposing a more accurate solution. These values may be included in the MultiCool software to improve the predictions in the presence of alternative base materials.

6.2.2 Influence of Sustainable Technologies on In-Place Thermal Properties

In agreement with the UHI concept, the temperature of all pavement sections included in the study presented daily fluctuations and varied with the depth within the asphalt layers, decreasing during the day and increasing at night. The thermal energy stored by each pavement seemed to be more susceptible to the total thickness of the asphalt layers, rather than the materials used to build it. A statistical analysis of the absorbed energy revealed slight differences between the section containing GTR-modified binder and all other

sections included in the study. However, the specific contribution of the analyzed sustainable technologies to the UHI effect was unclear, warranting further research.

Practical equations were proposed to calculate the field thermal conductivity of the pavement based on one-dimensional heat transfer mechanisms on a large planar wall. Using the internal layer temperatures and environmental conditions, two different daily values of the field thermal conductivity were calculated for each section, over a 170 day analysis period. Each value considered an independent boundary condition, one at the surface of the pavement and another at the asphalt-base interface, to assign a rather empirical value to the conduction properties of the asphalt concrete. Even if the obtained values seemed to fall within the ranges found in the literature for the thermal conductivity of asphalt concrete, the proposed field thermal conductivity consisted of an extensive property that accounted for the conditions in the field. It was suggested to avoid comparing these two parameters as they represent different properties of the material. Nonetheless, the proposed "field thermal conductivity" may be used to compare the heat conduction between the sections included in this study.

A statistical analysis of the obtained values for the field thermal conductivity established that the use of sustainable technologies such as increased RAP contents, RAS, and GTR-modified binders has a significant effect on the thermal properties of asphalt concrete pavements.

Sufficient statistical evidence was found indicating that the use of high RAP contents may decrease the thermal conductivity of the pavement, thus reducing the rate of heat transfer through the material. In that way, in service pavements built with RAP mixtures gain and loose heat at slower rate in comparison with conventional asphalt

mixtures. This would generate more stable pavement temperatures and less extreme peak values. In other words, less heat would be absorbed by RAP-pavements during the day and released into the atmosphere at night, reducing the contribution of the pavement to the UHI effect in comparison with conventional materials. From the results, it was inferred that the presence of larger amounts of aged binder and aggregates from different sources contained in the RAP may have been affecting the thermal properties of the layer by reducing the thermal conductivity of the asphalt mixture. Furthermore, the results obtained for sections S5 and N5 seemed to indicate that higher RAP contents generate more significant decreases in the thermal conductivity, than average RAP contents. However, only a more detailed laboratory study of the thermal conductivity of the mixtures used in section S5 would allow quantifying this effect with sufficient certainty.

A similar result was obtained for the sections containing RAS. Sufficient statistical evidence was found revealing a difference in the heat transfer between the control section and the section containing RAS. This allowed inferring that, in the same way as RAP; the stiffening effect of including RAS in the mixture resulted in the reduction of the thermal conductivity of the mixture and affected the conduction heat transfer within the asphalt layers. This effect could have been amplified the presence of aggregates from different sources included the RAS used for this study.

The use of the GTR-modified binder seemed to have a less significant effect on the thermal conductivity of the mixture. Nonetheless, the results from this study indicated that the GTR-modified binders were slightly increasing the thermal conductivity of asphalt concrete. It was inferred that the presence of enlarged rubber particles within the asphalt binder phase of the mixture had an effect on the thermal properties of the GTR

section in comparison to the control section. However, the results warranted further laboratory verification of the thermal properties of mixtures containing GTR-modified binders to more precisely determine the effect on the heat transfer within the asphalt layer.

6.3 RECOMMENDATIONS

Based on the results obtained in this study, it is recommended to continue using the MultiCool program for predicting the cooling of sustainable asphalt concrete materials. A conservative approach may be taken by considering a possible variation in the prediction of approximately ± 18°F, as suggested in the original validation of the software. Additionally, in the case of mixtures containing RAS and GTR-modified binders, and in the presence of FCM base layers, where the time available for compaction may be significantly reduced, it is recommended to initiate the compaction process as soon as soon as the mixture is stable enough to withstand the weight of the rollers without any excessive deformations of the mat.

It is recommended to continue the study of the field thermal conductivities to include a longer period of time, possibly the duration of the research cycle at the Test Track. This would allow assessing the influence of changing weather conditions, as well as the effect of mixture aging on the heat transfer of asphalt concrete. Similarly, the study could be extended to other sections at the Test Track, to increase amount of available information and support the conclusions from this study.

Given the observed effects of sustainable technologies on the thermal interactions of the sections included in this study, it is suggested that a laboratory study be performed

to determine the specific thermal conductivity of the mixtures used in this study. The results would not only allow a better assessment of the thermal properties of sustainable asphalt concrete materials in support of the findings included in this study, but could also be used to modify the inputs in the MultiCool software and improve cooling predictions.

An appealing alternative would be to calculate the thermal properties of the individual sustainable materials (i.e. RAP, RAS, GTR-modified binders) and develop equations to correlate them to the thermal properties of the mixture. This approach, similar to the solution suggested by Côté et al. (2013) for thermal conductivity, would allow calculating more precise heat transfer mechanisms based on the actual properties of the materials. In the same way, the equations could be included in the MultiCool software, where the user could have the option to specify the components of the mixtures and obtain a more accurate prediction of the cooling of the asphalt layer.

REFERENCES

American Association of State Highway and Transportation Officials. AASHTOWare Pavement Software. http://www.aashtoware.org/Pavement/Pages/default.aspx. Accessed August 29, 2013.

Asphalt Academy. *Bitumen Stabilised Materials, a Guideline for the Design and Construction of Bitumen Emulsion and Foamed Bitumen Stabilised Materials*. Second Edition. Asphalt Academy, South Africa, 2009.

Asphalt Institute. Manual Series 4 – The Asphalt Handbook. Seventh Edition. Asphalt Institute Inc., Lexington, KY, 2007.

Asphalt Recycling and Reclaiming Association. *Basic Asphalt Recycling Manual*. ARRA, Annapolis, MD, 2001.

ASTM Standard C177–10. *Standard Test Method for Steady-State Heat Flux Measurements and Thermal Transmission Properties by Means of the Guarded-Hot-Plate Apparatus*. ASTM International, West Conshohocken, PA, 2010. www.astm.org.

ASTM Standard C518-10. *Standard Test Method for Steady-State Thermal Transmission Properties by Means of the Heat Flow Meter Apparatus*. ASTM International, West Conshohocken, PA, 2010. www.astm.org.

ASTM Standard C1114-06. *Standard Test Method for Steady-State Transmission Properties by Means of the Thin Heater Apparatus*. ASTM International, West Conshohocken, PA, 2006. www.astm.org.

ASTM Standard C1045-07. *Standard Test Method for Calculating Thermal Transmission Properties under Steady State Conditions*. ASTM International, West Conshohocken, PA, 2007. www.astm.org.

ASTM Standard D5334-08. *Standard Test Method for Determination of Thermal Conductivity of Soil and Soft Rock by Thermal Needle Probe Procedure*. ASTM International, West Conshohocken, PA, 2008. www.astm.org.

ASTM Standard D2493-09. *Standard Viscosity-Temperature Chart for Asphalts*. ASTM International, West Conshohocken, PA, 2009. www.astm.org.

ARA Inc., ERES Consultants Division. Part 2 Design Inputs: Chapter 3 Environmental Effects. *Guide for Mechanistic-Empirical Pavement Design Guide of New and Rehabilitated Pavement Structures*, Final Report, NCHRP 1-37A, 2004.

Bahia, H. U., T. P. Friemel, P. A. Peterson, J. S. Russel, and B. Poehnelt. Optimization of Constructability and Resistance to Traffic: A New Design Approach for HMA Using the Superpave Compactor. *Journal of Association of Asphalt Paving Technologists*, Vol. 67, 1998, pp. 189-213.

Bahia, H. U., D. I. Hanson, M. Zeng, H. Zai, M. A. Khatri, and R. M. Anderson. NCHRP Report 459: Characterization of Modified Asphalt Binders in Superpave Mix Design. National Cooperative Highway Research Program, Transportation Research Board of the National Academies, National Academy Press, Washington, D.C., 2001.

Bahia, H. U., A. Fahim, and K. Nam. Prediction of Compaction Temperatures Using Binder Rheology. In *Transportation Research Circular, No. E-C105*, Transportation Research Board of the National Academies, Washington, D.C., 2006, pp. 3-17.

Bergman, T. L., A. S. Lavine, F. P. Incropera, and D. P. Dewitt. Fundamentals of Heat and Mass Transfer. Seventh Edition. John Wiley and Sons, Inc., Hoboken, NJ, 2011.

Bijleveld, F., S. Miller, A. De Bondt, and A. Doree. Too Hot to Handle, Too Cold to Control: Influence of Compaction Temperature on the Mechanical Properties of Asphalt. In *Proceedings of the 5th Eurasphalt & Eurobitume Congress.* Istanbul, Turkey, 2012, pp. 231-242.

Cabrera, J.G. Assessment of the Workability of Bituminous Mixtures. *Highways and Transportation*, Vol. 38, No. 11, 1991, pp. 17–23.

Carlson, J.D., R. Bhardwaj, P. E. Pelan, K. E. Kaloush, J. S. Golden. Determining Thermal Conductivity of Paving Materials Using Cylindrical Sample Geometry. In *ASCE Journal of Materials in Civil Engineering*, Vol. 22, No. 2, 2010, pp. 186–195.

Cengel, Y. and A. Ghajar. Heat and Mass Transfer Fundamentals and Applications. Fourth Edition. McGraw-Hill Education, New York, NY, 2010.

Chadbourn, B. A., J. A. Luoma, D. E. Newcomb, and V. R. Voller. Considerations of Hot-Mix Asphalt Thermal Properties During Compaction. Quality Management of Hot-Mix Asphalt, ASTM STP1299. American Society for Testing and Materials, 1996.

Chadbourn, B. A., D. E. Newcomb, V. R. Voller, R. A. De Sombre, J. A. Luoma, and D. H. Timm. *An Asphalt Paving Tool for Adverse Conditions.* Report MN/RC-1998-18. Minnesota Department of Transportation, 1998.

Chang, C., Y. Chang, and J. Chen. Effect of Mixture Characteristics on Cooling Rate of Asphalt Pavements. In *ASCE Journal of Transportation Engineering*, Vol. 135, No. 5, 2009, pp. 297–304.

Copeland, A. *Reclaimed Asphalt Pavement in Asphalt Mixtures: State of the Practice*. Publication No. FHWA-HRT-11-021, Federal Highway Administration, Washington, DC, 2011.

Corlew, J. S. and Dickson, P.F. Methods for Calculating Temperature Profiles of Hot-Mix Asphalt Concrete as Related to the Construction of Asphalt Pavements. *Journal of Association of Asphalt Paving Technologists*, Vol. 37, 1968, pp. 101-140.

Côté, J., J.M. Konrad, P. T. Dorchies. Use of Low Density Asphalt in Base-Course as a Mitigation for Frost Action in Pavements. In *Proceedings of the 12th Cold Region Engineering Specialty Conference*. American Society of Civil Engineers, Edmonton, 2004, pp. 16-19.

Côté, J. and J.M. Konrad. Thermal Conductivity of Base Course Materials. *Canadian Geotechnical Journal*, Vol. 42, 2005, pp. 61-78.

Côté, J., V. Grosjean, and J.M. Konrad. Thermal Conductivity of Bitumen Concrete. *Canadian Journal of Civil Engineering*, Vol. 40, 2013, pp. 172-180.

Daines, M. *Cooling Time of Bituminous Layers and Time Available for their Compaction*. Report NRR 4, Transport and Road Research Laboratory, 1985.

Decker, D. S. State-of-the-Practice for Cold Weather Compaction of Hot-Mix Asphalt Pavements. In *Transportation Research Circular, No. E-C105*, Transportation Research Board of the National Academies, Washington, D.C., 2006, pp. 27-33.

De Sombre, R., D. E. Newcomb, B. Chadbourn, and V. Voller. Parameters to Define the Laboratory Compaction Temperature Range of Hot-Mix Asphalt. *Journal of Association of Asphalt Paving Technologists*, Vol. 67, 1998, pp.125-142.

Devore, J. L. *Probability and Statistics for Engineering and the Sciences.* Fourth Edition. International Thomson Publishing Company, Belmont, 1995.

Dynapac Road Construction Equipment. http://www.dynapac.com/knowledge/End-user-Support/PaveComp/. Accessed August 18, 2013.

Eurovia, a subsidiary of Vinci. http://www.eurovia.com/en/cases/gradius-calculates-optimal-paving-temperature. Accessed August 18, 2013.

Federal Highway Administration. Quantifying Pavement Albedo. https://www.fbo.gov/?s=opportunity&mode=form&id=550f071692baac6d8a6dc550b76d733a&tab=core&_cview=1. Accessed September 8, 2013.

Foo, K. Y., D. I. Hanson, T. A. Lynn. Evaluation of Roofing Shingles in Hot Mix Asphalt. In *Journal of Materials in Civil Engineering*, Vol. 11, No. 1, pp. 15-20, 1999.

Fwa, T. F., B. H. Low, and S. A. Tan. Laboratory Determination of Thermal Properties of Asphalt Mixtures by Transient Heat Conduction. In *Transportation Research Record: Journal of the Transportation Research Board, No. 1492*, Transportation Research Board of the National Academies, Washington, D.C., 1995, pp. 118-128.

Gui, J., P. Phelan, K. Kaloush, and J. Golden. Impact of Pavement Thermophysical Properties on Surface Temperatures. In *Journal of Materials in Civil Engineering*, Vol. 19, No. 8, pp. 683-690, 2007.

Guler, M., H. U. Bahia, P. J. Bosscher, and M. E. Plesha. Device for Measuring Shear Resistance of Hot-Mix Asphalt in Gyratory Compactor. In *Transportation Research Record: Journal of the Transportation Research Board, No. 1723*, Transportation Research Board of the National Academies, Washington, D.C., 2000, pp. 116-124.

Guttman, N. B. and J. D. Matthews. Computation of Extraterrestrial Solar Radiation, Solar Elevation Angle, and True Solar Time of Sunrise and Sunset. In *Solmet Final Report, Vol. 2,* National Climatic Center, U.S. Department of Commerce, 1979, pp. 49-52.

Gudimettla, J. M., A. L. Cooley, and E. R. Brown. Workability of Hot Mix Asphalt. Report No. 03-03, National Center for Asphalt Technology, Auburn, AL, 2003.

Halles, F., G. Thenoux and A. Gonzalez. Stiffness Evolution of Granular Material s Stabilized with Foamed Bitumen and Cement. Presented at Transportation Research Board 92nd Annual Meeting, Washington, DC, 2013.

Harvey, J., A. Chong, and J. Roessler. Climate Regions for Mechanistic-Empirical Pavement Design in California and Expected Effects on Performance. Report Prepared for the California Department of Transportation, California, 2000.

Heitzman, M. A. *State of the Practice – Design and Construction of Asphalt Paving Materials with Crumb Rubber Modifier*. Publication No. FHWA 92-022, Federal Highway Administration, Washington, DC, 1992.

Hermansson, A. Simulation Model for Calculating Pavement Temperatures Including Maximum Temperature. In *Transportation Research Record: Journal of the Transportation Research Board, No. 1699*, Transportation Research Board of the National Academies, Washington, D.C., 2000, pp. 134-131.

Hermansson, A. Mathematical Model for Calculation of Pavement Temperatures: Comparison of Calculated and Measured Temperatures. In *Transportation Research Record: Journal of the Transportation Research Board, No. 1764*, Transportation Research Board of the National Academies, Washington, D.C., 2001, pp. 180-188.

Highter, W. H. and D. J. Wall. Thermal Properties of Some Asphaltic Concrete Mixes. In *Transportation Research Record: Journal of the Transportation Research Board, No. 968*, Transportation Research Board of the National Academies, Washington, D.C., 1984, pp. 38-45.

Huang, Y. H. Pavement Analysis and Design. Second Edition. Pearson Education Inc., Upper Saddle River, NJ, 2004.

Huang, B., G. Li, D. Vukosavljevic, X. Shu, and B. Egan. Laboratory Investigation of Mixing Hot-Mix Asphalt with Reclaimed Asphalt Pavement. In *Transportation Research Record: Journal of the Transportation Research Board, No. 1929*, Transportation Research Board of the National Academies, Washington, D.C., 2005, pp. 37-45.

Huerne, H. L. *Compaction of Asphalt Road Pavements Using Finite Elements and Critical State Theory*. Dissertation submitted in partial fulfillment of the requirements for the Degree of Doctor of Philosophy. University of Twente, Enschede, Netherlands, 2004.

Hunter, R. and Mcguire, G. A Fast and Efficient Method for Predicting Cooling Profiles in Bituminous Materials. *Civil Engineering*, 1986, pp. 24-25.

Jenkins, K. and Van de Ven, M. Guidelines for the Mix Design and Performance Prediction of Foamed Bitumen Mixes. Presented at 20th South African Transport Conference, Pretoria, South Africa, 2001.

Jenkins, K., M. Van de Ven, and J. de Groot. Characterization of Foamed Bitumen. Presented at 7th Conference on Asphalt Pavements for Southern Africa, Pretoria, South Africa, 1999.

Jordan, P. and Thomas, M. *Prediction of Cooling Curves for Hot-Mix Paving Materials by a Computer Program.* Report 729, Transport and Road Research Laboratory, 1976.

Kaloush, K. E., M. W. Witczak, A. C. Sotil, and G. B. Way. Laboratory Evaluation of Asphalt Rubber Mixtures Using the Dynamic Modulus Test. Presented at Transportation Research Board 82nd Annual Meeting, Washington, DC, 2003

Kandhal, P. S. and R. B. Mallick. *Pavement Recycling Guidelines for State and Local Governments – Participant's Reference Book.* Publication No. FHWA-98-042, Federal Highway Administration, Washington, DC, 1997.

Kari, W.J. Mix Properties as They Affect Compaction. *Journal of Association of Asphalt Paving Technologists*, Vol. 36, 1967, pp. 295-309.

Khatri, A., H. U. Bahia, and D. Hanson. Mixing and Compaction Temperature for Modified Binders Using the Superpave Gyratory Compactor. *Journal of Association of Asphalt Paving Technologists*, Vol. 70, 2001, pp. 424-466.

Kavianipour, A., J. V. Beck. Thermal Property Estimation Utilizing the Laplace Transform with Application to Asphaltic Pavement. In *International Journal of Heat and Mass Transfer*, Vol. 20, No. 3, pp. 259-267, 1977.

Kersten, M. S. Thermal Properties of Soils. In *University of Minnesota Institute of Technology Engineering Experiment Station Bulletin No. 28*, Vol. 52, No. 21, 1949.

Khosravifar, S., C. W. Schwartz and D. G. Goulias. Mechanistic Structural Properties of Foamed Asphalt Stabilized Base Materials. Presented at Transportation Research Board 92nd Annual Meeting, Washington, DC, 2013.

Khosravifar, S., D. Goulias, and C. Schwartz. Laboratory Evaluation of Foamed Asphalt Stabilized Base Materials. Presented at ASCE GeoCongress 2012, Oakland, CA, 2012.

Kim, Y. and H. Lee. Development of Mix Design Procedure for Cold In-Place Recycling with Foamed Asphalt. In *Journal of Materials in Civil Engineering*, Vol. 18, No. 1, pp. 116-124, 2006.

Kim, Y. and H. Lee. Influence of Reclaimed Asphalt Pavement Temperature on Mix Design Process of Cold In-Place Recycling Using Foamed Asphalt. In *Journal of Materials in Civil Engineering*, Vol. 23, No. 7, pp. 961-968, 2011.

Kim, Y., H. Lee and M. Heitzman. Dynamic Modulus and Repeated Load Tests of Cold In-Place Recycling Mixtures Using Foamed Asphalt. In *Journal of Materials in Civil Engineering*, vol. 21, No. 6, pp. 279-285, 2009.

Lee, H. and Y. Kim. *Development of a Mix Design Process for Cold-In-Place Rehabilitation Using Foamed Asphalt*. Final Report for TR-474 Phase I. University of Iowa, Iowa, 2003.

Leiva-Villacorta, F. and R. C. West. Analysis of HMA Field Compactability Using Accumulated Compaction Pressure Concept. In *Transportation Research Record: Journal of the Transportation Research Board, No. 2057*, Transportation Research Board of the National Academies, Washington, D.C., 2008, pp. 89-98.

Leiva-Villacorta, F. *Relationships Between Laboratory Measured Characteristics of HMA and Field Compactability*. Thesis submitted in partial fulfillment of the requirements for the Degree of Master of Science. Auburn University, Auburn, AL, 2007.

Loizos, A. and V. Papavasiliou. Evaluation of Foamed Asphalt Cold In-Place Pavement Recycling Using Nondestructive Techniques. In *Journal of Transortation Engineering*, Vol. 132, No. 12, pp. 970-978, 2006.

Luca, J. and D. E. Mrawira. New Measurements of Thermal Properties of Superpave Asphalt Concrete. In *Journal of Materials in Civil Engineering*, vol. 17, No. 1, pp. 72-79, 2005.

Mamlouk, M. S., J. P. Zaniewski. Materials for Civil and Construction Engineers. Second Edition. Pearson Education, Upper Saddle River, NJ, 2009.

Mieczkowski, P. The Effect of Weather and Climatic Factors on Temperature Drops in Built-In Asphalt Mixtures. In *Foundations of Civil and Environmental Engineering*, No. 9, pp. 95-104, 2007.

Mrawira, M. E. and J. Luca. Thermal Properties and Transient Temperature Response of Full-Depth Asphalt Pavements. In *Transportation Research Record: Journal of the Transportation Research Board, No. 1809*, Transportation Ressearch Board of the National Academies, Washington, D.C., 2002, pp. 160-171.

Mrawira, M. E. and J. Luca. Effect of Aggregate Type, Gradation, and Compaction Level on Thermal Properties of Hot-Mix Asphalts. *Canadian Journal of Civil Engineering*, Vol. 33, 2006, pp. 1410-1414.

National Asphalt Pavement Association. *Roller Operations for Quality*. Information Series 121. National Asphalt Pavement Association, Lanham, 2002.

National Asphalt Pavement Association. *TK-001 Compaction Toolkit*. http://store.asphaltpavement.org/index.php?productID=236. Accessed May 29, 2013.

National Center for Asphalt Technology (NCAT). Hot Mix Asphalt Materials, Mixture Design and Construction. Third Edition. NAPA Research and Education Foundation, Lanham, MD, 2009.

National Center for Asphalt Technology. Research Synopsis – TRB Report 2098: Strategies for Design and Construction of High-Reflectance Asphalt Pavements. http://www.ncat.us/files/research-synopses/pavement-reflectivity.pdf. Accessed September 8, 2013.

Ongel, A. and J. Harvey. *Analysis of 30 years of Pavement Temperatures using the Enhanced Integrated Climate Model (EICM)*. Draft Report Prepared for the California Department of Transportation, California, 2004.

Price, I. Determining if Skewness and Kurtosis Are Significantly Non-Normal. School of Psychology, University of New England. http://www.une.edu.au/WebStat/unit_materials/c4_descriptive_statistics/determine_skew_kurt.html. Accessed September 9, 2013.

Priest, A. L. and D. H. Timm. *Methodology and Calibration of Fatigue Transfer Functions for Mechanistic-Empirical Flexible Pavement Design*. Report No. 06-03, National Center for Asphalt Technology, Auburn University, AL, 2006.

Prowell, B. D., G. C. Hurley, B. Frank. *Warm-Mix Asphalt: Best Practices*. Second Edition. National Asphalt Pavement Association, Lanham, MD, 2011.

Putman, B. J. and S. N. Amirkhanian. Crumb Rubber Modification of Binders: Interaction and Particle Effects. Clemson University Department of Civil Engineering, Clemson, SC, 2006.

Romanoschi, S., M. Hossain, A. Gisi, and M. Heitzman. Accelerated Pavement Testing Evaluation of the Structural Contribution of Full-Depth Reclamation Material with Foamed Asphalt. In *Transportation Research Record: Journal of the Transportation Research Board, No. 1896*, Transportation Research Board of the National Academies, Washington, D.C., 2004, pp. 199-207.

Robinette, C. and J. Epps. Energy, Emissions, Material Conservation, and Prices Associated with Construction, Rehabilitation, and Material Alternatives for Flexible Pavements. In *Transportation Research Record: Journal of the Transportation Research Board, No. 2179*, Transportation Research Board of the National Academies, Washington, D.C., 2010, pp. 10-22.

Saint John's University. *Kolmogorov-Smirnov Test*. http://www.physics.csbsju.edu/stats/KS-test.html. Accessed May 29, 2013.

Salomon, D. and H. Zhai. Ranking Asphalt Binders by Activation Energy for Flow. *Journal of Applied Asphalt Binder Technology*, Vol. 2, 2002, pp. 1-9.

Tageler, P. and Dempsey, B. A Method of Predicting Compaction Time for Hot-Mix Bituminous Concrete. *Journal of Association of Asphalt Paving Technologists*, Vol. 42, 1973, pp. 499-523.

Solaimanian, M. and T. W. Kennedy. Predicting Maximum Pavement Surface Temperature Using Maximum air Temperature and Solar Radiation. In *Transportation Research Record: Journal of the Transportation Research Board, No. 1417*, Transportation Research Board of the National Academies, Washington, D.C., 1993, pp. 1-11.

Taha, H. Urban Climates and Heat Islands: Albedo, Evapotranspiration, and Anthropogenic Heat. *Energy and Buildings*, Vol. 25, No. 2, 1997, pp. 99-103.

Tang, Y. and J. E. Haddock. Field Testing of the Zero Shear Viscosity Method. In *Transportation Research Circular, No. E-C105*, Transportation Research Board of the National Academies, Washington, D.C., 2006, pp. 18-26.

Tan, S. W., T. F. Fwa, C. T. Chuai, and B. H. Low. Determination of Thermal Properties of Pavement Materials and Unbound Aggregates by Transient Heat Conduction. In *Journal of Testing and Evaluation*, vol. 25, 1997, pp. 15-22.

Taylor, A. J. and D. H. Timm. *Mechanistic Characterization of Resilient Moduli for Unbound Pavement Layer Materials*. Report No. 09-06, National Center for Asphalt Technology, Auburn University, AL, 2009.

Timm, D. H., V. R. Voller, E. Lee, and J. Harvey. CalCool: A Multi-Layer Asphalt Pavement Cooling Tool for Temperature Prediction During Construction. In *International Journal of Pavement Engineering*, Vol. 2, 2001, pp. 169–185.

Timm, D. H. Design, Construction and Instrumentation of the 2006Test Track Structural Study. Report No. 09-01, National Center for Asphalt Technology, Auburn University, AL, 2009.

Turner, W. C. and J. F. Malloy. Thermal Insulation Handbook. Robert E. Krieger Publishing Company Inc., Malabar, FL, 1981.

United States Environmental Protection Agency (EPA). Reducing Urban Heat Island: Compendium of Strategies. http://www.epa.gov/heatisland/resources/pdf/BasicsCompendium.pdf. Accessed August 26th 2013.

Van der Walt, N., P. Botha, C. Semmelink, F. Bloemfontein, and N. Salminen. The Use of Foamed Bitumen in Full-Depth In-Place Recycling of Pavement Layers Illustrating the Basic Concept of Water Saturation in the Foam Process. Presented at 7th Conference on Asphalt Pavements for Southern Africa, Pretoria, South Africa, 1999.

Varsenev, A., Bijleveld F., T. Hartmann, and A. G. Doree. A Real System for Prediction Cooling Within the Asphalt Layer to Support Rolling Operations. In *Proceedings of the 5th Eurasphalt & Eurobitume Congress.* Istanbul, Turkey, 2012, pp. 231-242.

Vargas-Nordcbeck, A., and D. H. Timm. Validation of Cooling Curves Prediction Model for Nonconventional Asphalt Concrete Mixtures. In *Transportation Research Record: Journal of the Transportation Research Board, No. 2228*, Transportation Research Board of the National Academies, Washington, D.C., 2011a, pp. 111–119.

Vargas-Nordcbeck, A. and D. H. Timm. Evaluation of Pavement Temperatures of Various Pavement Sections. *Transportation and Development Institute Congress*. Chicago, IL, 2011b, pp. 782-791.

Vargas Nordcbeck, A. *Physical and Structural Characterization of Sustainable Asphalt Pavement Sections at the NCAT Test Track*. Dissertation submitted in partial fulfillment of the requirements for the Degree of Doctor of Philosophy. Auburn University, Auburn, AL, 2012.

Wang, L. Mechanics of Asphalt: Microstructure and Micromechanics. McGraw-Hill Companies, Inc., New York, NY, 2011.

Way, G. B., K. E. Kaloush, and K. P. Biligiri. Asphalt-Rubber Standard PracticeGuide. First Edition. Rubber Pavements Association, Tempe, AZ, 2011.

West, R. C., D. E. Watson, P. A. Turner, and J. R. Casola. NCHRP Report 648: Mixing and Compaction Temperatures of Asphalt Binders in Hot-Mix Asphalt. National Cooperative Highway Research Program, Transportation Research Board of the National Academies, National Academy Press, Washington, D.C., 2010.

West, R., D. Timm, R. Willis, B. Powell, N. Tran, D. Watson, M. Sakhaeifar, R. Brown, M. Robbins, A. Vargas-Nordbeck, F. Leiva-Villacorta, X. Guo, and J. Nelson. *Phase IV NCAT Pavement Test Track Findings*, *Final Report*. Report No. 12-10, National Center for Asphalt Technology, Auburn University, AL, 2012.

Williamson, R. H. Effects of Environment on Pavement Temperatures. In *Proceedings of the 3rd International Conference on the Design of Asphalt Pavements*, International Society for Asphalt Pavements, London, England, 1972, pp. 144-158.

Wise J. and R. Lorio. A Practical Guide for Estimating the Compaction Window Time for Thin Layer Hot Mix Asphalt. . In *Proceedings of the 8th Conference on Asphalt Pavements for Southern Africa.* Sun City, South Africa, 2004.

Wirtgen Group. *Foamed Bitumen - The Innovative Binding Agent for Road Construction.* Wirtgen GmbH, 2002.

Wirtgen Group. *Wirtgen Cold Recycling Manual*. Windhagen, Germany, Wirtgen GmbH, 2012.

Wolfe, R. K., G. L. Heath , and D. C. Colony. Cooling Curve Prediction of Asphaltic Concrete. In *Journal of Transportation Engineering*, vol. 109, No. 1, pp. 137-147, 1983.

World Road Association. *Pavement Recycling Guidelines for In-Place Recycling with Cement, In-Place Recycling with Emulsion or Foamed Bitumen, Hot Mix Recycling in Plant.* Report 78-02-E AIPCR/PIARC, 2003.

Yildrim, Y., M. Solaiman, and T. Kennedy. *Mixing and Compaction Temperatures for Hot Mix Asphalt Concrete*. Report No. 1250-5, Center for Transportation Research, The University of Texas at Austin, Austin, TX, 2000.

APPENDIX A

AS-BUILT PROPERTIES

6/14/2013

Quadrant: N
Section: 3
Sublot: 1

Laboratory Diary

General Description of Mix and Materials

Design Method:	SMA
Compactive Effort:	75 gyrations
Binder Performance Grade:	76-22
Modifier Type:	SBS
Aggregate Type:	SMA 12.5 RAP
Design Gradation Type:	SMA

Avg. Lab Properties of Plant Produced Mix

Sieve Size	Target	QC
25 mm (1"):	100	100
19 mm (3/4"):	100	100
12.5 mm (1/2"):	86	88
9.5 mm (3/8"):	66	70
4.75 mm (#4):	27	32
2.36 mm (#8):	20	22
1.18 mm (#16):	NA	20
0.60 mm (#30):	16	18
0.30 mm (#50):	NA	16
0.15 mm (#100):	NA	15
0.075 mm (#200):	10.0	11.6
Binder Content (Pb):	6.4	6.1
Eff. Binder Content (Pbe):	6.4	6.1
Dust-to-Binder Ratio:	1.6	1.9
Rice Gravity (Gmm):	2.631	2.635
Avg. Bulk Gravity (Gmb):	2.549	2.572
Avg Air Voids (Va):	3.1	2.4
Agg. Bulk Gravity (Gsb):	2.944	2.933
Avg VMA:	18.9	17.6
Avg. VFA:	84	87

Construction Diary

Relevant Conditions for Construction

Completion Date:	August 24, 2012
24 Hour High Temperature (F):	0
24 Hour Low Temperature (F):	0
24 Hour Rainfall (in):	0.00
Planned Subot Lift Thickness (in):	2.0
Paving Machine:	0.00

Plant Configuration and Placement Details

Component	% Setting
Binder Content (Plant Setting)	6.2

As-Built Subot Lift Thickness (in):	2.1
Total Thickness of All 2012 Subots (in):	9.7
Approx. Underlying HMA Thickness (in):	0.0
Type of Tack Coat Utilized:	0.0
Undiluted Target Tack Rate (gal/sy):	0.00
Approx. Avg. Temperature at Plant (F):	325
Avg. Measured Mat Compaction:	95.7%

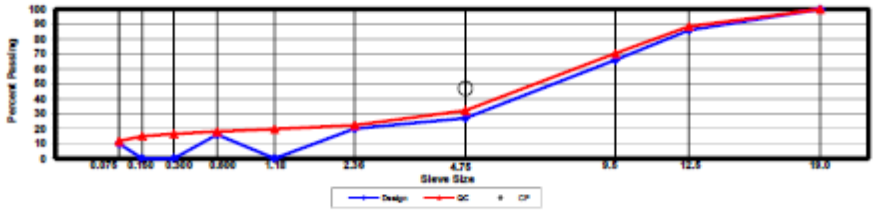

General Notes:
1) Mixes are referenced by quadrant (E=East, N=North, W=West, S=South, L=Lee Rd 159), section number, and subiot (top=1);
2) SMA and OGFC refer to stone matrix asphalt and open-graded friction course, respectively; and
3) Mixes not containing hydrated lime were run with either Gripper X antistrip or Evotherm Q1 warm mix additive at a 0.5% rate

6/14/2013

Quadrant: N
Section: 3
Sublot: 2

Laboratory Diary

General Description of Mix and Materials

Design Method:	Superpave
Compactive Effort:	65 gyrations
Binder Performance Grade:	67-22
Modifier Type:	NA
Aggregate Type:	Im-19.0D w/Rap 30
Design Gradation Type:	DGA

Avg. Lab Properties of Plant Produced Mix

Sieve Size	Target	QC
25 mm (1"):	100	100
19 mm (3/4"):	97	99
12.5 mm (1/2"):	87	91
9.5 mm (3/8"):	NA	77
4.75 mm (#4):	NA	49
2.36 mm (#8):	35	36
1.18 mm (#16):	NA	28
0.60 mm (#30):	NA	20
0.30 mm (#50):	NA	12
0.15 mm (#100):	NA	8
0.075 mm (#200):	6.0	5.9
Binder Content (Pb):	4.7	4.6
Eff. Binder Content (Pbe):	4.5	4.5
Dust-to-Binder Ratio:	1.3	1.3
Rice Gravity (Gmm):	2.517	2.536
Avg. Bulk Gravity (Gmb):	2.416	2.415
Avg Air Voids (Va):	4.0	4.8
Agg. Bulk Gravity (Gsb):	2.697	2.717
Avg VMA:	14.6	15.3
Avg. VFA:	73	69

Construction Diary

Relevant Conditions for Construction

Completion Date:	August 16, 2012
24 Hour High Temperature (F):	0
24 Hour Low Temperature (F):	0
24 Hour Rainfall (in):	0.00
Planned Subot Lift Thickness (in):	2.0
Paving Machine:	0.00

Plant Configuration and Placement Details

Component	% Setting
Binder Content (Plant Setting)	5.5

As-Built Sublot Lift Thickness (in):	2.1
Total Thickness of All 2012 Sublots (in):	9.7
Approx. Underlying HMA Thickness (in):	0.0
Type of Tack Coat Utilized:	0.0
Undiluted Target Tack Rate (gal/sy):	0.00
Approx. Avg. Temperature at Plant (F):	330
Avg. Measured Mat Compaction:	92.9%

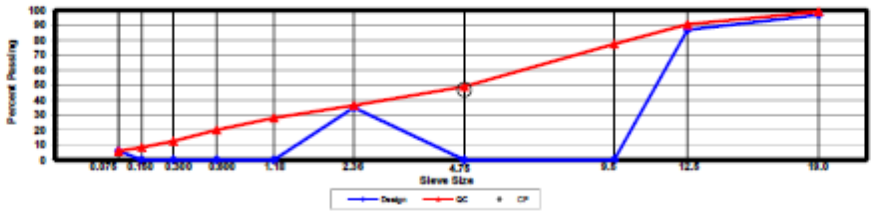

General Notes:
1) Mixes are referenced by quadrant (E=East, N=North, W=West, S=South, L=Lee Rd 159), section number, and sublot (top=1);
2) SMA and OGFC refer to stone matrix asphalt and open-graded friction course, respectively; and
3) Mixes not containing hydrated lime were run with either Gripper X antistrip or Evotherm Q1 warm mix additive at a 0.5% rate

6/14/2013

Quadrant: N
Section: 3
Sublot: 3

Laboratory Diary

General Description of Mix and Materials

Design Method:	Superpave
Compactive Effort:	65 gyrations
Binder Performance Grade:	67-22
Modifier Type:	NA
Aggregate Type:	Im-19.0D w/Rap 30
Design Gradation Type:	DGA

Avg. Lab Properties of Plant Produced Mix

Sieve Size	Target	QC
25 mm (1"):	100	100
19 mm (3/4"):	97	97
12.5 mm (1/2"):	87	85
9.5 mm (3/8"):	NA	74
4.75 mm (#4):	NA	45
2.36 mm (#8):	35	33
1.18 mm (#16):	NA	26
0.60 mm (#30):	NA	18
0.30 mm (#50):	NA	12
0.15 mm (#100):	NA	8
0.075 mm (#200):	6.0	5.8
Binder Content (Pb):	4.7	4.4
Eff. Binder Content (Pbe):	4.5	4.2
Dust-to-Binder Ratio:	1.3	1.4
Rice Gravity (Gmm):	2.517	2.585
Avg. Bulk Gravity (Gmb):	2.416	2.459
Avg Air Voids (Va):	4.0	4.9
Agg. Bulk Gravity (Gsb):	2.697	2.765
Avg VMA:	14.6	15.0
Avg. VFA:	73	67

Construction Diary

Relevant Conditions for Construction

Completion Date:	August 15, 2012
24 Hour High Temperature (F):	0
24 Hour Low Temperature (F):	0
24 Hour Rainfall (in):	0.00
Planned Subot Lift Thickness (in):	2.0
Paving Machine:	0.00

Plant Configuration and Placement Details

Component	% Setting
Binder Content (Plant Setting)	5.5

As-Built Subot Lift Thickness (in):	1.9
Total Thickness of All 2012 Subots (in):	9.7
Approx. Underlying HMA Thickness (in):	0.0
Type of Tack Coat Utilized:	0.0
Undiluted Target Tack Rate (gal/sy):	0.00
Approx. Avg. Temperature at Plant (F):	330
Avg. Measured Mat Compaction:	93.6%

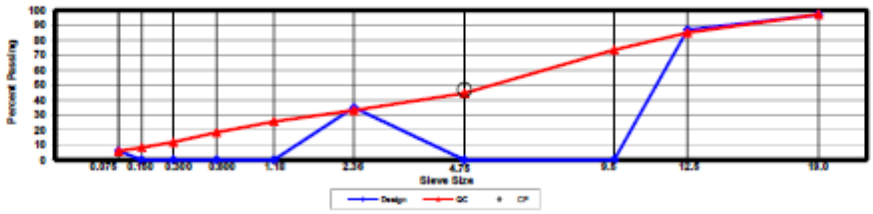

General Notes:
1) Mixes are referenced by quadrant (E=East, N=North, W=West, S=South, L=Lee Rd 159), section number, and subot (top=1);
2) SMA and OGFC refer to stone matrix asphalt and open-graded friction course, respectively; and
3) Mixes not containing hydrated lime were run with either Gripper X antistrip or Evotherm Q1 warm mix additive at a 0.5% rate

6/14/2013

Quadrant: N
Section: 4
Sublot: 1

Laboratory Diary

General Description of Mix and Materials

Design Method:	SMA
Compactive Effort:	75 gyrations
Binder Performance Grade:	76-22
Modifier Type:	SBS
Aggregate Type:	SMA 12.5 RAP
Design Gradation Type:	SMA

Avg. Lab Properties of Plant Produced Mix

Sieve Size	Target	QC
25 mm (1"):	100	100
19 mm (3/4"):	100	100
12.5 mm (1/2"):	86	90
9.5 mm (3/8"):	66	70
4.75 mm (#4):	27	27
2.36 mm (#8):	20	22
1.18 mm (#16):	NA	20
0.60 mm (#30):	16	18
0.30 mm (#50):	NA	17
0.15 mm (#100):	NA	15
0.075 mm (#200):	10.0	12.1
Binder Content (Pb):	6.4	6.0
Eff. Binder Content (Pbe):	6.4	6.0
Dust-to-Binder Ratio:	1.6	2.0
Rice Gravity (Gmm):	2.631	2.646
Avg. Bulk Gravity (Gmb):	2.549	2.582
Avg Air Voids (Va):	3.1	2.4
Agg. Bulk Gravity (Gsb):	2.944	2.942
Avg VMA:	18.9	17.5
Avg. VFA:	84	86

Construction Diary

Relevant Conditions for Construction

Completion Date:	August 24, 2012
24 Hour High Temperature (F):	0
24 Hour Low Temperature (F):	0
24 Hour Rainfall (in):	0.00
Planned Subot Lift Thickness (in):	2.0
Paving Machine:	0.00

Plant Configuration and Placement Details

Component	% Setting
Binder Content (Plant Setting)	6.2

As-Built Sublot Lift Thickness (in):	2.0
Total Thickness of All 2012 Subiots (in):	8.2
Approx. Underlying HMA Thickness (in):	0.0
Type of Tack Coat Utilized:	0.0
Undiluted Target Tack Rate (gal/sy):	0.00
Approx. Avg. Temperature at Plant (F):	325
Avg. Measured Mat Compaction:	95.3%

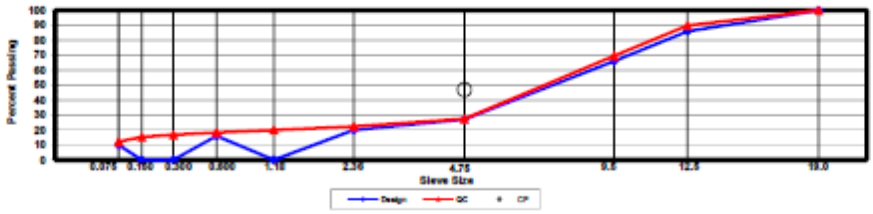

General Notes:
1) Mixes are referenced by quadrant (E=East, N=North, W=West, S=South, L=Lee Rd 159), section number, and subiot (top=1);
2) SMA and OGFC refer to stone matrix asphalt and open-graded friction course, respectively; and
3) Mixes not containing hydrated lime were run with either Gripper X antistrip or Evotherm Q1 warm mix additive at a 0.5% rate

6/14/2013

Quadrant: N
Section: 4
Sublot: 2

Laboratory Diary

General Description of Mix and Materials

Design Method:	Superpave
Compactive Effort:	65 gyrations
Binder Performance Grade:	67-22
Modifier Type:	NA
Aggregate Type:	Im-19.0D w/Rap 30
Design Gradation Type:	DGA

Avg. Lab Properties of Plant Produced Mix

Sieve Size	Target	QC
25 mm (1"):	100	100
19 mm (3/4"):	97	99
12.5 mm (1/2"):	87	91
9.5 mm (3/8"):	NA	81
4.75 mm (#4):	NA	51
2.36 mm (#8):	35	37
1.18 mm (#16):	NA	28
0.60 mm (#30):	NA	20
0.30 mm (#50):	NA	13
0.15 mm (#100):	NA	9
0.075 mm (#200):	6.0	6.3
Binder Content (Pb):	4.7	4.6
Eff. Binder Content (Pbe):	4.5	4.4
Dust-to-Binder Ratio:	1.3	1.4
Rice Gravity (Gmm):	2.517	2.584
Avg. Bulk Gravity (Gmb):	2.416	2.480
Avg Air Voids (Va):	4.0	4.0
Agg. Bulk Gravity (Gsb):	2.697	2.773
Avg VMA:	14.6	14.7
Avg. VFA:	73	73

Construction Diary

Relevant Conditions for Construction

Completion Date:	August 15, 2012
24 Hour High Temperature (F):	0
24 Hour Low Temperature (F):	0
24 Hour Rainfall (in):	0.00
Planned Sublot Lift Thickness (in):	2.0
Paving Machine:	0.00

Plant Configuration and Placement Details

Component	% Setting
Binder Content (Plant Setting)	5.5

As-Built Sublot Lift Thickness (in):	1.9
Total Thickness of All 2012 Sublots (in):	8.2
Approx. Underlying HMA Thickness (in):	0.0
Type of Tack Coat Utilized:	0.0
Undiluted Target Tack Rate (gal/sy):	0.00
Approx. Avg. Temperature at Plant (F):	330
Avg. Measured Mat Compaction:	92.6%

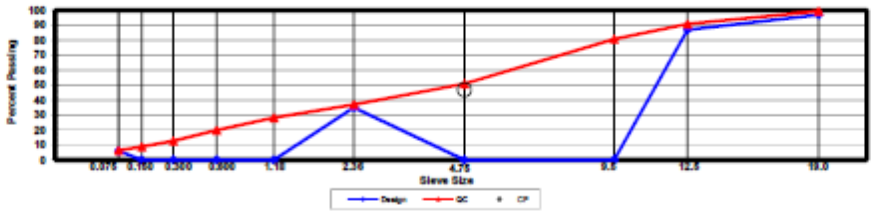

General Notes:
1) Mixes are referenced by quadrant (E=East, N=North, W=West, S=South, L=Lee Rd 159), section number, and sublot (top=1);
2) SMA and OGFC refer to stone matrix asphalt and open-graded friction course, respectively; and
3) Mixes not containing hydrated lime were run with either Gripper X antistrip or Evotherm Q1 warm mix additive at a 0.5% rate

3/19/2013

Quadrant: N
Section: 5
Sublot: 1

Laboratory Diary

General Description of Mix and Materials

Design Method:	Superpave
Compactive Effort:	80 gyrations
Binder Performance Grade:	67-22
Modifier Type:	NA
Aggregate Type:	Granite/RAP/Sand
Design Gradation Type:	ARZ

Avg. Lab Properties of Plant Produced Mix

Sieve Size	Target	QC
25 mm (1"):	100	100
19 mm (3/4"):	100	100
12.5 mm (1/2"):	100	100
9.5 mm (3/8"):	99	99
4.75 mm (#4):	74	73
2.36 mm (#8):	52	51
1.18 mm (#16):	38	40
0.60 mm (#30):	26	29
0.30 mm (#50):	16	18
0.15 mm (#100):	10	11
0.075 mm (#200):	6.2	7.0
Binder Content (Pb):	5.6	5.2
Eff. Binder Content (Pbe):	5.1	4.7
Dust-to-Binder Ratio:	1.2	1.5
Rice Gravity (Gmm):	2.459	2.494
Avg. Bulk Gravity (Gmb):	2.361	2.414
Avg Air Voids (Va):	4.0	3.2
Agg. Bulk Gravity (Gsb):	2.647	2.669
Avg VMA:	15.8	14.2
Avg. VFA:	75	77

Construction Diary

Relevant Conditions for Construction

Completion Date:	August 20, 2012
24 Hour High Temperature (F):	84
24 Hour Low Temperature (F):	71
24 Hour Rainfall (in):	0.01
Planned Subot Lift Thickness (in):	1.3
Paving Machine:	Roadtec

Plant Configuration and Placement Details

Component	% Setting
Binder Content (Plant Setting)	5.2
89 Columbus Granite	41.0
M10 Columbus Granite	29.0
Shorter Coarse Sand	10.0
EAP Unfractionated RAP	20.0
Green Foam	2.0
As-Built Sublot Lift Thickness (in):	1.4
Total Thickness of All 2012 Sublots (in):	6.1
Approx. Underlying HMA Thickness (in):	0.0
Type of Tack Coat Utilized:	NTSS-1HM
Undiluted Target Tack Rate (gal/sy):	0.05
Approx. Avg. Temperature at Plant (F):	270
Avg. Measured Mat Compaction:	91.6%

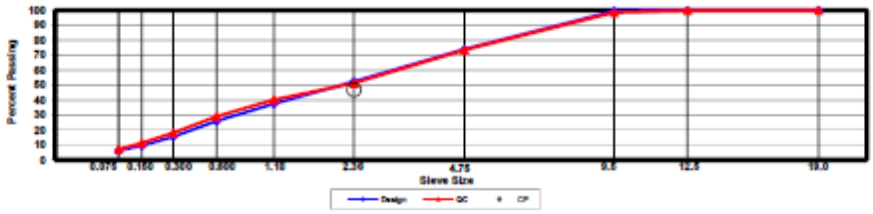

General Notes:
1) Mixes are referenced by quadrant (E=East, N=North, W=West, and S=South), section # (sequential) and sublot (top=1);
2) SMA and OGFC refer to stone matrix asphalt and open-graded friction course, respectively; and
3) Mixes not containing hydrated lime were run with either Gripper X antistrip or Evotherm Q1 warm mix additive at a 0.5% rate

3/19/2013

Quadrant: N
Section: 5
Sublot: 2

Laboratory Diary

General Description of Mix and Materials

Design Method:	Superpave
Compactive Effort:	80 gyrations
Binder Performance Grade:	67-22
Modifier Type:	NA
Aggregate Type:	Lms/RAP/Sand
Design Gradation Type:	ARZ

Avg. Lab Properties of Plant Produced Mix

Sieve Size	Target	QC
25 mm (1"):	100	99
19 mm (3/4"):	97	96
12.5 mm (1/2"):	88	90
9.5 mm (3/8"):	78	83
4.75 mm (#4):	56	61
2.36 mm (#8):	42	48
1.18 mm (#16):	32	39
0.60 mm (#30):	21	27
0.30 mm (#50):	12	15
0.15 mm (#100):	7	9
0.075 mm (#200):	5.0	5.5
Binder Content (Pb):	4.8	4.6
Eff. Binder Content (Pbe):	4.2	4.0
Dust-to-Binder Ratio:	1.2	1.4
Rice Gravity (Gmm):	2.546	2.540
Avg. Bulk Gravity (Gmb):	2.444	2.448
Avg Air Voids (Va):	4.0	3.6
Agg. Bulk Gravity (Gsb):	2.705	2.687
Avg VMA:	13.8	13.0
Avg. VFA:	72	72

Construction Diary

Relevant Conditions for Construction

Completion Date:	August 16, 2012
24 Hour High Temperature (F):	92
24 Hour Low Temperature (F):	72
24 Hour Rainfall (in):	0.00
Planned Subot Lift Thickness (in):	2.3
Paving Machine:	Roadtec

Plant Configuration and Placement Details

Component	% Setting
Binder Content (Plant Setting)	4.6
78 Opelika Limestone	27.0
57 Opelika Limestone	17.0
Shorter Coarse Sand	21.0
EAP Unfractionated RAP	35.0
Green Foam	2.0
As-Built Sublot Lift Thickness (in):	1.7
Total Thickness of All 2012 Sublots (in):	6.1
Approx. Underlying HMA Thickness (in):	0.0
Type of Tack Coat Utilized:	NTSS-1HM
Undiluted Target Tack Rate (gal/sy):	0.05
Approx. Avg. Temperature at Plant (F):	285
Avg. Measured Mat Compaction:	93.1%

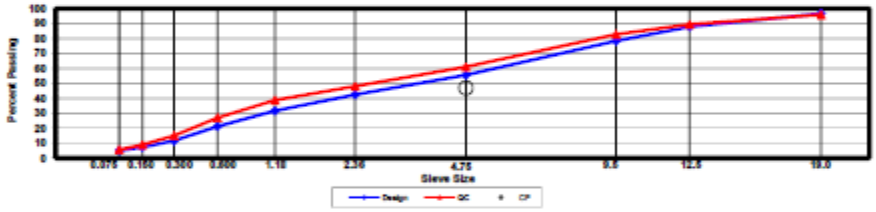

General Notes:
1) Mixes are referenced by quadrant (E=East, N=North, W=West, and S=South), section # (sequential) and sublot (top=1);
2) SMA and OGFC refer to stone matrix asphalt and open-graded friction course, respectively; and
3) Mixes not containing hydrated lime were run with either Gripper X antistrip or Evotherm Q1 warm mix additive at a 0.5% rate

3/19/2013

Quadrant: N
Section: 5
Sublot: 3

Laboratory Diary

General Description of Mix and Materials

Design Method:	Superpave
Compactive Effort:	80 gyrations
Binder Performance Grade:	67-22
Modifier Type:	NA
Aggregate Type:	Lms/RAP/Sand
Design Gradation Type:	ARZ

Avg. Lab Properties of Plant Produced Mix

Sieve Size	Target	QC
25 mm (1"):	100	99
19 mm (3/4"):	97	96
12.5 mm (1/2"):	88	91
9.5 mm (3/8"):	78	84
4.75 mm (#4):	56	63
2.36 mm (#8):	42	49
1.18 mm (#16):	32	39
0.60 mm (#30):	21	26
0.30 mm (#50):	12	14
0.15 mm (#100):	7	9
0.075 mm (#200):	5.0	5.7
Binder Content (Pb):	4.8	4.7
Eff. Binder Content (Pbe):	4.2	4.1
Dust-to-Binder Ratio:	1.2	1.4
Rice Gravity (Gmm):	2.546	2.563
Avg. Bulk Gravity (Gmb):	2.444	2.447
Avg Air Voids (Va):	4.0	4.5
Agg. Bulk Gravity (Gsb):	2.705	2.722
Avg VMA:	13.8	14.4
Avg. VFA:	72	69

Construction Diary

Relevant Conditions for Construction

Completion Date:	August 15, 2012
24 Hour High Temperature (F):	92
24 Hour Low Temperature (F):	69
24 Hour Rainfall (in):	0.00
Planned Sublot Lift Thickness (in):	2.5
Paving Machine:	Roadtec

Plant Configuration and Placement Details

Component	% Setting
Binder Content (Plant Setting)	4.6
78 Opelika Limestone	27.0
57 Opelika Limestone	17.0
Shorter Coarse Sand	21.0
EAP Unfractionated RAP	35.0
Green Foam	2.0
As-Built Sublot Lift Thickness (in):	3.0
Total Thickness of All 2012 Sublots (in):	6.1
Approx. Underlying HMA Thickness (in):	0.0
Type of Tack Coat Utilized:	NA
Undiluted Target Tack Rate (gal/sy):	NA
Approx. Avg. Temperature at Plant (F):	280
Avg. Measured Mat Compaction:	93.5%

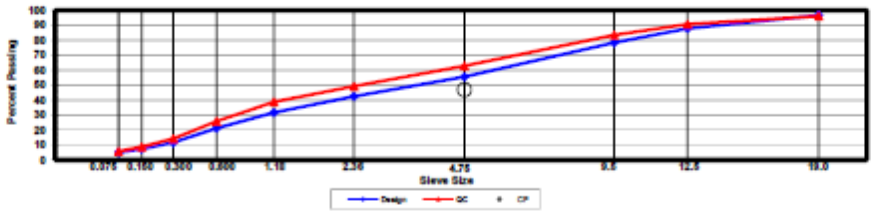

General Notes:
1) Mixes are referenced by quadrant (E=East, N=North, W=West, and S=South), section # (sequential) and sublot (top=1);
2) SMA and OGFC refer to stone matrix asphalt and open-graded friction course, respectively; and
3) Mixes not containing hydrated lime were run with either Gripper X antistrip or Evotherm Q1 warm mix additive at a 0.5% rate

5/23/2013

Quadrant: S
Section: 5
Sublot: 1

Laboratory Diary

General Description of Mix and Materials

Design Method:	SMA
Compactive Effort:	50 blows
Binder Performance Grade:	67-22
Modifier Type:	NA
Aggregate Type:	Gm/C-FRAP/Flyash
Design Gradation Type:	SMA

Avg. Lab Properties of Plant Produced Mix

Sieve Size	Target	QC
25 mm (1"):	100	100
19 mm (3/4"):	100	100
12.5 mm (1/2"):	100	100
9.5 mm (3/8"):	98	98
4.75 mm (#4):	46	52
2.36 mm (#8):	21	25
1.18 mm (#16):	15	19
0.60 mm (#30):	13	15
0.30 mm (#50):	11	12
0.15 mm (#100):	9	10
0.075 mm (#200):	8.3	7.4
Binder Content (Pb):	6.9	6.3
Eff. Binder Content (Pbe):	6.3	5.8
Dust-to-Binder Ratio:	1.3	1.3
Rice Gravity (Gmm):	2.416	2.439
Avg. Bulk Gravity (Gmb):	2.319	2.330
Avg Air Voids (Va):	4.0	4.5
Agg. Bulk Gravity (Gsb):	2.644	2.649
Avg VMA:	18.4	17.6
Avg. VFA:	78	75

Construction Diary

Relevant Conditions for Construction

Completion Date:	May 22, 2013
24 Hour High Temperature (F):	87
24 Hour Low Temperature (F):	68
24 Hour Rainfall (in):	0.00
Planned Subot Lift Thickness (in):	1.3
Paving Machine:	Blaw Knox

Plant Configuration and Placement Details

Component	% Setting
Binder Content (Plant Setting)	6.3
89 Columbus Granite	65.0
M10 Columbus Granite	6.0
EAP Coarse Fractionated RAP	25.0
Green Foam	2.0
Flyash	4.0
Cellulose	0.3
As-Built Sublot Lift Thickness (in):	1.0
Total Thickness of All 2012 Sublots (in):	6.0
Approx. Underlying HMA Thickness (in):	0.0
Type of Tack Coat Utilized:	NTSS-1HM
Undiluted Target Tack Rate (gal/sy):	0.08
Approx. Avg. Temperature at Plant (F):	285
Avg. Measured Mat Compaction:	93.5%

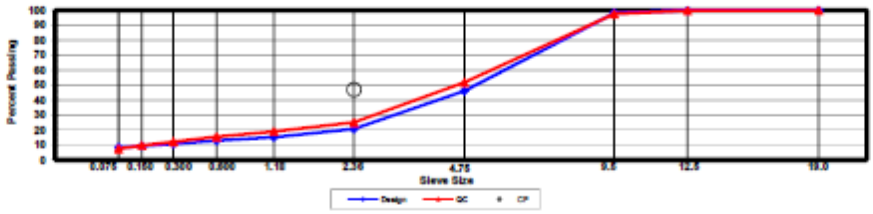

General Notes:
1) Mixes are referenced by quadrant (E=East, N=North, W=West, S=South, L=Lee Rd 159), section number, and sublot (top=1);
2) SMA and OGFC refer to stone matrix asphalt and open-graded friction course, respectively; and
3) Mixes not containing hydrated lime were run with either Gripper X antistrip or Evotherm Q1 warm mix additive at a 0.5% rate

5/23/2013

Quadrant: S
Section: 5
Sublot: 2

Laboratory Diary

General Description of Mix and Materials

Design Method:	Superpave
Compactive Effort:	80 gyrations
Binder Performance Grade:	67-22
Modifier Type:	NA
Aggregate Type:	RAP/Lms/Sand
Design Gradation Type:	ARZ

Avg. Lab Properties of Plant Produced Mix

Sieve Size	Target	QC
25 mm (1"):	100	100
19 mm (3/4"):	96	96
12.5 mm (1/2"):	84	90
9.5 mm (3/8"):	77	81
4.75 mm (#4):	51	56
2.36 mm (#8):	41	45
1.18 mm (#16):	31	38
0.60 mm (#30):	20	27
0.30 mm (#50):	10	15
0.15 mm (#100):	6	9
0.075 mm (#200):	4.3	4.9
Binder Content (Pb):	4.8	5.0
Eff. Binder Content (Pbe):	4.1	4.3
Dust-to-Binder Ratio:	1.1	1.1
Rice Gravity (Gmm):	2.527	2.514
Avg. Bulk Gravity (Gmb):	2.426	2.439
Avg Air Voids (Va):	4.0	3.0
Agg. Bulk Gravity (Gsb):	2.676	2.670
Avg VMA:	13.7	13.2
Avg. VFA:	71	77

Construction Diary

Relevant Conditions for Construction

Completion Date:	May 21, 2013
24 Hour High Temperature (F):	89
24 Hour Low Temperature (F):	65
24 Hour Rainfall (in):	0.00
Planned Sublot Lift Thickness (in):	2.3
Paving Machine:	Blaw Knox

Plant Configuration and Placement Details

Component	% Setting
Binder Content (Plant Setting)	5.0
78 Opelika Limestone	14.0
57 Opelika Limestone	15.0
Shorter Coarse Sand	21.0
EAP Coarse Fractionated RAP	30.0
EAP Fine Fractionated RAP	20.0
Green Foam	2.0
As-Built Sublot Lift Thickness (in):	2.4
Total Thickness of All 2012 Sublots (in):	6.0
Approx. Underlying HMA Thickness (in):	0.0
Type of Tack Coat Utilized:	NTSS-1HM
Undiluted Target Tack Rate (gal/sy):	0.10
Approx. Avg. Temperature at Plant (F):	330
Avg. Measured Mat Compaction:	95.8%

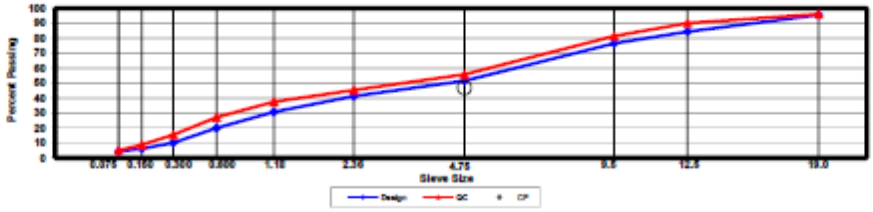

General Notes:
1) Mixes are referenced by quadrant (E=East, N=North, W=West, S=South, L=Lee Rd 159), section number, and sublot (top=1);
2) SMA and OGFC refer to stone matrix asphalt and open-graded friction course, respectively; and
3) Mixes not containing hydrated lime were run with either Gripper X antistrip or Evotherm Q1 warm mix additive at a 0.5% rate

5/23/2013

Quadrant: S
Section: 5
Sublot: 3

Laboratory Diary

General Description of Mix and Materials

Design Method:	Superpave
Compactive Effort:	80 gyrations
Binder Performance Grade:	76-22E
Modifier Type:	NA
Aggregate Type:	Lms/Sand/RAP
Design Gradation Type:	ARZ

Avg. Lab Properties of Plant Produced Mix

Sieve Size	Target	QC
25 mm (1"):	100	100
19 mm (3/4"):	97	98
12.5 mm (1/2"):	88	91
9.5 mm (3/8"):	78	84
4.75 mm (#4):	56	63
2.36 mm (#8):	42	48
1.18 mm (#16):	32	39
0.60 mm (#30):	21	27
0.30 mm (#50):	12	15
0.15 mm (#100):	7	8
0.075 mm (#200):	5.0	5.3
Binder Content (Pb):	4.7	4.7
Eff. Binder Content (Pbe):	4.1	4.1
Dust-to-Binder Ratio:	1.2	1.3
Rice Gravity (Gmm):	2.549	2.529
Avg. Bulk Gravity (Gmb):	2.447	2.436
Avg Air Voids (Va):	4.0	3.7
Agg. Bulk Gravity (Gsb):	2.705	2.682
Avg VMA:	13.7	13.5
Avg. VFA:	71	73

Construction Diary

Relevant Conditions for Construction

Completion Date:	May 21, 2013
24 Hour High Temperature (F):	89
24 Hour Low Temperature (F):	65
24 Hour Rainfall (in):	0.00
Planned Subot Lift Thickness (in):	2.5
Paving Machine:	Blaw Knox

Plant Configuration and Placement Details

Component	% Setting
Binder Content (Plant Setting)	4.7
78 Opelika Limestone	27.0
57 Opelika Limestone	17.0
Shorter Coarse Sand	21.0
EAP Unfractionated RAP	35.0
Evotherm Q1	0.5
As-Built Sublot Lift Thickness (in):	2.7
Total Thickness of All 2012 Sublots (in):	6.0
Approx. Underlying HMA Thickness (in):	0.0
Type of Tack Coat Utilized:	NA
Undiluted Target Tack Rate (gal/sy):	NA
Approx. Avg. Temperature at Plant (F):	285
Avg. Measured Mat Compaction:	92.8%

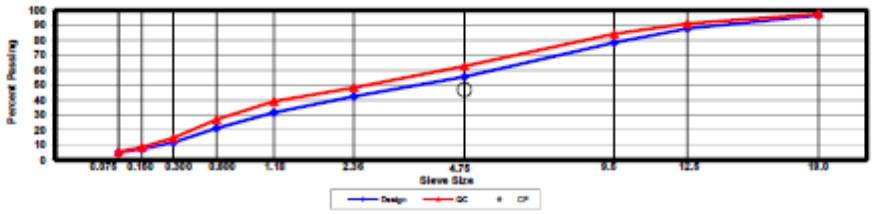

General Notes:
1) Mixes are referenced by quadrant (E=East, N=North, W=West, S=South, L=Lee Rd 159), section number, and sublot (top=1);
2) SMA and OGFC refer to stone matrix asphalt and open-graded friction course, respectively; and
3) Mixes not containing hydrated lime were run with either Gripper X antistrip or Evotherm Q1 warm mix additive at a 0.5% rate

3/19/2013

Quadrant: S
Section: 6
Sublot: 1

Laboratory Diary

General Description of Mix and Materials

Design Method:	SMA
Compactive Effort:	80 gyrations
Binder Performance Grade:	67-22
Modifier Type:	NA
Aggregate Type:	Gm/Flyash/PC-RAS
Design Gradation Type:	SMA

Avg. Lab Properties of Plant Produced Mix

Sieve Size	Target	QC
25 mm (1"):	100	100
19 mm (3/4"):	100	100
12.5 mm (1/2"):	100	100
9.5 mm (3/8"):	100	100
4.75 mm (#4):	54	54
2.36 mm (#8):	25	24
1.18 mm (#16):	18	20
0.60 mm (#30):	15	16
0.30 mm (#50):	12	13
0.15 mm (#100):	11	11
0.075 mm (#200):	9.1	8.7
Binder Content (Pb):	6.7	5.5
Eff. Binder Content (Pbe):	6.3	5.1
Dust-to-Binder Ratio:	1.4	1.7
Rice Gravity (Gmm):	2.417	2.473
Avg. Bulk Gravity (Gmb):	2.320	2.383
Avg Air Voids (Va):	4.0	3.6
Agg. Bulk Gravity (Gsb):	2.651	2.667
Avg VMA:	18.5	15.6
Avg. VFA:	78	77

Construction Diary

Relevant Conditions for Construction

Completion Date:	August 23, 2012
24 Hour High Temperature (F):	91
24 Hour Low Temperature (F):	65
24 Hour Rainfall (in):	0.00
Planned Sublot Lift Thickness (in):	1.3
Paving Machine:	Roadtec

Plant Configuration and Placement Details

Component	% Setting
Binder Content (Plant Setting)	5.7
89 Columbus Granite	82.0
M10 Columbus Granite	9.0
Wedowee PC-RAS	5.0
Green Foam	2.0
Flyash	4.0
As-Built Sublot Lift Thickness (in):	1.3
Total Thickness of All 2012 Sublots (in):	6.0
Approx. Underlying HMA Thickness (in):	0.0
Type of Tack Coat Utilized:	NTSS-1HM
Undiluted Target Tack Rate (gal/sy):	0.05
Approx. Avg. Temperature at Plant (F):	275
Avg. Measured Mat Compaction:	92.1%

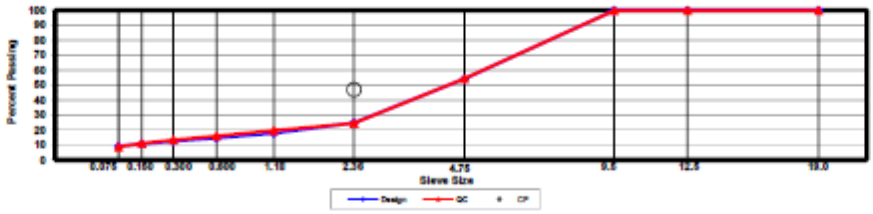

General Notes:
1) Mixes are referenced by quadrant (E=East, N=North, W=West, and S=South), section # (sequential) and sublot (top=1);
2) SMA and OGFC refer to stone matrix asphalt and open-graded friction course, respectively; and
3) Mixes not containing hydrated lime were run with either Gripper X antistrip or Evotherm Q1 warm mix additive at a 0.5% rate

3/19/2013

Quadrant: S
Section: 6
Sublot: 2

Laboratory Diary

General Description of Mix and Materials

Design Method:	Superpave
Compactive Effort:	80 gyrations
Binder Performance Grade:	67-22
Modifier Type:	NA
Aggregate Type:	Lms/RAP/Sand/RAS
Design Gradation Type:	ARZ

Avg. Lab Properties of Plant Produced Mix

Sieve Size	Target	QC
25 mm (1"):	99	99
19 mm (3/4"):	95	94
12.5 mm (1/2"):	80	85
9.5 mm (3/8"):	70	76
4.75 mm (#4):	51	57
2.36 mm (#8):	41	45
1.18 mm (#16):	30	36
0.60 mm (#30):	20	25
0.30 mm (#50):	11	14
0.15 mm (#100):	7	9
0.075 mm (#200):	4.7	5.6
Binder Content (Pb):	4.9	4.9
Eff. Binder Content (Pbe):	4.3	4.3
Dust-to-Binder Ratio:	1.1	1.3
Rice Gravity (Gmm):	2.549	2.546
Avg. Bulk Gravity (Gmb):	2.447	2.457
Avg Air Voids (Va):	4.0	3.1
Agg. Bulk Gravity (Gsb):	2.715	2.712
Avg VMA:	14.0	13.5
Avg. VFA:	72	77

Construction Diary

Relevant Conditions for Construction

Completion Date:	August 22, 2012
24 Hour High Temperature (F):	89
24 Hour Low Temperature (F):	69
24 Hour Rainfall (in):	0.00
Planned Sublot Lift Thickness (in):	2.3
Paving Machine:	Roadtec

Plant Configuration and Placement Details

Component	% Setting
Binder Content (Plant Setting)	4.8
78 Opelika Limestone	35.0
57 Opelika Limestone	15.0
Shorter Coarse Sand	20.0
EAP Unfractionated RAP	25.0
Wedowee PC-RAS	5.0
Evotherm Q1	0.5
As-Built Sublot Lift Thickness (in):	2.4
Total Thickness of All 2012 Sublots (in):	6.0
Approx. Underlying HMA Thickness (in):	0.0
Type of Tack Coat Utilized:	NTSS-1HM
Undiluted Target Tack Rate (gal/sy):	0.05
Approx. Avg. Temperature at Plant (F):	280
Avg. Measured Mat Compaction:	94.0%

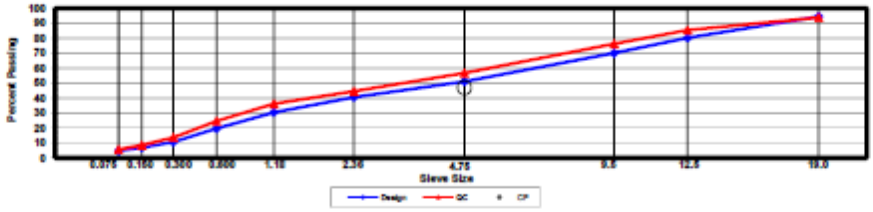

General Notes:
1) Mixes are referenced by quadrant (E=East, N=North, W=West, and S=South), section # (sequential) and sublot (top=1);
2) SMA and OGFC refer to stone matrix asphalt and open-graded friction course, respectively; and
3) Mixes not containing hydrated lime were run with either Gripper X antistrip or Evotherm Q1 warm mix additive at a 0.5% rate

3/19/2013

Quadrant: S
Section: 6
Sublot: 3

Laboratory Diary

General Description of Mix and Materials

Design Method:	Superpave
Compactive Effort:	80 gyrations
Binder Performance Grade:	76-22
Modifier Type:	SBS
Aggregate Type:	Lms/RAP/Sand/Gm
Design Gradation Type:	ARZ

Avg. Lab Properties of Plant Produced Mix

Sieve Size	Target	QC
25 mm (1"):	100	97
19 mm (3/4"):	95	93
12.5 mm (1/2"):	81	84
9.5 mm (3/8"):	72	78
4.75 mm (#4):	55	60
2.36 mm (#8):	44	48
1.18 mm (#16):	33	39
0.60 mm (#30):	21	27
0.30 mm (#50):	11	15
0.15 mm (#100):	7	9
0.075 mm (#200):	4.7	5.9
Binder Content (Pb):	5.4	5.3
Eff. Binder Content (Pbe):	4.8	4.8
Dust-to-Binder Ratio:	1.0	1.2
Rice Gravity (Gmm):	2.520	2.530
Avg. Bulk Gravity (Gmb):	2.470	2.487
Avg Air Voids (Va):	2.0	1.7
Agg. Bulk Gravity (Gsb):	2.703	2.714
Avg VMA:	13.4	13.2
Avg. VFA:	85	87

Construction Diary

Relevant Conditions for Construction

Completion Date:	August 17, 2012
24 Hour High Temperature (F):	89
24 Hour Low Temperature (F):	70
24 Hour Rainfall (in):	0.00
Planned Subot Lift Thickness (in):	2.5
Paving Machine:	Roadtec

Plant Configuration and Placement Details

Component	% Setting
Binder Content (Plant Setting)	5.3
78 Opelika Limestone	21.0
57 Opelika Limestone	24.0
M10 Columbus Granite	10.0
Shorter Coarse Sand	20.0
EAP Unfractionated RAP	25.0
Green Foam	2.0

As-Built Sublot Lift Thickness (in):	2.3
Total Thickness of All 2012 Sublots (in):	6.0
Approx. Underlying HMA Thickness (in):	0.0
Type of Tack Coat Utilized:	NA
Undiluted Target Tack Rate (gal/sy):	NA
Approx. Avg. Temperature at Plant (F):	285
Avg. Measured Mat Compaction:	96.5%

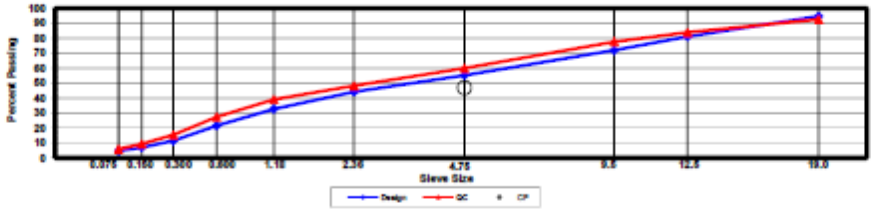

General Notes:
1) Mixes are referenced by quadrant (E=East, N=North, W=West, and S=South), section # (sequential) and sublot (top=1);
2) SMA and OGFC refer to stone matrix asphalt and open-graded friction course, respectively; and
3) Mixes not containing hydrated lime were run with either Gripper X antistrip or Evotherm Q1 warm mix additive at a 0.5% rate

6/14/2013

Quadrant: S
Section: 12
Sublot: 1

Laboratory Diary

General Description of Mix and Materials

Design Method:	SMA
Compactive Effort:	75 gyrations
Binder Performance Grade:	76-22
Modifier Type:	SBS
Aggregate Type:	SMA 12.5 RAP
Design Gradation Type:	SMA

Avg. Lab Properties of Plant Produced Mix

Sieve Size	Target	QC
25 mm (1"):	100	100
19 mm (3/4"):	100	100
12.5 mm (1/2"):	86	90
9.5 mm (3/8"):	66	71
4.75 mm (#4):	27	32
2.36 mm (#8):	20	22
1.18 mm (#16):	NA	19
0.60 mm (#30):	16	18
0.30 mm (#50):	NA	17
0.15 mm (#100):	NA	15
0.075 mm (#200):	10.0	12.2
Binder Content (Pb):	6.4	6.1
Eff. Binder Content (Pbe):	6.4	6.1
Dust-to-Binder Ratio:	1.6	2.0
Rice Gravity (Gmm):	2.631	2.636
Avg. Bulk Gravity (Gmb):	2.549	2.573
Avg Air Voids (Va):	3.1	2.4
Agg. Bulk Gravity (Gsb):	2.944	2.932
Avg VMA:	18.9	17.6
Avg. VFA:	84	86

Construction Diary

Relevant Conditions for Construction

Completion Date:	August 24, 2012
24 Hour High Temperature (F):	0
24 Hour Low Temperature (F):	0
24 Hour Rainfall (in):	0.00
Planned Subot Lift Thickness (in):	2.0
Paving Machine:	0.00

Plant Configuration and Placement Details

Component	% Setting
Binder Content (Plant Setting)	6.2

As-Built Sublot Lift Thickness (in):	2.0
Total Thickness of All 2012 Sublots (in):	9.1
Approx. Underlying HMA Thickness (in):	0.0
Type of Tack Coat Utilized:	0.0
Undiluted Target Tack Rate (gal/sy):	0.00
Approx. Avg. Temperature at Plant (F):	325
Avg. Measured Mat Compaction:	95.8%

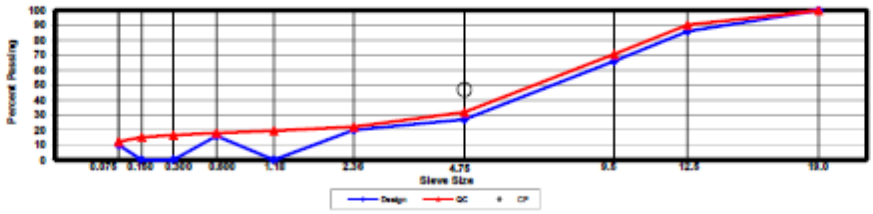

General Notes:
1) Mixes are referenced by quadrant (E=East, N=North, W=West, S=South, L=Lee Rd 159), section number, and sublot (top=1);
2) SMA and OGFC refer to stone matrix asphalt and open-graded friction course, respectively; and
3) Mixes not containing hydrated lime were run with either Gripper X antistrip or Evotherm Q1 warm mix additive at a 0.5% rate

6/14/2013

Quadrant: S
Section: 12
Sublot: 2

Laboratory Diary

General Description of Mix and Materials

Design Method:	Superpave
Compactive Effort:	65 gyrations
Binder Performance Grade:	67-22
Modifier Type:	NA
Aggregate Type:	Im-19.0D w/Rap 30
Design Gradation Type:	DGA

Avg. Lab Properties of Plant Produced Mix

Sieve Size	Target	QC
25 mm (1"):	100	100
19 mm (3/4"):	97	100
12.5 mm (1/2"):	87	91
9.5 mm (3/8"):	NA	78
4.75 mm (#4):	NA	53
2.36 mm (#8):	35	39
1.18 mm (#16):	NA	30
0.60 mm (#30):	NA	21
0.30 mm (#50):	NA	13
0.15 mm (#100):	NA	9
0.075 mm (#200):	6.0	6.4
Binder Content (Pb):	4.7	4.7
Eff. Binder Content (Pbe):	4.5	4.6
Dust-to-Binder Ratio:	1.3	1.4
Rice Gravity (Gmm):	2.517	2.537
Avg. Bulk Gravity (Gmb):	2.416	2.437
Avg Air Voids (Va):	4.0	4.0
Agg. Bulk Gravity (Gsb):	2.697	2.725
Avg VMA:	14.6	14.8
Avg. VFA:	73	73

Construction Diary

Relevant Conditions for Construction

Completion Date:	August 15, 2012
24 Hour High Temperature (F):	0
24 Hour Low Temperature (F):	0
24 Hour Rainfall (in):	0.00
Planned Subot Lift Thickness (in):	2.0
Paving Machine:	0.00

Plant Configuration and Placement Details

Component	% Setting
Binder Content (Plant Setting)	5.5

As-Built Sublot Lift Thickness (in):	1.9
Total Thickness of All 2012 Sublots (in):	9.1
Approx. Underlying HMA Thickness (in):	0.0
Type of Tack Coat Utilized:	0.0
Undiluted Target Tack Rate (gal/sy):	0.00
Approx. Avg. Temperature at Plant (F):	330
Avg. Measured Mat Compaction:	93.3%

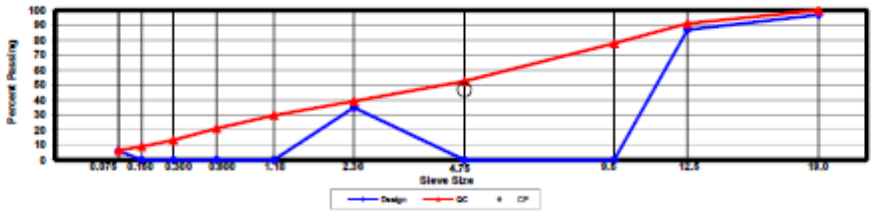

General Notes:
1) Mixes are referenced by quadrant (E=East, N=North, W=West, S=South, L=Lee Rd 159), section number, and sublot (top=1);
2) SMA and OGFC refer to stone matrix asphalt and open-graded friction course, respectively; and
3) Mixes not containing hydrated lime were run with either Gripper X antistrip or Evotherm Q1 warm mix additive at a 0.5% rate

3/19/2013

Quadrant: S
Section: 13
Sublot: 1

Laboratory Diary

General Description of Mix and Materials

Design Method:	SMA
Compactive Effort:	80 gyrations
Binder Performance Grade:	ARB12(-30)
Modifier Type:	GTR
Aggregate Type:	Granite/Flyash
Design Gradation Type:	SMA

Avg. Lab Properties of Plant Produced Mix

Sieve Size	Target	QC
25 mm (1"):	100	100
19 mm (3/4"):	100	100
12.5 mm (1/2"):	100	100
9.5 mm (3/8"):	100	100
4.75 mm (#4):	55	58
2.36 mm (#8):	25	26
1.18 mm (#16):	18	20
0.60 mm (#30):	15	17
0.30 mm (#50):	12	14
0.15 mm (#100):	10	11
0.075 mm (#200):	8.6	8.5
Binder Content (Pb):	6.4	5.7
Eff. Binder Content (Pbe):	6.0	5.2
Dust-to-Binder Ratio:	1.4	1.6
Rice Gravity (Gmm):	2.433	2.456
Avg. Bulk Gravity (Gmb):	2.336	2.375
Avg Air Voids (Va):	4.0	3.3
Agg. Bulk Gravity (Gsb):	2.648	2.645
Avg VMA:	17.3	15.3
Avg. VFA:	77	78

Construction Diary

Relevant Conditions for Construction

Completion Date:	September 7, 2012
24 Hour High Temperature (F):	92
24 Hour Low Temperature (F):	72
24 Hour Rainfall (in):	0.19
Planned Subot Lift Thickness (in):	1.3
Paving Machine:	Roadtec

Plant Configuration and Placement Details

Component	% Setting
Binder Content (Plant Setting)	5.4
89 Columbus Granite	79.0
M10 Columbus Granite	15.0
Evotherm Q1	0.5
Flyash	6.0
As-Built Sublot Lift Thickness (in):	1.2
Total Thickness of All 2012 Sublots (in):	6.4
Approx. Underlying HMA Thickness (in):	0.0
Type of Tack Coat Utilized:	NTSS-1HM
Undiluted Target Tack Rate (gal/sy):	0.05
Approx. Avg. Temperature at Plant (F):	275
Avg. Measured Mat Compaction:	92.9%

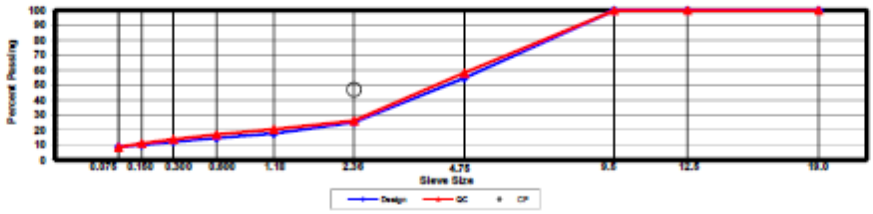

General Notes:
1) Mixes are referenced by quadrant (E=East, N=North, W=West, and S=South), section # (sequential) and sublot (top=1);
2) SMA and OGFC refer to stone matrix asphalt and open-graded friction course, respectively; and
3) Mixes not containing hydrated lime were run with either Gripper X antistrip or Evotherm Q1 warm mix additive at a 0.5% rate

3/19/2013

Quadrant: S
Section: 13
Sublot: 2

Laboratory Diary

General Description of Mix and Materials

Design Method:	Superpave
Compactive Effort:	80 gyrations
Binder Performance Grade:	ARB12(-30)
Modifier Type:	GTR
Aggregate Type:	Lms/RAP/Sand
Design Gradation Type:	ARZ

Avg. Lab Properties of Plant Produced Mix

Sieve Size	Target	QC
25 mm (1"):	100	100
19 mm (3/4"):	97	96
12.5 mm (1/2"):	88	87
9.5 mm (3/8"):	78	81
4.75 mm (#4):	56	60
2.36 mm (#8):	42	46
1.18 mm (#16):	32	36
0.60 mm (#30):	21	25
0.30 mm (#50):	12	13
0.15 mm (#100):	7	8
0.075 mm (#200):	5.0	5.2
Binder Content (Pb):	4.7	4.8
Eff. Binder Content (Pbe):	4.1	4.3
Dust-to-Binder Ratio:	1.2	1.2
Rice Gravity (Gmm):	2.550	2.538
Avg. Bulk Gravity (Gmb):	2.448	2.445
Avg Air Voids (Va):	4.0	3.6
Agg. Bulk Gravity (Gsb):	2.705	2.700
Avg VMA:	13.7	13.8
Avg. VFA:	71	74

Construction Diary

Relevant Conditions for Construction

Completion Date:	September 6, 2012
24 Hour High Temperature (F):	74
24 Hour Low Temperature (F):	73
24 Hour Rainfall (in):	0.00
Planned Sublot Lift Thickness (in):	3.0
Paving Machine:	Roadtec

Plant Configuration and Placement Details

Component	% Setting
Binder Content (Plant Setting)	4.8
78 Opelika Limestone	27.0
57 Opelika Limestone	17.0
Shorter Coarse Sand	21.0
EAP Unfractionated RAP	35.0
Green Foam	2.0
As-Built Sublot Lift Thickness (in):	3.2
Total Thickness of All 2012 Sublots (in):	6.4
Approx. Underlying HMA Thickness (in):	0.0
Type of Tack Coat Utilized:	NTSS-1HM
Undiluted Target Tack Rate (gal/sy):	0.05
Approx. Avg. Temperature at Plant (F):	280
Avg. Measured Mat Compaction:	94.4%

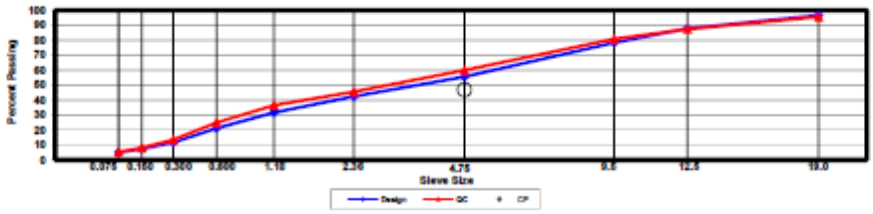

General Notes:
1) Mixes are referenced by quadrant (E=East, N=North, W=West, and S=South), section # (sequential) and sublot (top=1);
2) SMA and OGFC refer to stone matrix asphalt and open-graded friction course, respectively; and
3) Mixes not containing hydrated lime were run with either Gripper X antistrip or Evotherm Q1 warm mix additive at a 0.5% rate

3/19/2013

Quadrant: S
Section: 13
Sublot: 3

Laboratory Diary

General Description of Mix and Materials

Design Method:	AZ
Compactive Effort:	75 blows
Binder Performance Grade:	AZ20(-16)
Modifier Type:	GTR
Aggregate Type:	Lms/Sand/Hyd Lime
Design Gradation Type:	GAP

Avg. Lab Properties of Plant Produced Mix

Sieve Size	Target	QC
25 mm (1"):	100	100
19 mm (3/4"):	100	100
12.5 mm (1/2"):	98	94
9.5 mm (3/8"):	80	80
4.75 mm (#4):	31	39
2.36 mm (#8):	14	15
1.18 mm (#16):	10	11
0.60 mm (#30):	7	8
0.30 mm (#50):	4	5
0.15 mm (#100):	3	4
0.075 mm (#200):	2.4	3.4
Binder Content (Pb):	7.7	7.2
Eff. Binder Content (Pbe):	7.0	6.5
Dust-to-Binder Ratio:	0.3	0.5
Rice Gravity (Gmm):	2.496	2.493
Avg. Bulk Gravity (Gmb):	2.361	2.389
Avg Air Voids (Va):	5.5	4.2
Agg. Bulk Gravity (Gsb):	2.774	2.750
Avg VMA:	21.7	19.4
Avg. VFA:	74	78

Construction Diary

Relevant Conditions for Construction

Completion Date:	September 5, 2012
24 Hour High Temperature (F):	88
24 Hour Low Temperature (F):	73
24 Hour Rainfall (in):	0.03
Planned Subot Lift Thickness (in):	1.8
Paving Machine:	Roadtec

Plant Configuration and Placement Details

Component	% Setting
Binder Content (Plant Setting)	7.8
78 Opelika Limestone	92.0
Shorter Coarse Sand	7.0
Evotherm Q1	0.5
Hyd Lime	1.0
As-Built Sublot Lift Thickness (in):	2.0
Total Thickness of All 2012 Sublots (in):	6.4
Approx. Underlying HMA Thickness (in):	0.0
Type of Tack Coat Utilized:	NA
Undiluted Target Tack Rate (gal/sy):	NA
Approx. Avg. Temperature at Plant (F):	300
Avg. Measured Mat Compaction:	92.3%

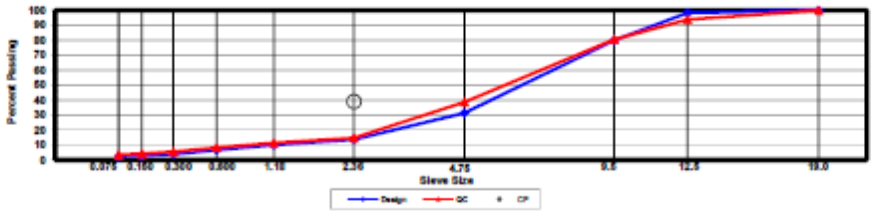

General Notes:
1) Mixes are referenced by quadrant (E=East, N=North, W=West, and S=South), section # (sequential) and sublot (top=1);
2) SMA and OGFC refer to stone matrix asphalt and open-graded friction course, respectively; and
3) Mixes not containing hydrated lime were run with either Gripper X antistrip or Evotherm Q1 warm mix additive at a 0.5% rate